Dissertation

Skin regeneration and wound healing after mesenchymal stromal cell treatment is dose dependent

submitted by

Dr. med. univ. Gertraud EYLERT

for the Academic Degree of

Doctor of Medical Science

(Dr. scient. med.)

at the

Medical University of Graz

Department of Surgery

Division of Plastic, Aesthetic and Reconstructive Surgery

under the Supervision of

Univ.-Prof. Dr. med. univ. Lars-Peter KAMOLZ, MSc

2021

Declarations (English, Deutsch)

Declaration

I hereby declare that this thesis is my own original work and that I have fully acknowledged by name all of those individuals and organizations that have contributed to this thesis. Due acknowledgement has been made in the text to all other material used. Throughout this thesis and in all related publications I followed the "Standards of Good Scientific Practice" and the guidelines from the Medical University of Graz.

Graz, March 2021

Eidesstattliche Erklärung

Ich erkläre ehrenwörtlich, dass ich die vorliegende Arbeit selbständig angefertigt und abgefasst und jene Personen und Institutionen, die am Zustandekommen der Forschungsdaten beteiligt waren, namentlich genannt habe. Andere als die angegebenen Quellen habe ich nicht verwendet und die den benutzten Quellen wörtlich oder inhaltlich entnommenen Stellen habe ich als solche kenntlich gemacht. Die Arbeit an der Dissertation und daraus entstandener Publikationen wurde gemäss den Regeln der „Good Scientific Practice" und der Richtlinien der Medizinischen Universität Graz durchgeführt.

Graz, März 2021

Investigators, Dissertation Committee

Principal Investigators, Doctoral Student
Dr. med. univ. Gertraud Eylert, MSc
Medical University of Graz
Auenbruggerplatz 2
8036 Graz
Austria
Email: gertraud.eylert@stud.medunigraz.at

Supervisor for Doctoral Study
Univ. Prof. Dr. med. univ. Lars-Peter Kamolz, MSc
Professor, Medical University of Graz
Department of Surgery
Head of the Division of Plastic Aesthetic and Reconstructive Surgery
Auenbruggerplatz 29
8036 Graz
Austria
Email: lars.kamolz@medunigraz.at

Principal Investigators (Research Institution), Co-Supervisor for Doctoral Study
Marc Jeschke, MD, PhD, FACS, FCCM, FRCS (C)
Professor, University of Toronto
Director, Ross Tilley Burn Centre
Senior Scientist, Sunnybrook Research Institute
Department of Surgery and Plastic Surgery
Department of Immunology
2075 Bayview Avenue, Room D704
M4N 3M5 Toronto
Canada
Email: marc.jeschke@sunnybrook.ca

Co-Supervisor for Doctoral Study
Ao. Univ.-Prof. Mag. Dr. rer. nat. Ingrid Lang-Olip
Department of Cell Biology, Histology and Embryology
Gottfried Schatz Research Center for Cell Signaling, Metabolism and Aging
Medical University of Graz
Neue Stiftingtalstraße 6/II
8010 Graz
Austria
Email: ingrid.lang@medunigraz.at

Acknowledgments

This research opportunity was possible due to the support of Prof. Dr. Lars-Peter Kamolz, MSc, Head of the Division of Plastic, Aesthetic and Reconstructive Surgery at the Medical University of Graz, Austria, who provided encouraging and took “a-step-beyond” by applying for the research opportunity abroad. I would like to thank all my supervisors for their support guiding me through this PhD thesis project.

The main research was conducted in Prof. Dr. Marc G. Jeschke`s stem cell laboratory in Toronto, Canada. During my dedicated two-year full-time research fellowship in Canada, I was also able to complete a Master`s program in Regenerative Medicine at the University of Toronto with Dr. Jeschke as my supervisor (09/2017–06/2019). I was able to finish a MSc thesis with the title “Bio-Printing of Mesenchymal Stem Cells for Skin Reconstruction after Burns”, which was completed in accordance with the University of Toronto and in transparency with the Medical University of Graz and my supervisors in this PhD program (02/2017–07/2021). Dr. Jeschke’s help has enabled me to lay the foundation of my career as a surgeon scientist in plastic surgery.

I would like to thank Prof. Dr. Ingrid Lang-Olip for her valuable feedback and the opportunity to learn the initial mesenchymal stem cell work and analysis in her cell biology laboratory. Furthermore, Prof. Dr. Lang-Olip introduced me to the SPRINT Cost Action, a European Cooperation in Science and Technology, which has been a great networking opportunity in the perinatal tissue research community.

Furthermore, I would like to thank PD Mag. Dr. Lohberger for her support in the Doctoral School of Bones, Muscles, Joints and Skin, as well as Miriam Sedej, PhD, for helping me organizing my doctoral study.

Finally, I would like to thank my family and friends for all their help and their constant belief in me during this research time.

Funding

I was supported by the following societies:

- Medical University Graz, Division of Plastic, Aesthetic and Reconstructive Surgery, Travel/Education Support for Canada (September 2017) (EUR 3.000,-)
- Research Award 18-month, Austrian Surgeon Association (January 2018) (EUR 13.5000,-)
- SPRINT COST Grant, European Cooperation in Science Technology (August 2019) (EUR 650,-)
- Medical University Graz, Travel Grant for Congress (October 2019) (EUR 500,-)
- Literar-Mechana, Doctoral Study Stipend (January 2020) (EUR 9.000,-)
- Medical University Graz, Research Scholarship for Dissertation Projects (January 2020) (EUR 3.565,39)
- SIE Grant - Plastic Surgeon Dr. Suzanne Noël Scholarship supported by the Austrian Soroptimist Club Belvedere Vienna, granted by the Soroptimist International Europe (October 2020-2021) (EUR 5.000,-)

Statement of Contributions

The following people/organizations have been instrumental in the collection of materials and data for this thesis:

- The Integra Life Science Corporation for providing Integra®.
- The obstetrical and gynecological department of Sunnybrook, Dr. Herer and Dr. Zaltz, for the collection of umbilical cords.
- Reinhard Dolp, MD, MSc in Dr. Jeschke`s Stem Cell Laboratory, who established the protocol for cell seeding into Integra®, with technical laboratory contribution assisted by Alexandra Parousis. Reinhard Dolp conduced the *in vitro* experiments with the artificial scaffold and performed stem cell grafting surgeries on pigs (09/2015–06/2017). Both taught me how to seed the Integra® with the cells and how to conduct my own pig experiments.
- The staff in the Dr. Marc Jeschke`s Stem Cell Laboratory at Sunnybrook Research Institute with the laboratory technical support by Alexandra Parousis, MSc; Andrea-Kaye Datu, MSc; Haidun Liu, MSc; and Elisa Tran, MSc, who helped me to conduct my own experiments.
- The staff in the Comparative Research Department at Sunnybrook Research Institute, who helped me with the anaesthesia for the pig experiments.
- Geneve Awong, PhD, Core Facility Managerin–Centre for Flow Cytometry and Microscopy–who helped me with the flowcytometry, and in specifically with the cell sorting, the cell tracing experiment, and gating the nanoparticles and labeled cells.
- The students Stefania Priore and Viola Reiner who helped me with the histological staining and scanning of the slides.
- Verification of the analyzed data was confirmed blindly by Stefania Priore; Viola Reiner; Prof. Ingrid Lang-Olip, MSc, PhD; Frederike Reischies, MD, PhD; Yanran Wang, MSc; Andrea Kaye Datu; MSc and Haidun Liu, MSc.
- In Prof. Dr. Lang-Olip`s laboratory, Christine Daxböck taught me the initial mesenchymal stromal/stem cell isolation of the umbilical cord, Wharton`s Jelly and Amnion; in addition, Monika Sundl taught me (immuno)-histological staining.
- My collaborator Richard Cheng, MSc and PhD-candidate, assisted in the setting up and optimization of the confocal microscope in the Engineer Department at the University of Toronto for stem cell imaging of the labeled cells, contributed blindly in the stem cell counting and provided help with Illustrator graphs for the publications for this project.

- Statistical analysis shown in this thesis was performed with the help from Mark Pelechaty, MA (Data Scientist).
- Lastly, the final thesis with the title "Skin regeneration and wound healing after mesenchymal stromal cell treatment is dose dependent" evolved after my observation in the first project with the hand-held bioprinter, were I observed in the ongoing trial that actually a lower dose of mesenchymal stromal/stem cells leads to better wound healing than the believed high dosages. Following this, Dr. Marc G. Jeschke and Dr. Lars-Peter Kamolz allowed me to write my doctoral thesis on this topic–"the dosage phenomenon". Subsequently, I was assigned to analyze the whole data set available of the transplanted stem cell seeded Integra® trial in the Jeschke Lab again. I combined my pig tissue data set of the two years (2017–2019) and took in additional tissue biopsies from the available stored pig experiments (2015–2017). Therefore, I contributed in all necessary parts for this project: the study design, the isolation and characterization of the mesenchymal stromal/stem cells, the cell sorting and all flow cytometry experiments, including the cell labeling, and viability experiments, the *in vivo* porcine experiments, all histology and immunohistochemistry, microscopy, and analysis using the necessary protocol, results, and statistics, as well as the writing and editing of the manuscripts and the final thesis.

Plagiarism and Publications

Animal research must be conducted in accordance with ethical standards. In my projects, the same animals have been used to answer two different hypotheses due to the costly nature of animal studies. The created full-thickness porcine burn wound healing model (left and right side/flank of the pigs) answered the research question in my completed MSc thesis "Bio-Printing of Mesenchymal Stem Cells for Skin Reconstruction after Burns" (2019), which investigated the safety and efficacy of a novel hand-held bio-printer. In this following PhD thesis, the conducted research experiments investigated whether skin regeneration and wound healing after mesenchymal stromal cell treatment is dose dependent.

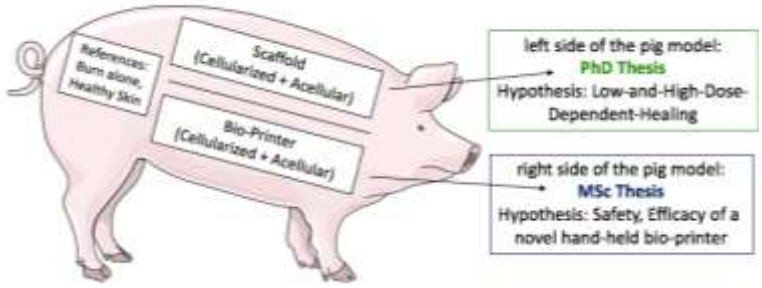

Explanation Hypothesis-Model on the created full-thickness burn porcine model.

My supervisors are aware of my previously published work, and permission was granted for this PhD thesis. The following previously published work appears in parts of this thesis:

- Amini-Nik, Dolp, **Eylert**, et. al, Stem cells derived from burned skin - The future of burn care. *EBIOMedicine*, 37, pp.509–520, 2018
- **Eylert, G.** (2019) MSc Thesis. Bio-Printing of Mesenchymal Stem Cells for Skin Reconstruction after Burns(Eylert 2019).
- Cheng & **Eylert**, Gariepy, He, et al., Handheld instrument for wound-conformal delivery of skin precursor sheets improves healing in full-thickness burns. *Biofabrication*, 2020
- Dolp & **Eylert**, Auger, Aijaz et al., 2021. Biological characteristics of stem cells derived from burned skin-a comparative study with umbilical cord stem cells. *Stem cell research & therapy*, 12(1), p.137
- **Eylert**, Dolp, Parousis et al., Skin regeneration is accelerated by a lower dose of multipotent mesenchymal stromal/stem cells-a paradigm change. *Stem cell research & therapy*, 12(1), p.82, 2021

The project and main funding of the following research including the publications is attributed to Dr. Marc G. Jeschke, PhD, in the Sunnybrook Research Institute. The publication costs (of the main article of this thesis “Skin regeneration is accelerated by a lower dose of multipotent mesenchymal stromal/stem cells – a paradigm change” (Eylert et al. 2021)) is attributed to the Medical University of Graz. The article is available and licensed under a Creative Commons Attribution 4.0 International License, via BMC, Stem Cell Research & Therapy, Open Access, 2021.

The other two publications contributing to this thesis are “Stem cells derived from burned skin - The future of burn care” (Amini-Nik, Dolp, Eylert, et. al 2018) – the article is available and published under Creative Commons licensing, which enables authors to retain copyright while allowing others to copy, distribute, and make some uses of their work, provided full credit is given to them as originators, and “Handheld instrument for wound-conformal delivery of skin precursor sheets improves healing in full-thickness burns” (Cheng & Eylert, Gariepy, He, et al. 2020), which is available and published under Creative Commons Attribution 3.0 Unported (CC BY 3.0), which allows free share and adapt, Biofabrication, IOPublishing, 2020.

Table of contents

DECLARATIONS (ENGLISH, DEUTSCH) ..... **II**
INVESTIGATORS, DISSERTATION COMMITTEE ..... **III**
ACKNOWLEDGMENTS ..... **IV**
FUNDING ..... **V**
STATEMENT OF CONTRIBUTIONS ..... **VI**
PLAGIARISM AND PUBLICATIONS ..... **VIII**
TABLE OF CONTENTS ..... **X**
LIST OF ABBREVIATIONS ..... **XIII**
LIST OF FIGURES ..... **XV**
LIST OF TABLES ..... **XVI**
ABSTRACT ..... **XVII**
ABSTRAKT (DEUTSCH) ..... **XVIII**

CHAPTER 1 INTRODUCTION AND BACKGROUND **1**
A BURN INJURY 2
ANATOMY OF THE SKIN 2
WOUND HEALING AND TISSUE REPAIR 3
CURRENT STANDARDS OF BURN CARE 4
REGENERATIVE MEDICINE 4
CHAPTER 2 PROJECT RATIONALE **6**
RATIONALE FOR THIS THESIS PROJECT 7
RATIONALE FOR USING UMBILICAL CORD MESENCHYMAL STROMAL/STEM CELLS 8
RATIONALE FOR USING THE SKIN SUBSTITUTE –THE DERMAL REGENERATION TEMPLATE, INTEGRA® 8
RATIONALE FOR THE LOW-TO-HIGH CELL DOSE MODEL 9
RATIONALE FOR THE PORCINE WOUND HEALING MODEL, YORKSHIRE PIG 9
CHAPTER 3 HYPOTHESIS AND AIM **10**
HYPOTHESIS 11
NOVELTY (ORIGINALITY) 11
RESEARCH OBJECTIVE AND AIMS 11
OUTCOME MEASURES AND ENDPOINTS 11
Outcome measures for skin regeneration and wound healing *11*
Endpoints of the study: *12*
CHAPTER 3 MATERIAL AND METHODS **13**
STUDY DESIGN 14
ETHICAL APPROVAL AND GUIDELINES 14
MESENCHYMAL STROMAL/STEM CELLS 14
Mesenchymal stromal/stem cell extraction *14*
Criteria and characteristics of mesenchymal stromal/stem cells *16*
Mesenchymal stromal/stem cell differentiation - in vitro *16*
Cell sorting, flow cytometry assay *17*
THE SKIN SUBSTITUTE, SCAFFOLD 17
Cell integration into the dermal regeneration template *17*
CONTROLS 18
Acellular controls *18*
Treatment references *19*

Cell labeling and detecting the presence of labeled cells 19
Preclinical Trial 21
Experimental overview *21*
Burn treatment *22*
Animals and housing *22*
Burn wound infliction *23*
Surgical wounds *23*
Mesenchymal stromal/stem cell transplantation, the dose-model *23*
Wound dressing changes, biopsies *24*
Pig`s health score assessment *25*
Endpoints *25*
Study Assessment, Outcome Measurement Analysis 25
Safety Assessment of the treatments *25*
Outcome Measurement Analysis *26*
Macroscopical assessment (Photography) *26*
Assessment of the histology *27*
Masson`s Trichrome *28*
Immunohistochemistry *28*
Statistics 29

CHAPTER 4 RESULTS 30

Overview of results 31
Creation of comparable baseline conditions for the experiments 31
Extracted cells from the Umbilical Cord are Mesenchymal Stromal/Stem cells *32*
Full-thickness burns are reproducible *33*
Presence of grafted mesenchymal stromal/stem cells on the wounds 34
Skin tissue regeneration after Integra® treatment 35
Mesenchymal stromal/stem cells therapy enhances skin regeneration and wound healing 36
Efficacy of a low-to-high mesenchymal stromal/stem cells treatment 38
Macroscopical Wound Healing *38*
Epithelialization 38
Scarring 38
Epidermal Regeneration *39*
Epidermal Thickness 39
Appendages 41
Dermal Regeneration *44*
Collagen Formation 44
Neovascularization 44
Fibrosis 44
Inflammation 44
Skin regeneration and wound healing after MSC treatment is dose-dependent 46

CHAPTER 5 DISCUSSION 50

General Discussion 51
The existence of a cell-dose phenomenon 51
Regeneration findings and their meaning 53
Negative findings 55
MSCs therapy via Integra® 55
Umbilical cord mesenchymal stromal cells in wound healing 56
Animal Model 56
Ethical concerns 57
Limitations 58

CHAPTER 6 CONCLUSION 60

Conclusion 61
Recommendations 61

CHAPTER 7 FUTURE DIRECTIONS 62

Future Directions 63

REFERENCES 64

APPENDIX I: TIMEFRAME, MILESTONES OF THE THESIS PROJECT 74
APPENDIX II: PUBLICATION LIST FOR THIS THESIS PROJECT 75
SUPPLEMENTARY MATERIAL 76
SUPPLEMENTARY MATERIAL FIGURE 1 76
SUPPLEMENTARY MATERIAL FIGURE 2 77
SUPPLEMENTARY MATERIAL TABLE 1 81

List of Abbreviations

Ab/Am	Antibiotic-antimycotic solution
ATMP	Advanced Therapy Medicinal Product
BASG	Austrian Federal Office for Safety in Health Care
BD	Burn-derived
BrdU	Bromodeoxyuridine
CD	Cluster of Differentiation
CCL2	Monocyte chemoattractant protein-1
CXCL	Chemokine
DMEM	Dulbecco's Modified Eagle Medium
DRT	Dermal Regeneration Template
ECM	Extracellular Matrix
EGF	Epidermal growth factor
EMA	European Medicines Agency
EtOH	Ethanol
FBS	Fetal bovine serum
FDA	Food and Drug Administration
GVHD	Graft-versus-host disease
HBSS	Hank`s Balanced Salt Solution
IGF	Insulin-like growth factor
ISCT	International Society for Cellular Therapy
M1	Macrophages type 1
M2	Macrophages type 2
MMPS	Matrix metalloproteinases
MSC	Multipotent Mesenchymal Stromal/Stem Cell
MPCs	Mesenchymal precursor cells
N	Number
P	Passage
PBS	Phosphate-buffered saline
PDGF	Platelet-derived growth factor
REB	Research Ethics Board
SC	Stem cell

SD	Standard deviation
SMA	Smooth muscle actin
TBSA	Total body surface area
TGF	Tissue growth factor
TNF	Tumor necrosis factor
TIMPs	Tissue inhibitors of metalloproteinases
UC	Umbilical cord
UC-MSC	Umbilical cord mesenchymal stromal cells
VEGF	Vascular endothelial growth factor
VSS	Vancouver Scare Scale
WHO	World Health Organization

List of Figures

Figure 1: Conventional stem cell extraction from the Wharton`s Jelly. 15
Figure 2: Schematic purpose of the DRT, cell labeling 20
Figure 3: Creation of a low-to-high cell dose 24
Figure 4: Wound Healing Analysis, Scar Assessment 27
Figure 5: Histology Example. 28
Figure 6: Overview of the experiment. 31
Figure 7: Mesenchymal stromal/stem cell differentiation. 32
Figure 8: Burn Confirmation 34
Figure 9: Cell viability after labeling cells 35
Figure 10: Tissue regeneration 36
Figure 11: Ranking assessment, descriptive data summary of the study 37
Figure 12: Data distribution, macroscopical wound healing 39
Figure 13: Data Distribution, outcome measures 40
Figure 14: Epidermal and Dermal Regeneration 41
Figure 15: Appendages, Neoformation 43
Figure 16: Inflammation 46
Figure 17: Data summary of the study 47
Figure 18: Cell dose curves for each outcome measures 48

List of Tables

Table 1: Experimental Overview. 21

Abstract

Skin regeneration and wound healing after mesenchymal stromal/stem cell treatment is dose dependent

Background: Skin regeneration and wound healing is crucial, especially after a burn injury. Mesenchymal stromal cell (MSC) therapy is under investigation in promising (pre)clinical trials to restore the damaged skin; however, the optimal cell dosage for therapy remains unknown.

Hypothesis: Different low-to-high MSC dosages promote outcome measures differently in skin regeneration and wound healing.

Methods: We conducted a porcine study (N = 8 Yorkshire pigs) and seeded between 200–2,000,000 cells/cm^2 of umbilical cord mesenchymal stromal cells (UC-MSCs) on a biodegradable collagen-based dermal regeneration template (DRT) Integra® and grafted it onto full-thickness burn excised wounds. On day 28, we compared the different low-to-high cell dose groups, the acellular control, a burn wound, and healthy skin.

Result: We found that the low dose with 40,000 cells/cm^2 regenerates the full-thickness burn excised wounds most efficaciously, followed by the dose groups 5,000 cells/cm^2 and 200,000 cells/cm^2. The low dose of 40,000 cells/cm^2 accelerated re-epithelialization, reduced scarring, regenerated epidermal thickness superiorly, enhanced neovascularization, reduced fibrosis and reduced type 1 and type 2 macrophages compared to other cell dosages and the acellular control.

Importance: This regenerative cell therapy study using MSCs shows efficacy when utilizing a low dose, which changes the paradigm that more cells lead to better wound healing outcome.

Abstrakt (Deutsch)

Hautregenerierung und Wundheilung ist nach mesenchymaler Stammzelltherapie dosisabhängig

Hintergrund: Hautregenerierung und Wundheilung ist wesentlich, speziell nach einer Verbrennung. Mesenchymale Stammzelltherapie wird in vielversprechenden (vor-)
klinischen Studien untersucht um die Haut wiederherzustellen. Die optimale Zelldosis dieser Therapie kennt man jedoch noch nicht.

Hypothese: Wir haben eine Studie mit Schweinen durchgeführt (N = 8 Yorkshire Schweine) und zwischen 200–2.000.000 Zellen/cm^2 mesenchymale Stammzellen von der Nabelschnur auf ein biologisch abbaubares Hautsubstitut, Integra®, und auf zuvor ausgeschnittene Verbrennungswunden transplantiert. Vier Wochen danach haben wir die verschiedenen niedrigen bis hohen Zelldosen der Gruppen mit einer azellulären Kontrollgruppe, verbrannten Wunden und gesunder Haut verglichen.

Resultat: Die Wunden mit 40.000 Zellen/cm^2 haben die voll ausgeschnittenen verbrannten Wunden am besten regeneriert, gefolgt von der Dosis mit 5.000 Zellen/cm^2 und 200.000 Zellen/cm^2. Die niedrige Dosis von 40.000 Zellen/cm^2 haben die Wunden beschleunigt reepithelialisiert, haben Vernarbung reduziert, haben die Epidermis besser regeneriert, haben die Neovaskularisierung vorangetrieben, die Fibrose reduziert und die Typ 1 und 2 Makrophagen reduziert verglichen mit den anderen Zelldosen und der azellulären Kontrolle.

Wichtigkeit: Diese Zelltherapiestudie, welche die mesenchymale Stammzelltherapie untersucht hat gezeigt, dass eine niedrige Zelldosis am wirksamsten regeneriert; dies ändert den Glauben, dass höhere Dosen besser für Wundheilung sind.

Chapter 1
Introduction and Background

The contents in this chapter has been partially modified and published previously as follows:

- Amini-Nik, Dolp, **Eylert**, et. al, Stem cells derived from burned skin - The future of burn care. *EBIOMedicine*, 37, pp.509–520, 2018
- **Eylert, G**. (2019) MSc Thesis. Bio-Printing of Mesenchymal Stem Cells for Skin Reconstruction after Burns.
- Cheng & **Eylert** et al., Handheld instrument for wound-conformal delivery of skin precursor sheets improves healing in full-thickness burns. *Biofabrication*, 2020
- **Eylert** et al., Skin regeneration is accelerated by a lower dose of multipotent mesenchymal stromal/stem cells-a paradigm change. *Stem cell research & therapy*, 12(1), p.82, 2021

A burn injury

A burn is one of the most severe skin injuries a human can suffer from, and according to the World Health Organization (WHO) in 2000, 12% of all worldwide diseases accounted for such an injury (Niels & Stephen 2006). It is estimated that 330,000 deaths occur due to such a disease (World Health Organization, Report, 2002). Major burns lead to profound systemic (hypermetabolic) responses (Jeschke et al. 2008) that have serious long-term effects (Greenhalgh 2019), including browning (Abdullahi & Jeschke 2017) and scarring (Finnerty et al. 2016). Infections are the leading causes of the high morbidity and mortality rates (Lindberg et al. 1965), highlighting the importance of quick and permanent wound closure in burn patients (Nicholas et al. 2016). Generally, the larger the burn is (measured in total body surface area percentage, TBSA %), the more difficult the treatment is (Jeschke, Kamolz, et al. 2017). Furthermore, the thickness of injury is determined and classified in first, second, third (dermis and hypodermis) and deeper fourth-degree burns (skeletal muscle, bones), as well as superficial, partial- and full-thickness burns (which is equivalent to a third degree burn affecting the dermis and hypodermis).

Anatomy of the skin

The skin is the largest organ in the human body, with its essential functions being a barrier against external factors such as mechanical stress and injury and bacterial infection and immunity, maintaining temperature and having important sensory functions (Yousef & Badri 2019; Yousef & Varacallo 2019). Human skin, with a total thicknesses ranging from a few hundred microns to several millimeters depending on the location, has a multilayered and stratified organization, which is structured as the epidermis, dermis and hypodermis/subcutaneous (adipose) fat tissue (Oltulu et al. 2018). The epidermis is the upper-most layer comprised of differentiated epithelial cells known as keratinocytes (Prodinger et al. 2017). The epithelial layer is tightly packed through cell-cell junctions and interact with support cells such as melanocytes and Langerhans cells to provide the critical barrier (Yousef & Badri 2019; Yousef & Varacallo 2019). The layer evolves from ectodermal precursors (Dekoninck & Blanpain 2018; Kretzschmar & Watt 2014; Prodinger et al. 2017) anchored to the basal layer and appendages; however, high plasticity has been recently shown (Dekoninck & Blanpain 2018), and the epidermal layer can regenerate also from the mesenchymal lineage (Lynch & Watt 2018a; Driskell & Watt 2015; Dekoninck & Blanpain 2018). These mesenchymal stromal cells build the papillary (upper loose connective tissue) and reticular (lower dense connective tissue) dermis, which is a

layer of loosely arranged extracellular matrix and, in healthy skin, abundant collagen-1 (Thulabandu et al. 2017), which provides the tissue structure. The dermal papillae are extensions from the dermis, which reach toward the epidermal layer and provide nutrients and oxygen to the basal layer. In the dermis, dermal fibroblasts are the most populated cell type, responsible for secretion, degradation and homeostasis in this layer derived from the mesenchymal lineage (Grinnell 2003; Lynch & Watt 2018b; Nolte et al. 2008). Hair follicles, sweat glands, sebaceous glands, lymphatic and blood vessels may cross through (Yousef & Badri 2019; Yousef & Varacallo 2019). The hypodermis, also referred to as the subcutaneous fat tissue, is located below the dermis and contains the majority of adipocytes, also derived from the mesenchymal lineage (Qomi & Sheykhhasan 2017), playing a significant role in fat storage for energy and thermal regulation, while supporting cells such as endothelial cells, smooth muscle cells, fibroblasts and hair follicles (Watt 2014).

Wound healing and tissue repair

Wound healing and repair is a physiological response to restore tissue homeostasis, and it is a tightly regulated process, which can be divided into four distinct phases: (1) haemostasis (minutes after injury – 2 days), (2) inflammation (minutes after injury – day 7), (3) proliferation and regeneration (day 2-day 28), and (4) remodeling (day 14 – 2 years) (Gurtner et al. 2008; A. J. Singer & Clark 1999). The first phase, haemostasis, is characterized primarily by platelet activity, secreted growth factors such as epidermal growth factor (EGF), platelet-derived growth factor (PDGF) and transforming growth factor beta (TGF-beta) from local stromal and epithelial cells at the injury site that activate, aggregate and form a temporary plug. Subsequently, circulating fibrinogen in the plasma is polymerized with the protease thrombin which forms a mesh and further impedes blood loss. This matrix acts as a provisional scaffold for stromal and epithelial cell migration. In the inflammatory phase, macrophages and neutrophils are recruited to the wound area by vasodilatation and platelet-secreted factors such as PDGF, CCL2 (Monocyte chemoattractant protein-1), CXCL1 (Chemokine), and CXCL8. In addition, they clear clearing debris, dead cells, bacteria and other pathogens from the wound site and secrete growth factors such as EGF, VEGF (Vascular endothelial growth factor), TNF (Tumor necrosis factor), and IGF (Insulin-like growth factor) to promote epidermal and dermal cell division. After, the proliferation and regeneration phase is characterized by formation of a highly vascularized granular tissue where fibroblasts actively proliferate and secrete extracellular matrix proteins such as collagen and fibronectin (Bielefeld et al. 2012; Gurtner et al. 2008).

Within this newly formed granular tissue, fibroblasts differentiate into myofibroblasts and actively contract to pull on the extracellular matrix to decrease the overall size of the wound (Hinz et al. 2001; Hinz 2016); the epithelial cells at the wound edges also allow for rapid cell division and exhibit increase collective cell migration to cover the wound (Bielefeld et al. 2012; Gurtner et al. 2008). In the remodeling phase, the tissue is reorganized by enzymes such as matrix metalloproteinases (MMPS) and tissue inhibitors of metalloproteinases (TIMPs), leading to scar formation (Walraven & Hinz 2018).

Wound healing is carefully orchestrated and regulated. However, (mesenchymal) stem cells promote wound healing beneficially in various pathways (Cha & Falanga 2007; N. G. Singer & Caplan 2010; Isakson et al. 2015).

Current standards of burn care

In addition to primary care including (fluid) resuscitation, there is a clear need to restore the physiological barrier of the skin as quickly as possible to prevent further water loss or infection (Greenhalgh 2019). Therefore, in burn treatment, skin substitutes play an important role and provide temporary or permanent wound coverage (Shahrokhi & Jeschke 2019; Nicholas et al. 2016; Kamolz, et al. 2014; Wurzer et al. 2016) if autologous, allo- or xenografting therapy are unavailable. Cellularized skin substitutes aim to mimic skin and are being developed (Nicholas 2016; Beier et al. 2010; Adibfar et al. 2019; Sheikholeslam et al. 2018; Germain et al. 2018). Many acellular skin substitutes are widely used, and Integra® is one of the most recognized scaffolds worldwide and is approved for acute as well as chronic wounds (Yannas & Burke 1980; Yannas et al. 2010). It is a synthetic biodegradable dermal matrix bilayer consisting of a bottom acellular dermal part—a porous crosslink of bovine type I collagen and shark cartilage—and an upper-protecting silicon layer. The acellular Integra® scaffold as a dermal regeneration template (DRT) provides a construct for endogenous cell ingrowth and dermal stroma synthesis following healing.

Regenerative Medicine

Regenerative medicine with stem cell therapy is a novel approach in modern medicine based on the assumption that stem cells and their progenitors can regenerate and repair damaged tissue (Gurtner et al. 2008). The first descripted attempt in regenerative stem cell (SC) therapy was done by transplanting bone marrow, which is a rich source of hematopoietic stem and progenitor cells as well as mesenchymal stromal cells (Friedenstein et al. 1966; Caplan 2019).

Generally, stem and progenitor cells display two fundamental properties of self-renewal by lacking specialization and the ability to differentiate, producing a copy of the cell itself either symmetrically or asymmetrically (Ruddy & Morshead 2018).

The multipotent mesenchymal stromal/stem cells (MSCs) derive from the second germ layer and differentiate into multiple soft tissues, such as the bone, cartilage, skeletal, adipose and dermal tissue (Prodinger et al. 2017), making them potentially powerful candidates for cellular therapy. There are multiple sources for MSCs, such as the umbilical cord (Weiss & Troyer 2006), the placenta, the bone marrow, the adipose tissue, the dental pulp, the breast milk, and the burned skin tissue (Amini-Nik et al., 2018; Dolp & Eylert et al. 2021) itself.

Although the benefits of MSCs have been proven on the bench, and MSCS have been successfully applied in clinical trials (Jeschke et al. 2019), the therapy seems to be limited. Success rates in clinical trials are low and promising early results turned out to be irreproducible in larger cohorts (Le Blanc & Davies 2018; C et al. 2017; Yau et al. 2019). Possible explanations for the low efficiency may include the use of inappropriate cell types, insufficient quality and quantity of applied cells, limited delivery of the cells to the target organ, sub-optimal timing of the transplantation after the disease onset, wrong application mode and others, as authors recently proposed (Reinisch, 2020). However, we recently observed in an umbilical cord stem cell study a cell-dosing phenomenon indicating that the dose seems to be key.

Chapter 2
Project Rationale

The contents in this chapter has been partially modified and published previously as follows:

- Amini-Nik, Dolp, **Eylert**, et. al, Stem cells derived from burned skin - The future of burn care. *EBIOMedicine*, 37, pp.509–520, 2018
- **Eylert, G**. (2019) MSc Thesis. Bio-Printing of Mesenchymal Stem Cells for Skin Reconstruction after Burns(Eylert 2019).
- Cheng & **Eylert** et al., Handheld instrument for wound-conformal delivery of skin precursor sheets improves healing in full-thickness burns. *Biofabrication*, 2020
- **Eylert** et al., Skin regeneration is accelerated by a lower dose of multipotent mesenchymal stromal/stem cells-a paradigm change. *Stem cell research & therapy*, 12(1), p.82, 2021

Rationale for this thesis project

Skin regeneration and wound healing are tremendously important if a skin injury (Kamolz et al. 2015), such as a burn injury, occurs. Regeneration and healing of the epidermis and dermis are crucial to lowering the risk of infections that are associated with high mortality (Clark et al. 2007; Jeschke et al., 2015). To date, however, there is no optimal treatment for a severe skin burn. One approach is wound coverage with autologous skin graft transplantations, which is considered the gold standard in burn care. However, autologous grafting comes with additional challenges, such as the artificial creation of an additional wound when harvesting healthy skin from the donor to cover the burn wound, as well as wound healing problems after grafting, including wound healing disorders, or even a failure of the transplant itself. Alternatively, allografts and xenografts can be used, but they raise additional ethical concerns and issues concerning availability and/or also potential rejection. Therefore, skin substitutes play an important role and provide temporary or permanent wound coverage (Frueh et al. 2017) if autologous, allografting or xenografting therapy are unavailable.

In recent years, preclinical and clinical trials (Can et al., 2017) have been conducted to investigate wound healing using mesenchymal stromal/stem cells (MSCs) (Fitzsimmons et al. 2018; Jeschke et al. 2019) incorporated into Integra® (Amini-Nik, et al., 2018; Cheng & Eylert et al. 2020). However, the critical cell dosing of MSCs is still unknown and difficult to compare based on previous reports. Publications utilizing the DRT for wound healing include MSCs cell dosages that vary between 5,000–2,000,000 cells/cm^2 (Cheng & Eylert et al. 2020; Amini-Nik et al., 2018; Isakson et al. 2015) and are tested on different models, such as rodents (Spater et al. 2018; Formigli et al., 2015; Fierro et al., 2015; Meruane et al. 2012; Isakson et al. 2015), pigs (Amini-Nik et al., 2018; Cheng & Eylert et al. 2020; Wood et al. 2007) and humans (Falanga 2012a). These studies including models that were either given cell dosages once (Cheng & Eylert et al. 2020; Wood et al. 2007; Amini-Nik et al., 2018; Esteban-Vives et al. 2018) or multiple times (Isakson et al. 2015) on acute (Amini-Nik et al., 2018; Cheng & Eylert et al. 2020; Wood et al. 2007; Esteban-Vives et al. 2018) and chronic wounds (Falanga 2012a), either on partial (Esteban-Vives et al. 2018) or full-thickness (Wood et al. 2007; Cheng & Eylert et al. 2020; Amini-Nik et al., 2018) (burn) wounds, making comparisons even more difficult.

However, we previously observed in a stem cell study using a bioprinter with direct cell depositioning onto burn wounds that a lower dose regenerated the skin (Cheng & Eylert et al. 2020). This raises the challenging question of which dose is optimal, as the general research principle from these previous papers is that more cells lead to better wound healing outcomes. (Eylert et al. 2021)

The translational research presented here aims to answer the important question of optimal dosing of MSCs for future clinical applications.

Rationale for using umbilical cord mesenchymal stromal/stem cells

The literature describes several sources of mesenchymal stromal stem cells that have shown to enhance wound healing (Kamolz et al. 2014; Takeo et al. 2015; Isakson et al. 2015; Formigli et al., 2015). The rationale for using umbilical cord mesenchymal stromal/stem cells (UC-MSCs) extracted from Wharton`s Jelly was based on the following considerations: The umbilical cords we received were readily available as a biological side product (a collaboration with Sunnybrook Obstetrical and Gynecological Department), were free of costs and originated from a possible noninvasive harvesting technique (Mahmood et al. 2015). Currently, perinatal tissue, such as the amnion and the umbilical cord, are being used in wound care. The umbilical cord and their extracted cells have impressive healing capabilities (Davis 1910; Matthews et al. 1981; Jeschke et al. 2019). In addition, clinical trials (Can et al., 2017) have shown their safety (Couto et al. 2019), and they are known to be nontumorigenic, with a high proliferation capacity (Saleh & Reza 2017). These cells have a superior multipotent potential compared to other MSC sources, including the adipose or chorionic tissue (Jing Li et al. 2018). Furthermore, UC-MSCs possess a lack of HLA-DR expression and have excellent immunosuppressive properties with a low risk of graft-versus-host disease (Jing Li et al. 2018). Furthermore, UC-MSCs are described as having a great potential for banking (Weiss & Troyer 2006). The Jeschke laboratory has previously shown that UC-MSC extracted from Wharton`s Jelly enhances wound healing by accelerating the differentiation of cells in wounds (Bakhtyar et al. 2017). Other research groups have demonstrated UC-MSCs possess characteristics that could be advantageous for wound healing, such as their potency under ischemic-like stress conditions (Himal et al. 2017); additionally, they have the ability to differentiate into fibroblast-like cells (Mahmood et al. 2015), they show increased expression of re-epithelialization, neovascularization and fibroproliferation factors (Arno et al., 2014; Arno et al., 2014), and they can also decrease inflammation (Lee et al. 2016).

Thus, UC-MSCs have the potential to become an economical and effective treatment option for wound healing in burn patients (Jeschke et al. 2019). (Eylert et al. 2021)

Rationale for using the skin substitute –the dermal regeneration template, Integra®

The acellular DRT Integra® (LifeScience Corporation) is one of the most widely used scaffolds worldwide and is the standard of care in burn treatment (Shahrokhi et al. 2014; Wurzer et al.

2016) if a skin substitute is needed for wound coverage. The main purpose of the DRT is to provide a stiff scaffold for endogenous cell ingrowth, allowing tissue remodeling and promoting skin regeneration and wound healing. DRT is a synthetic biodegradable bilayer consisting of a bottom acellular dermal matrix–a porous crosslink of bovine type I collagen and shark cartilage–and an upper-protecting silicon layer. Previously, we (Amini-Nik et al., 2018; Cheng & Eylert et al. 2020) and other groups (Spater et al. 2018; Formigli et al., 2015; Fierro et al., 2015; Meruane et al. 2012; Isakson et al. 2015; Wood et al. 2007) have confirmed that the DRT is a reliable cell carrier for tissue engineering, allows cell ingrowth (Jones et al. 2003; Hamrahi et al. 2012) as well as cell differentiation (Morena et al. 2016), and therefore promotes wound healing. In addition, researchers have been able to show that the collagen-crosslinked matrix provides an environment for the differentiation of cells (Hamrahi et al. 2012). (Eylert et al. 2021)

Rationale for the low-to-high cell dose model

Recently, it was found in the stem cell research group in the Jeschke Lab that a macroscopical dose-phenomenon exists using a novel hand-held bio-printer when transplanting MSCs onto burn full-thickness wounds (Cheng & Eylert et al. 2020; Eylert 2019). Cell dosages up to 50,000,000 MSCs per wound were used; however, the low dosages showed superior healing (Cheng & Eylert et al. 2020; Eylert 2019). In the literature, other research groups descripted comparable dose-models, however, the (most) optimal dose is not determined yet in tissue engineering (Wagner et al. 2019; Chahal et al. 2019; Cheng & Eylert et al. 2020; Wood et al. 2007). Ultimately, the goal is to treat patients with an ideal cellularized skin treatment in the future.

Rationale for the porcine wound healing model, Yorkshire pig

Yorkshire pigs (Abdullahi et al. 2014; Cheng & Eylert et al. 2020; Dolp 2017; Eylert et al. 2021) were used (N = 8) in this study, and they possess similar anatomic and physiologic skin characteristics and comparable pigmentation to humans (Grada et al. 2018). Large wound sizes did not allow spontaneous healing via contracture (Jeschke et al. 2017). The model has been validated by other authors as a sufficient full-thickness burn model (Singer & McClain 2003; A. J. Singer et al. 2016; Sullivan et al. 2001; Wood et al. 2007). (Eylert et al. 2021)

Chapter 3
Hypothesis and Aim

Hypothesis

We hypothesize that different multipotent mesenchymal stromal/stem cell dose concentrations delivered on an acellular dermal regeneration template Integra® promote outcome measures differently in skin regeneration and wound healing in a full-thickness skin burn model.

Novelty (Originality)

Skin regeneration and wound healing are investigated in full-thickness skin burn model using a low-to-high multipotent mesenchymal stromal/stem cell dose treatment.

Research Objective and Aims

The aims of this study are to investigate skin regeneration and wound healing using different dosages in a low-to-high MSCs concentration model incorporated in a DRT in the treatment of a full-thickness skin injury. Therefore, the defined objectives include the following:

1. Determine the presence of mesenchymal stromal/stem cells after cell-grafting on the wounds.
2. Determine and evaluate the efficacy of outcome measures in a low-to-high dose model after mesenchymal stromal/stem cell treatment is delivered on an acellular DRT.
3. Determine and compare different mesenchymal stromal/stem cell dosages for an optimized treatment using Integra® as an artificial skin graft.

Outcome Measures and Endpoints

To our knowledge, a multipotent mesenchymal stromal/stem cell treatment in a low-to-high-dose model has not been tested before. However, the question of an optimized dosing is of tremendous importance for current and future clinical trials for skin regeneration and wound healing for humans. Thus, we aim to answer our research question by defining outcome measures to determine the efficacy of a mesenchymal stromal/stem cell grafting treatment, where efficacy is defined as the potential for skin regeneration and wound healing outcome measures.

Outcome measures for skin regeneration and wound healing

Macroscopically:

- Epithelialization area (in %)
- Scarring (Vancouver Scar Scale, VSS)

Histologically:

- Epidermal thickness (µm)
- Dermal regeneration, collagen formation (Integrated Density, Unit/μm^2)
- Neovascularization (positive stained vessels, Unit/μm^2)
- Fibrosis (alpha-SMA positive stained cells, Integrated Density, Unit/μm^2)
- Inflammation, Type 1 and Type 2 macrophages (positive stained cells, Unit/μm^2)

Endpoints of the study:

- Healed wounds, day 28 (indicative of the remodeling phase in wound healing)
- Medium-term stagnation in wound healing (remodeling phase, wound healing)

Chapter 3
Material and Methods

The contents in this chapter of this thesis have been partially published previously as follows:

- Amini-Nik, Dolp, **Eylert**, et. al, Stem cells derived from burned skin - The future of burn care. *EBIOMedicine*, 37, pp.509–520, 2018
- **Eylert, G**. (2019) MSc Thesis. Bio-Printing of Mesenchymal Stem Cells for Skin Reconstruction after Burns(Eylert 2019).
- Cheng & **Eylert** et al., Handheld instrument for wound-conformal delivery of skin precursor sheets improves healing in full-thickness burns. *Biofabrication*, 2020
- Dolp & **Eylert** et al., 2021. Biological characteristics of stem cells derived from burned skin-a comparative study with umbilical cord stem cells. *Stem cell research & therapy*, 12(1), p.137
- **Eylert** et al., Skin regeneration is accelerated by a lower dose of multipotent mesenchymal stromal/stem cells-a paradigm change. *Stem cell research & therapy*, 12(1), p.82, 2021

Study design

A prospective, experimental large animal study was carried out at the Jeschke Stem Cell Laboratory (M7-140) at the Sunnybrook Research Institute in Toronto, affiliated with the University of Toronto, Canada. The animal experiments were performed between September 2015 and June 2019 by two surgeons (Reinhard Dolp, MD, MSc 09/2015–06/2017 (RD)) and Gertraud Eylert, MD, MSc 09/2017–06/2019 (GE)). This thesis project evaluates skin regeneration and wound healing in a full-thickness porcine wound healing model after mesenchymal stromal/stem cell treatment was incorporated and grafted with the acellular dermal regeneration template (DRT, matrix, scaffold), Integra®, using different low-to-high cell dose concentrations.

To confirm the previously observed hypothesis and to account for a higher sample size (N) for statistical analysis two data sets from two surgeons from the same registered trial have been pooled (RD, N = 17 (31%); GE, N = 38 (69%)) (Supplementary Material Figure 2). Biopsies were taken retrospectively (from RD, 2019) from the stored excised wounds (from the period 2015–2017). All tissue samples were processed from the same surgeon (GE) according to the same protocols and were further stained and analyzed from the same blinded team.

Ethical approval and Guidelines

This study was approved and performed in accordance with the guidelines and regulations of the Research Ethics Board (REB), Sunnybrook Health Science Centre (REB # 017-2011). All procedures were executed accordingly in agreement with the Animal Policy and Welfare Committee of the University of Toronto. Animal procedures were reviewed, approved and monitored by the Sunnybrook Research Institute and Sunnybrook Health Sciences Centre animal care and use committee (AUP # 16-600) from trained veterinarian technicians and doctors. Routine safety and health checks were performed. All controlled drug exemptions were obtained from Health Canada (44219.11.17, 44220.11.17) under the Controlled Drug and Substances Act. During the trials, no adverse events occurred. The investigated animals maintained their health during the entire experiment. Informed consent was obtained from patients or from their substitute decision makers for the donation the umbilical cords.

Mesenchymal stromal/stem cells

Mesenchymal stromal/stem cell extraction

Several sources of human mesenchymal stromal/stem cells are available; however, cells for this project were extracted from the umbilical cord tissue, which the Jeschke Stem Cell Laboratory

received as a donation from the Obstetrical and Gynaecology Department from the Sunnybrook Hospital, using the same technique from Professor Ingrid Lang-Olip's Laboratory for the extraction.

The umbilical cords were maximally stored after collection for a period of 24 hours in the fridge at 4 °C before processing. Stromal/stem cells were extracted with a scalpel from the extracellular matrix from the umbilical cord, from the Wharton`s Jelly in specifically, and they were further cultured in Dulbecco's Modified Eagle Medium (Gibco™ DMEM, Thermo Fischer Scientific, Canada) supplemented with 1% antibiotic-antimycotic solution (Gibco® Antibiotic-Antimycotic, Thermo Fischer Scientific, Canada), 1% L-Glutamin (Sigma Aldrich) and 10% fetal bovine serum (FBS) (Gibco™ fetal bovine serum, Life Technologies Corporation, USA). Briefly, for the cell extraction method, the umbilical cord was diced in 3 cm pieces and washed three times with 2% Ab/Am in phosphate-buffered saline (PBS; Wisent Inc., Canada). The amnion and subamnion were vertically opened with a scalpel incision. Wharton`s Jelly was excised in multiple < 0.5 cm^2 squares, which were placed in a 6-well cell culture dish and submerged in 4 mL of culture medium. Cells were placed in an incubator at 37 °C with 5% CO_2. Cell outgrowth was controlled from the tissue pieces every other day under a light microscope. Once cell outgrowth took place (usually between days 7–12), the tissue pieces were removed, and partial media change was performed. Once the cells reached 90% confluency, they were passaged and seeded into cell culture flasks (T75) (Figure 1). Further cell culturing with cell expansion and media changes took place every second or third day for the duration of the experiments.

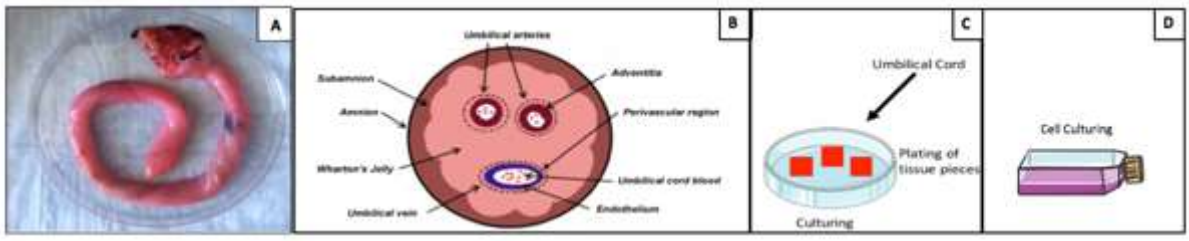

**Figure 1: Conventional stem cell extraction from the Wharton`s Jelly from the umbilical cord. (**A) Washed umbilical cord. (B) Schematic cross-section of the umbilical cord; Wharton`s Jelly is defined as the stroma. (C) Schematic small pieces of the excised Wharton`s Jelly in a 6-well dish. (D) Cell culturing for cell expansion. (Eylert 2019)

Criteria and characteristics of mesenchymal stromal/stem cells

According to the International Society for Cellular Therapy (ISCT) (2006), mesenchymal stromal/stem cells must meet the following minimal criteria to be identified and characterized as such *in vitro*: (1) they must adhere to a plastic surface; (2) they must express the Cluster of Differentiation (CD) protein 105, 90 and 73 while lacking CD 45, 34, and 14 or CD 11b, 79alpha, or CD 19 and HLA-DR; and (3) they must differentiate into main mesenchymal tissues: adipose tissue, cartilage, and bone tissue (Dominici et al. 2006).

Mesenchymal stromal/stem cell differentiation - *in vitro*

According to the aforementioned definition from the ISCT, cells extracted from the perinatal tissue were differentiated *in vitro*. After the cells reached a confluency of > 80% in the initial dish, cells were trypsinized and seeded into 6-well plates with a contraction of 100,000 cells/well and cultured until a confluency of 90%. After, the media was changed to a differentiation media for cartilage, adipose and bone tissue, according to the following protocols below.
Adipogenic differentiation: cells were cultured in low glucose DMEM supplemented with 10% FBS, 1% Ab/Am and 1mM of 3-isobutyl-1-methylxanthine (Sigma-Aldrich, Canada), 10 µg/mL of insulin (SAFC Biosciences, USA), 60 µM of indomethacin (Sigma-Aldrich, Canada), and 1 µM of dexamethasone (Sigma-Aldrich, Canada). Cells were placed in an incubator at 37 °C in 5% CO_2. The media was changed 2–3 times/week. Differentiation Staining: Oil Red O staining: After two weeks, the first staining was performed to confirm adipogenic differentiation. The media was removed, and wells were rinsed with PBS. Cells were then fixed in 10% formalin for 30 minutes, rinsed with distilled water and stained with Oil Red O for 5 min (Sigma-Aldrich). Following multiple rinses with water, cells were stained with hematoxylin (Sigma). Intracytoplasmic lipid droplets appear in red and nuclei appear in dark blue.
Chondrogenic differentiation: Cells were cultured in a low glucose DMEM supplemented with 10% FBS, 1% Ab/Am and 0.1 mM of L-ascorbic acid-2-phosphate (Sigma-Aldrich, Canada), 1% of Insulin-Transferrin-Selenium (Corning™ cellgro™ Insulin-Transferrin-Selenium, Corning Incorporated, USA), 100 nM of dexamethasone (Sigma-Aldrich, Canada), 0.1 mM of sodium pyruvate (Sigma Aldrich, Canada), and 10 ng/mL of TGF-β1. Cells were placed in an incubator at 37° C in 5% CO_2. The media was changed 2–3 times/week. Differentiation Staining: Alcian Blue staining: After 42 days the first staining was performed to confirm chondrogenic differentiation. Cells were fixed with 4% paraformaldehyde for 30 minutes (Electron Microscopy Sciences, USA), rinsed with 0% PBS and stained with Alcian Blue for 30 minutes

(Alcian Blue 8GX, Santa Cruz Biotechnology, Canada); they were washed multiple times. The cartilage extracellular matrix exhibited a strong blue stain.

Osteogenic differentiation: cells were cultured in low glucose DMEM supplemented with 10% FBS, 1% Ab/Am, 0.05 mM L-ascorbic acid-2-phosphate, (Sigma-Aldrich, Canada), 10 mM β-glycerophosphate disodium salt hydrate (Sigma-Aldrich, Canada), and 100 nM dexamethasone (Sigma-Aldrich, Canada). Cells were placed in an incubator at 37 °C in 5% CO_2. The media was changed 2–3 times/week. Differentiation Staining: Alizarin Red staining: After three weeks of osteogenic differentiation, the media was removed, and wells were rinsed with PBS. Cells were fixed with 4% Paraformaldehyde for 30 minutes (Electron Microscopy Sciences, USA), rinsed with 0% PBS, and stained with Alizarin Red for 45 minutes (Alcian Blue 8GX, Santa Cruz Biotechnology, Canada), and washed multiple times. Calcium deposits appear in a strong red.

Cell sorting, flow cytometry assay

Flow cytometry was performed after initial cell extraction and expansion to sort for MSCs expressing markers positive markers CD73, CD90 and CD105 (and negative markers, including the following: CD34, CD45, CD11b, CD19, and HLA-DR) by using a BD ™ LSR II Flow Cytometer (BD Biosciences, Canada), using FACSDIVA™ (BD Biosciences, Canada) and FlowJo™ software for graphical and statistical analysis. Live cells were selected and gated out with the negative markers CD34-/CD11b-/CD45- (FITC) (Invitrogen) and CD19-/HLA-DR- (AF700, PE-Cy7) (eBioscience), and positive markers were gated for CD73+ (PE) (eBioscience), CD90+ (BV510) (eBioscience) and CD105+ (APC) (eBioscience).

For cell sorting cells had a passage number of three with a confluency of 90% in the flasks. They were trypsinized, washed and resuspended in flow buffer consisting of Hank's Balanced Salt Solution (HBSS; Wisent Inc., Canada) supplemented with 1% bovine serum albumin (WISENT Inc., Canada). After, they were incubated with the conjugated antibodies (ratio 1:100) for 30 minutes on ice in the dark. After washing with flow buffer, DAPI (1:200) was added, and cells were analyzed with the BD™ LSR II flow cytometer with the above-mentioned laser channels.

The skin substitute, scaffold

Cell integration into the dermal regeneration template

The extracted and cultured MSCs were sorted and expanded until the anticipated cell count was reached for the grafting experiment. Shortly before the experiment, another flowcytometry

analysis was performed in order to confirm the cell surface markers. The cells were incorporated into the DRT on the day of each surgical experiment and were grafted on the burn excised wounds (Cheng & Eylert et al. 2020; Eylert et al. 2021). (Figure 2, 6)

As previously described (Amini-Nik, et al., 2018; Cheng & Eylert et al. 2020; Eylert et al. 2021), the cells were trypsinized, spun down and distributed in 50 mL Falcon tubes containing 25% + of cells and 2 mL of cell medium (Gibco™ DMEM, enriched with 1% antibiotic-antimycotic solution, 1% L-glutamine and with 10% FBS) depending on the design of each experimental protocol (using between 200–50,000,000 cells per treatment per wound). One milliliter of standard cell culture medium was pipetted to each cell pellet. The cells were then resuspended and transferred into a Petri dish and homogenously pipetted with a multi-channel pipette (VWR High Performance Signature^{TM}) on the acellular Integra® (Meshed bilayer Integra®, Integra LifeScience Corporation) on top of the bovine collagen, with the silicone side facing down on a sterile cell culture disk. The cells were seeded on DRT, which builds connections with the wound bed after surgical placement. The acellular control was prepared similarly with a mix of PBS and DMEM. Importantly, the DRTs absorbed the entire volume of the cells and PBS suspensions. Both groups were then placed in the incubator at 37 °C before being surgically grafted onto the porcine wound healing model. Shortly before surgery, the cellularized scaffolds were assessed under the microscope for floating cells indicating cell death and/or failure to integrate. No floating cells could be detected in either of the scaffolds, indicating full cell integration. From initial scaffold preparation until surgical grafting, less than 90 min of time had passed.

Previously, our group could evaluate the depth of the seeding technique of 123 ± 21 µm in the 1.3 mm thick scaffold (Reinhard Dolp, MSc Thesis, T-Space, University of Toronto; Figure modified by Gertraud Eylert, submitted and published previously (Eylert et al. 2021), Supplementary Material Figure 1). Transplanting the seeded cells with the DMEM on the pig did not lead to an adverse event as previously shown (Amini-Nik et al., 2018; Cheng & Eylert et al. 2020; Eylert et al. 2021). Other researchers confirmed this (Fierro et al., 2015), and this is most likely due to the wet scaffold where cells stay attached in higher densities at the surface, presumably due to a high affinity of MSC to attach to collagen.

Controls

Acellular controls

To investigate the efficacy of skin regeneration and wound healing, the acellular DRT was compared to the cellularized MSCs-DRT-treatment. The acellular control contained no cells

(Integra® alone) and were placed and grafted in the same manner as the cellularized component (Cheng & Eylert et al. 2020; Eylert et al. 2021). The acellular DRT Integra® is used in the clinic as a gold-standard skin substitute scaffold in burn care (Jeschke et al. 2013; Shahrokhi & Jeschke 2019).

Treatment references

In addition to the cellularized and acellular treatment, burn wounds were created on the pigs (N = 4) that received no treatment. Biopsies were taken at determined time-points from these wounds, and from healthy skin of the pig (N = 9); they were subsequently examined and referred as the worst and physiologic/optimal skin condition. (Eylert et al. 2021)

Cell labeling and detecting the presence of labeled cells

Sorted UC-MSCs (1,000,000) were labeled with 6 µL of a lipid cell surface dye (DiO; Vybrant Cell Labeling Kit, eligible for flow cytometry, DiO yellow channel (V-22886) Abs 484(nm)/Em 501 (nm), FITC) at the last medium change before the experiment (on day 2). This technique was found to be a reliable labeling kit option for cells integrated into the DRT(Clover et al. 2015) (Figure 2).

Additionally, a cell viability analysis after labeling was performed according to the manufacturer`s protocol and assessed at 12 hours using Live/Dead® Viability/Cytotoxicity Kit, Invitrogen (Calcein 494/517nm, Ethidium homodimer-1/DNA 528/617nm) (Figure 2). The labeled cells were incorporated with a density of 40,000 cells/cm^2 into equally cut 5x5 cm meshed acellular DRT, and were grafted on full-thickness burn excised wounds on day 0. Full-thickness tissue biopsies of 4 mm diameter were taken on day 2, 4, 7 and 9 at every dressing change from rotational quadrants of the wounds. The tissue biopsies were immediately cut into small pieces with the surgical scissors and mixed with a collagenase solution for 60–90 minutes under 37 °C conditions until all visible tissue pieces were small enough for further processing. This cell suspension mix was filtered (10µm cell strainer, Falcon® Corning, USA) and washed with flow buffer and spun down. The cell pellet was then distributed into a small unstained control portion (10%–15%) and a large experimental tube (85%–90%) in order to show the labeled MSCs. The experimental tube was stained with CD90+ in order to indicate mesenchymal stromal cells as double positive with the labeling dye DiO (BV510) (eBioscience). Analysis was made with flow cytometry (BD FACSDIVA™ SOFTWARE) (Figure 2).

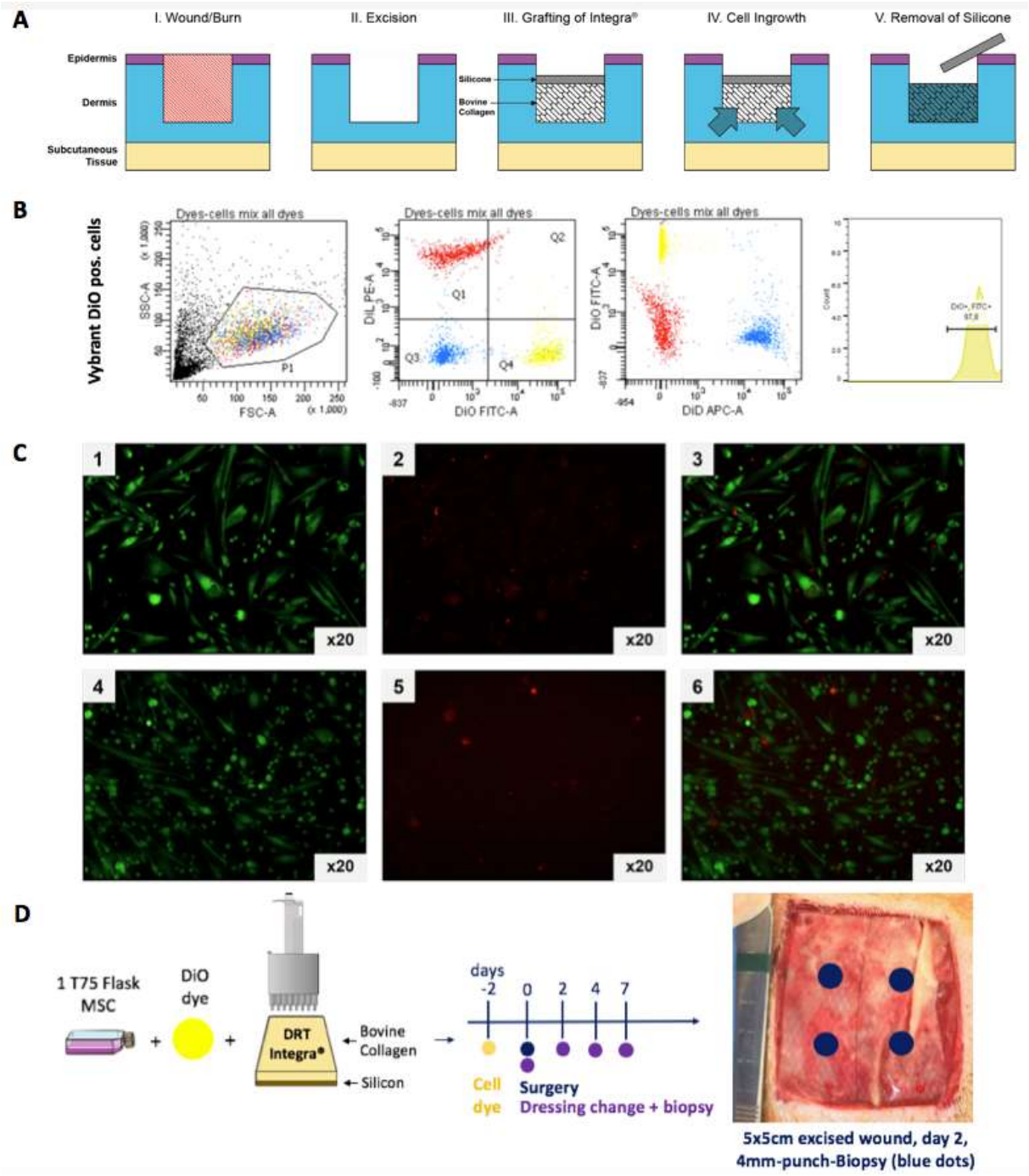

Figure 2: Schematic purpose of the DRT, cell labeling and viability and schematic experiment of the detection of labeled cells. (A) Schematic purpose of the DRT. Excision and removal of the wound tissue, grafting of the DRT for cell ingrowth and remodeling until the protecting silicon layer was removed. (B) Cell labeling kit via flowcytometry. Gated cell population containing three different cell surface labeling dyes (FSC and SCC). Histogram of DiO positive gated cells in the FITC, yellow channel. (C) Live-dead-staining, confocal microscope, magnification x 20. First row (1–3): After 12 hours after cells labeled and seeding: (1) live cells (calcein) (green channel), (2) dead cells (EthD) (red channel), (3) merged, labeled and dead

cells. Second row (4–6): unlabeled controls: (4) live cells (calcein) (green channel), (5) dead cells (EthD) (red channel), (6) merged, labeled and dead cells. (D) Schematic experiment of the detection of labeled cells on the wounds. Cells were labeled with a yellow lipid cell surface dye and grafted onto pig, at each wound dressing change every other day (day 2, 4, 7, and 9), and tissue biopsies (schematic: blue dots) were taken in a rotating application from the quadrant. (Eylert 2019; Eylert et al. 2021)

Preclinical Trial

Experimental overview

In general, the present study investigated eight Yorkshire pigs (N = 8), where umbilical cord mesenchymal stromal/stem cells were seeded in a density between 200-2,000,000 cells/cm^2 on a DRT onto 5x5cm full-thickness burn excised wounds investigating skin regeneration and wound healing. On day 28, comparisons were made between the different low-to-high cell dose groups, the acellular control, a burn wound and healthy skin. Analysis was made based on photography and histological samples from the wound center (Table 1).

Table 1: Experimental Overview.

Characteristics of the Pig-Models:
N = 8 pigs were included (2015–2019)
N = 55 wounds in total were analyzed
N = 1-10 wounds per pig (median 7, mean 6)
Nine conditions: 7 different wound treatments + 2 references
Each treatment was performed on 3–7 pigs
Each wound treatment was performed 3–12 times
Same Conditions:
UC-MSCs
Wound sizes (5x5cm), Biopsies from the wound centers (day 28)
Full-thickness-burn protocol (TBSA 25%), Same technicians
Same breeder
Same baseline condition of the pigs during experiments (Yorkshire, age, weight, size)

Burn treatment

The pigs received two treatments that were performed and based on the skin substitute Integra®. These two treatments were either cellularized with multipotent stromal cells or were acellular. We investigated 5x5cm full-thickness wounds and made comparisons regarding skin regeneration and wound healing. Additionally, we made comparisons to healthy skin and burn wounds alone as references. Treatment on the surgery day was assigned as day 0. Biopsies were taken at determined intervals. The eight pigs received the same treatment (Integra and UC-MSCs), although they had different amounts of wounds with different cell dosages. An ethically approved guideline was the creation of a TBSA of a maximum of 25%. Different experiments on the pigs using different sources and delivery strategies of multipotent stromal cells accounted for the unequal number of wounds per pig, in addition to the wide variety of different cell dose wounds.

Animals and housing

Eight Yorkshire male pigs (N = 8) were included in the study to determine the efficacy of the different cell dose MSCs treatments. Upon arrival, all pigs from the same breeder had a minimum weight of 20–25kg and were allowed to acclimatize for a minimum of 1–2 weeks prior to the start of the experiments, reaching the same baseline condition regarding weight and lengths. During the acclimatization period, animals received antibiotic therapy for approximately 1 week (e.g., 5–7 days, with a ceftiofur injection daily, intramuscular (im.)) after arrival from the farm. All procedures followed under the guidelines of the Sunnybrook Research Institute and Sunnybrook Health Sciences Animal Policy and Welfare Committee of the University of Toronto. The pigs were housed in individual pens at room temperature and at a 12 h light–dark cycle with food and water ad libitum at the Animal Facility of the Sunnybrook Research Institute. Feeding and daily care were performed by the in-house animal staff and overseen by the assigned veterinarian. Diet and animal care standard operation procedures were met. Experiments began when the pigs maintained a health score of 25/25 (assessed daily, using the following assessed items: (1) pupil size and reaction to light, (2) activity, (3) food intake, (4) posture and (5) hydration; there was a maximum of 5 points/item for an overall maximum of 25 points/day). All animals were fasted for at least 6 hours before any procedures, including burn infliction, surgery and wound dressing. All procedures were monitored daily and followed the standardized protocols overseen by the veterinarian. Pain medication and necessary antibiotic treatment were adjusted accordingly.

Burn wound infliction

For burn wound infliction, we used our standardized protocol (2 day before the transplantation (-2 days)) (Amini-Nik et al., 2018; Cheng & Eylert et al. 2020). After being acclimatized and treated with preventive antibiotics (ceftiofur injection daily, intramuscular (im.)) all pigs were exposed to burns (TBSA of a maximum of 25%). Briefly, under anesthesia and analgesia (buprenorphine 0.05mg/kg subcutaneous (sc.), ketamine starting dose 0.2 mg/kg sc., combined with atropine 0.5–1.0 mg depending on the heart rate, as well as isofluorane 5%/L/O2 intubation), 5x5 cm dorsal full-thickness burns were created using a heated silver device (200 °C) for 20 seconds under constant force measured using a digital force gauge (4.0 N, Mark-10 Corporation). The wounds were covered with wound dressing and sterile gauzes, which were kept in place by adhesive bandage and elastic stocking porcine suit. Additional analgesia (Tramadol 2–4 mg/kg/every 8 h orally) was administered regularly during the duration of the entire experiment and started 24 h post intervention. Full-thickness burns were confirmed histologically 48 hours post burn (Singer et al. 2016) via punch-biopsy as described previously (on day 0) (Cheng & Eylert et al. 2020; Eylert 2019; Dolp & Eylert et al. 2021).

Surgical wounds

After burn infliction (48 hours postburn) surgical wounds were completed. Pigs were monitored, and under general anesthesia and analgesia (buprenorphine, ketamine, isofluorane), hair was removed via electrical shaving followed by chemical depilation. The operation area was disinfected with chlorhexidine, skin excisions were marked and excision of the full-thickness burn was performed with a scalpel and monopolar electrocautery. Full-thickness burn excisional wounds were inflicted in all pigs of a size of 5x5 cm each, in two rows equidistant from the spine and each other. After the excision, wounds were covered and grafted as previously in the laboratory that prepared DRT treatments. The skin substitutes were secured with metal staples or sutured with Vicryl 2.0. The pigs were intraoperatively closely monitored, and 500-1000 mL of NaCl was administered intravenously (iv.). Daily antibiotic injections were continued between 3–5 days post surgery. After surgery and bandaging, pigs could recover in a warm, well-ventilated recovery pen with essential amounts of oxygen under observation.

Mesenchymal stromal/stem cell transplantation, the dose-model

In 2015–2017, the stem cell research group started transplanting multipotent stromal/stem cells onto burn excised full-thickness wounds (Reinhard Dolp, MS, MSc) to investigate the efficacy in skin regeneration and the wound healing (Dolp 2017). Cell dosages up to 10,000,000 cells

per wound were used. In a second period starting in 2017, we expanded the dose model exponentially using cells up to 50,000,000 cells per wound (Cheng & Eylert et al. 2020; Eylert 2019). Other research groups started with comparable exponential dose-models when used in tissue engineering (Wagner et al. 2019) and via direct injection (Chahal et al. 2019).

The arbitrary low-to-high cell dose counts for the MSC treatment groups account to an overall cell count per wound size (e.g., 200 cells/cm^2 = 5,000 cells/wound; 5,000 cells/cm^2 = 125,000 cells/wound; 40,000 cells/cm^2 = 1,000,000 cells/wound; 200,000 cells/cm^2 = 5,000,000 cells/wound; 400,000 cells/cm^2 = 10,000,000 cells/wound; and 2,000,000 cells/cm^2 = 50,000,000 cells/wound; etc.) (Figure 3).

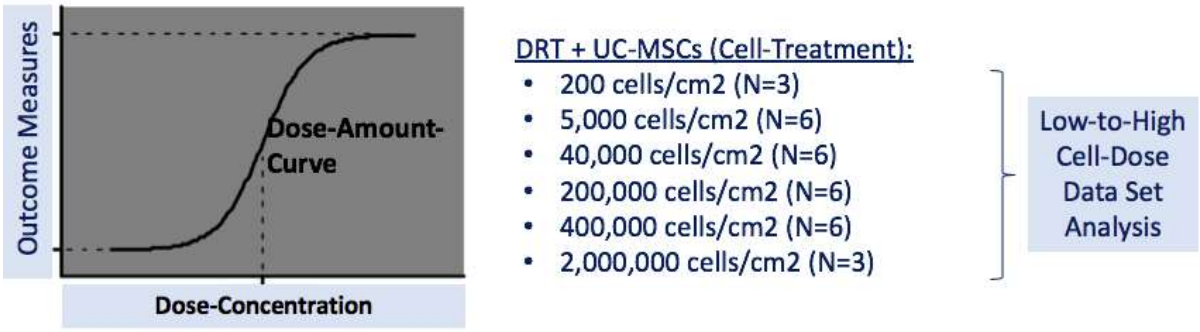

Figure 3: Creation of a low-to-high cell dose model.

Wound dressing changes, biopsies

All wound dressing changes and biopsies took place with the above-described general anesthesia method and under sterile conditions. Wound dressings were changed 3 times/week in the first 2–3 weeks until the wounds were granulated with signs of progressed wound healing. This was followed by dressing changes 2 times/week until the end of the experiment. Dressing layers consisted of the following materials: Polysporin® cream, followed by Jelonet®, on a layer of wet gauze; multiple layers of dry gauze (optional Tegaderm® transparent film dressing); cotton towel staples and an animal compression jacket suit (Compression Cl. 1). Full-tissue punch biopsies with a size of 4 mm (diameter), including the whole (epi-)dermis, part of the subcutis as well as fascia and muscle tissue depending on the healing progress, were taken regularly from the wound centers in a rotatory schemata (Figure 2), and from the wound center on day 28. The skin biopsies were first fixed in formalin and changed afterwards to 70% ethanol before processing and embedding the sample in paraffin for further analysis.

Pig`s health score assessment

Pigs were assessed for systemic (everyday) and local wound site complications (at each dressing change) according to our protocols. Assessments and health scoring were performed by our research group and additionally by an animal technician in the research facility.

Briefly, we assessed for local complications, such as (1) bleeding out of the wound site, (2) wound infections, (3) wound secretion, (4) edema, (5) detachment of the skin substitute scaffold, and (6) scar and/or contracture formation. Additionally, an assessment for systemically complications was performed on a daily basis with a standardized health-scoring system, which consisted of animal research pupil size and reactivity, activity, posture, food intake, and hydration. Each item was scored from 1-5, with 5 indicating the absence of problems. The scores of the 5 items were added up to a maximum score of 25, indicating a healthy, active and well-nourished pig. In addition, we assessed for respiratory distress, fever and any signs of abnormal behavior that might indicate systemic complications, such as shivering and abnormal behavior towards humans or other pigs; plus, an assessment for post surgical complications was performed without finding any deviations from the normal course using the Clavien-Dindo-Classification (Dindo et al. 2004).

During our experiments no adverse events occurred. All investigated animals maintained their health during the entire procedures and experiment.

Endpoints

The primary endpoint of wound healing after mesenchymal stromal cell treatment was wound closure – either fully epithelialized and/or almost epithelialized wounds on day 28, as per the definition in the remodeling phase (Gurtner et al. 2008). In comparison, human endpoints for wound healing are therapy refractory wounds with no infection, no pain and no distress, such as persistent hemorrhage, wound secretion or ambulatory difficulty.

At the termination of the experiment, chemical euthanasia was performed on the pigs by the animal staff under general anesthesia using phenobarbital IV (euthanyl 100-200 mg/kg iv.). Treated wounds were excised and processed.

Study Assessment, Outcome Measurement Analysis

Safety Assessment of the treatments

A safety assessment of the treatment was made in accordance with the guidelines for Wound Healing Assessment (UK, 2010) (Fletcher 2010). The general condition of the investigated pigs

was assessed, as well as the precondition of the wounds, any complications, a wound assessment before and after the burn and wound treatment, the safety of the treatment, time and sterility and an overall rating for any condition.

Outcome Measurement Analysis

The main outcome measures to determine skin regeneration and wound healing of this study are based on macroscopical findings of epithelialization (cm2 in %/wound) and Vancouver Scar Scale (Vancouver Scar Scale, VSS), as well as on the following histological markers: epidermal thickness (µm), collagen formation, integrated density (unit/µm2), neovascularization, CD31 (positive vessels/unit), fibrosis, aSMA, integrated density (positive cells/unit/µm2), type 1 macrophages, CD11b at the epidermal border region and in the dermis (positive cells/unit/µm2), and type 2 macrophages, CD163 at the epidermal border region and in the dermis (positive cells/unit/µm2).

Macroscopical assessment (Photography)

Photographs of the wounds were taken on day 0 and day 28 with an iPhone 5SE, using the ruler of a scalpel for scale on each photo. Images were transferred to a computer and have been analysed using an imaging software (Image J Version 1.51 for MAC).

Evaluation was made by measuring epithelialization area/image of each wound, using the initial burn excision wound size (on day 0) as reference and sparing the non-epithelialized area (on day 28), using the formula [(area without epithelialization in cm^2 on day 28 x 100)/initial wound size in cm^2 on day 0)] (Figure 4).

Furthermore, scarring was assessed using an established clinical scar scale – the Vancouver Scar Scale (VSS, assessing vascularity, pigmentation, pliability and height), which was introduced in 1990 (Sullivan et al. 1990). It is the most recognized and validated (Finlay et al. 2017) scar scale in burn care (Fearmonti 2010; Zuo et al., 2019; Idriss & Maibach 2009), and has been used previously for skin graft assessment (Zuo et al., 2019b; Cheng & Eylert et al. 2020; Eylert et al. 2021). The VSS can be assessed without the need of interviewing the patient (pig). One drawback is that the scale does not include the parameter of pruritus, which other scar scales also lack (Fearmonti 2010). Evaluation for scarring was performed by two external blinded researchers in plastic surgery research. (Figure 4).

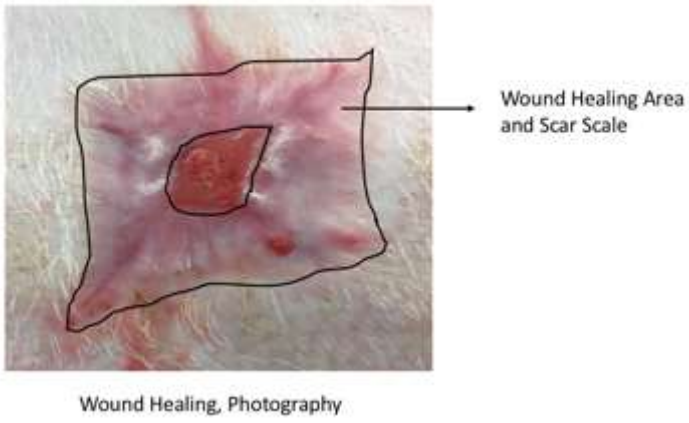

Table 2. *The Vancouver Scar Scale*

Scar characteristic		Score
Vascularity	Normal	0
	Pink	1
	Red	2
	Purple	3
Pigmentation	Normal	0
	Hypopigmentation	1
	Hyperpigmentation	2
Pliability	Normal	0
	Supple	1
	Yielding	2
	Firm	3
	Ropes	4
	Contracture	5
Height	Flat	0
	<2 mm	1
	2-5 mm	2
	>5 mm	3
Total score		**13**

Figure 4: Wound Healing Analysis, Scar Assessment. (left) Schematic wound on day 28 (photography), with measurement of the inner circle – the nonepithelialized area. The outer circle indicates the scar which was analysed using the Vancouver Scar Scale (VSS) (right). (Eylert 2019)

Assessment of the histology

Skin biopsies were assessed using histological samples, which were taken on day 28 from all centers of the wounds. The tissue was immediately fixed in 10% formalin, changed to 70% ethanol (EtOH), embedded in paraffin and cut into 5 µm sections. Histology was stained according to protocols. All histological tissue samples were first scanned via Leica light microscope (LEICADM 2000 LED) on three positions of each tissue sample according to a protocol (location and depth depending on the staining of interest) (Position 1, P1, etc.) (Figure 5) at the epidermis/epidermal border and in the dermis (measuring from the epidermis 2000 µm toward deep dermis). Second, these images were assessed by two blinded individuals. The three positions were averaged for one value per location and sample. An imaging software (Image J Version 1.51, Fiji Version 2.0.0 and Plug-Ins for MAC) was performed by two researchers for special analysis of the images.

The evaluation for the scanned images with the imaging software was performed as followed after setting the scales. The thickness of the epidermis was measured with the ruler function (µm) (Amini-Nik et al., 2018; Cheng & Eylert et al. 2020; Eylert et al. 2021); for collagen formation, the integrated density was measured (unit/µm2), extracted with the plug-in for Masson's Trichrome, and a binary was created while measurement of the integrated density was performed (Brianezi et al. 2015; Cheng & Eylert et al. 2020; Eylert et al. 2021); for neovascularization, a positive vessel for CD31 positive cells with a lumen was counted and an anatomical structure was counted once (Ertl et al. 2018; Ryan 1976) (positive vessels/unit); for fibrosis, the

positive aSMA cells were measured, after extracting with a colour deconvolution plug-in for the red/brown channel (H&E DAB) was taken, a binary was created and the integrated density was measured (positive cells/unit/µm2) (Brianezi et al. 2015); and for the inflammatory cell assessment, positive cells for type 1 and type 2 macrophages were manually counted and noted, using the wand tool (positive cells/unit/µm2) (Schliefsteiner et al. 2017).

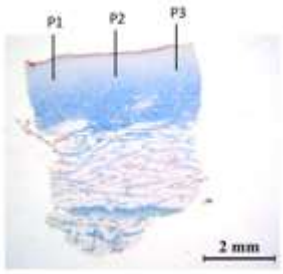

Figure 5: Histology Example. Analysis/imaging of multiple locations of each sample (Picture 1, P1, Picture 2, P2, Picture 3, P3). (Eylert 2019)

Masson`s Trichrome

Paraffin-embedded slides were dewaxed through CitriSolv and rehydrated through grades of ethanol for staining (Electron Microscopy Sciences). Samples were kept overnight in Bouin`s solution (Electron Microscopy Sciences, #26386-01) at room temperature, was were washed and stained with Weigert`s iron hematoxylin (A, B, Electron Microscopy Sciences, #26320-03, 26320-04) working solution (Sigma-Aldrich), Biebrich scarlet-acid fuchsin solution (Electron Microscopy Sciences, #26033-25), phosphomolybdic-phospho-acid solution (Electron Microscopy Sciences, #26364-01, 26356-05), aniline blue solution (Electron Microscopy Sciences, #26693-04), and they were washed multiple times and refreshed in acid acidic (1%), until fixated by rehydration and citrosol. After, the slides were mounted, and scanned via microscope and analyzed with an imaging software.

Immunohistochemistry

For immunohistochemistry, slides were deparaffinized and rehydrated for staining. First, antigen decloaking was performed with a pressure cooker at 110 °C for 4 min for antigen retrieval. Afterwards, samples were blocked with 3% H2O2 for 10 min. before antibody incubation overnight. The following antibodies were used: CD11b (ab133357, rabbit monoclonal, Abcam), CD163 (ab87099, rabbit polyclonal, Abcam), CD31 (ab28364, rabbit polyclonal, Abcam) and aSMA (ab18415, mouse, monoclonal, Abcam). Antibodies were visualized through HRP probe and polymer detection kits (Biocare) for either mouse or rabbit, followed by a betazoid DAB

chromogen kit (DAKO, Biocare). Slides were counterstained with hematosylin (Electron Microscopy Sciences), dehydrated and mounted with xylene-based mounting medium. Stained slides were scanned, and positively stained cells/structures were then quantified and measurements were performed using standardized protocols at the region of interest.

Statistics

After summarizing the data set, each outcome measures was analyzed descriptively (median, interquartile range, IQR, percent %) in the nonparametric data set using Microsoft Excel 2016 for Mac. Graphical presentation was performed using GraphPad Prism Version 8.0 for Mac.
For the graphical presentation of the dose curves and line of best fit the statistical program Python was used. Each graph illustrates a regression (or order 2), and the 95% confidence interval is indicated as the area in light blue (of the raw data set, without normalization).

Chapter 4
Results

The subsection “Creation of comparable conditions for the experiments”, showing that the cells used in this study are mesenchymal stromal/stem cells and the created burns are full-thickness burn wounds, have been published previously(Eylert 2019) and have been modified. The contents in this chapter of this thesis have been partially published previously as follows:

- Cheng & **Eylert** et al., Handheld instrument for wound-conformal delivery of skin precursor sheets improves healing in full-thickness burns. *Biofabrication*, 2020
- **Eylert** et al., Skin regeneration is accelerated by a lower dose of multipotent mesenchymal stromal/stem cells-a paradigm change. *Stem cell research & therapy*, 12(1), p.82, 2021

Overview of results

The aim of this study was to determine the efficacy of low-to-high-doses of mesenchymal stromal/stem cells (200–2,000,000 cells/cm^2) extracted from the Wharton`s Jelly from the umbilical cord, which were incorporated in Integra® to investigate wound healing and skin regeneration. The treatment was compared to an acellular control. Both treatments were applied once on full-thickness burn excised wounds (day 0) and evaluation were made 4 weeks after treatment (day 28), as per the definition in the remodeling wound healing phase, undergoing the initial inflammation and proliferation phase (Gurtner et al. 2008).

The main objectives of this study were to investigate if the transplanted and grafted stem cells on Integra® are present on the wounds, if the cells promote skin regeneration and wound healing and if differences of cell doses in outcome measures for wound healing can be determined. The results of this evaluation have implications for future clinical considerations in the treatment of (burn) wound healing (Figure 6). (Eylert et al. 2021)

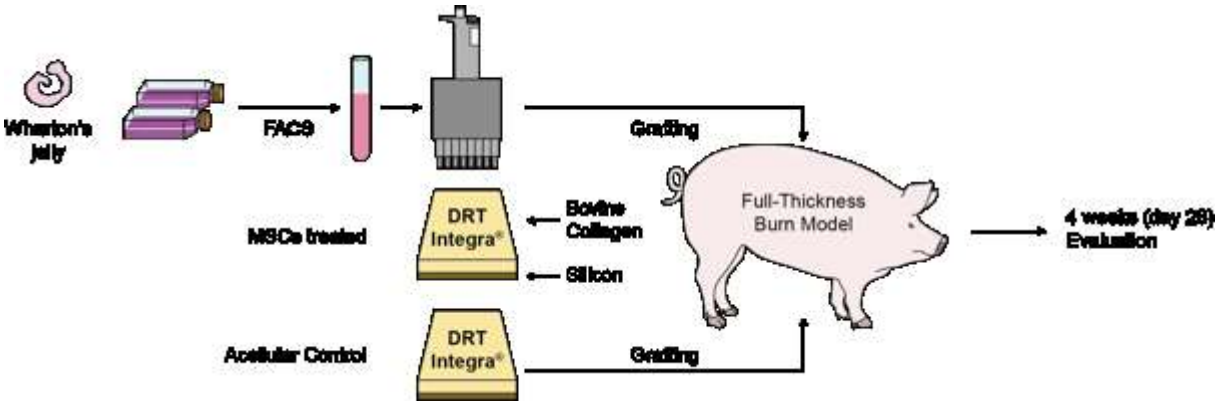

Figure 6: Overview of the experiment. Extraction of mesenchymal stromal/stem cells with following from the Wharton`s Jelly from the umbilical cord. Cells were sorted via flow cytometry and incorporated into the DRT Integra® and grafted on full-thickness inflicted burn excised pig models. Skin regeneration and wound healing were assessed 4 weeks after surgery. (Eylert et al. 2021)

Creation of comparable baseline conditions for the experiments

The creation of comparable baseline conditions for any experiments is detrimental. We therefore used established, published and peer-reviewed protocols for our experiments (Cheng & Eylert et al. 2020; Eylert et al. 2021).

Extracted cells from the Umbilical Cord are Mesenchymal Stromal/Stem cells

The cells were isolated from the Wharton`s Jelly of the umbilical cord and subsequently cultured. The extracted cells were differentiated according to differentiation protocols into the three main mesenchymal lineages: adipogenic, osteogenic and chondrogenic, as shown previously (Cheng et al. 2020; Eylert et al. 2021). Furthermore, the extracted and expanded cells were sorted for MSC surface markers according to the definition of the International Society of Cellular Therapy(Dominici et al. 2006) via flow cytometry (CD73+, CD90+, CD105+, CD11b-, CD19-, CD34-, CD45- and HLA-DR-) as shown previously (Cheng & Eylert et al. 2020; Eylert et al. 2021). This resulted in a sorted MSC population of 98.7%. These cells were than further cultured and expanded for the experiment for incorporation into Integra® (Figure 7).

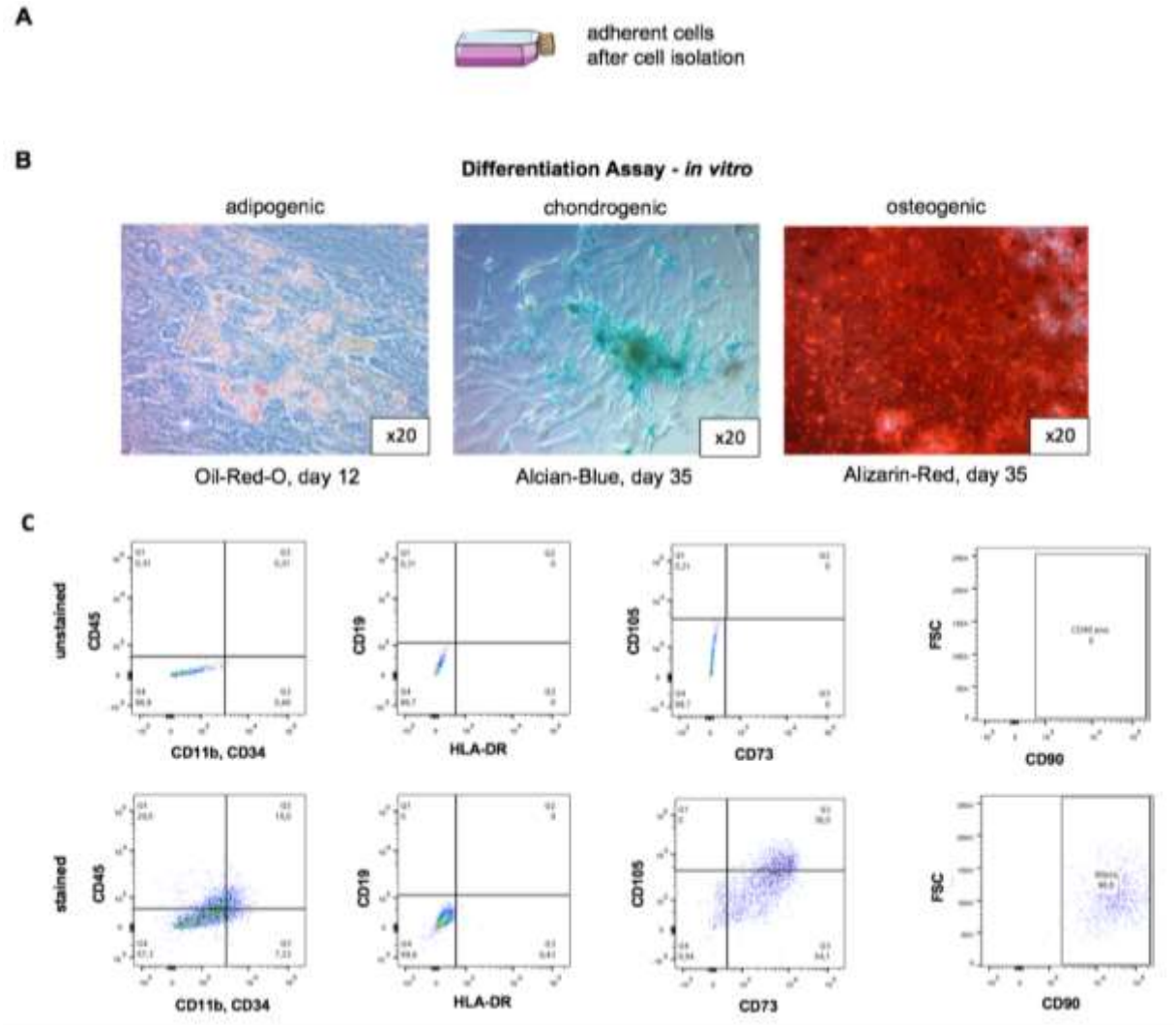

Figure 7 Mesenchymal stromal/stem cell differentiation. (Modified from: Eylert, G. MSc Thesis, 2019.) (A) Cells must first adhere on plastic. (B) Differentiation staining, *in vitro.* MSCs isolated from the Wharton's Jelly differentiating into adipocytes after 12 days with visible lipid

droplets as visualized with Oil-Red-O stain (left), differentiation into chondrocytes after 35 days of culture as visualized with Alcian-Blue (middle) and differentiation into osteocytes with visible calcium, stained with Alizarin-Red (right). (C) Flow cytometry results confirming triple positive stain for CD73, 90 and 105, while indicating as negative for CD34, CD45, CD11b, CD19, and HLA-DR. Upper panel: unstained cells; lower panel: stained cells. (Eylert et al. 2021)

Full-thickness burns are reproducible

The Yorkshire pig burn model has been validated from previous authors as a sufficient full-thickness burn excised wound healing model (Wood et al. 2007; Singer & McClain 2003; Sullivan et al. 2001; Abdullahi et al. 2014; Amini-Nik et al., 2018; Cheng & Eylert et al. 2020). The infliction of a full-thickness burn on the pigs was performed in accordance with all animal welfare guidelines and ethical approvals, according to a protocol from our burn research laboratory in Sunnybrook Research Hospital as previously published (Amini-Nik et al., 2018; Cheng & Eylert et al. 2020). The full-thickness injury was 48 h post burn and confirmed twice via histology using Masson`s Trichrome protocol, which assesses the depth of necrosis, collagen denaturation and microvascular injury (Singer et al. 2016). The thickness of the depth of the burn necrosis (Median 1939, SD 566), the depth of the collagen denaturation (Median 3068, SD 1671) and the depth of the microvascular injury (Median 5893, SD 1680) were reproducible in both models assessed without statistical differences. Furthermore, the induced injuries were similar regardless of the location of the pigs when using our standardized protocol (Figure 8).

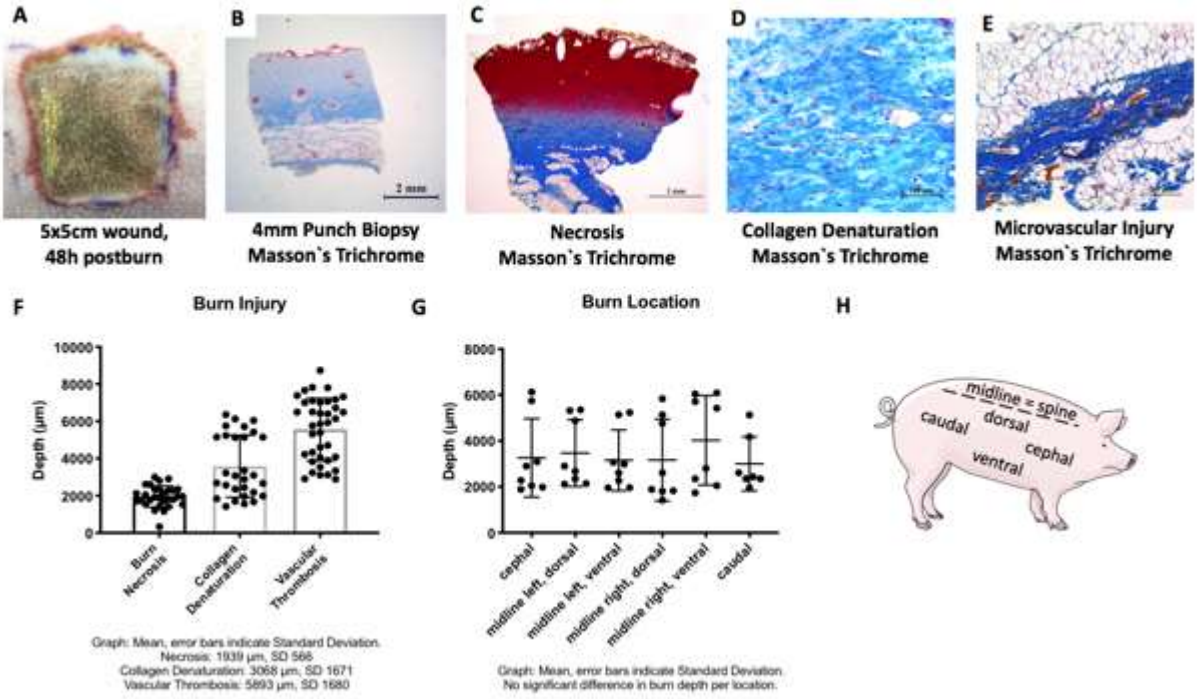

Figure 8: Burn Confirmation. (Modified from: Eylert, G. MSc Thesis, 2019.) (A) Burn wound, 48 h post burn. (B) Representative histology of burn tissue from a 4 mm punch biopsy, 48 h post burn, magnification x 1.25. (C) Necrosis, magnification x 5. (D) Collagen denaturation, magnification x 10. (E) Microvascular injury, magnification x 20. (F) Burn injury with measured depth of parameters. (G) Burn location with measured injury depths. (H) Schematic model of a pig with burn location indicated. (Eylert 2019; Eylert et al. 2021)

Presence of grafted mesenchymal stromal/stem cells on the wounds

The commercially available Integra® was used since it has been demonstrated from our group and others as being a reliable cell carrier for tissue engineering (Amini-Nik et al., 2018; Cheng & Eylert et al. 2020; Spater et al. 2018; Formigli et al., 2015; Fierro et al., 2015; Meruane et al. 2012; Wood et al. 2007; Foubert et al. 2015), allowing cell ingrowth (Hamrahi et al. 2012; Jones et al. 2003) as well as cell differentiation (Morena et al. 2016). Extracted sorted UC-MSCs were incorporated into the DRT with a cell density between 200–2,000,00 cells/cm2 according to our protocol (Figure 9) (Eylert et al. 2021).

Two Integra® treatment wounds were specially assessed for the presence of labeled cells after grafting. Cells were labeled with a lipid cell surface dye (DiO) and seeded with a density of 40,000 cells/cm^2 before incorporation into the DRT. Before incorporation, the dye was tested for cell toxicity. Cell viability was assessed at 12 hours after using the cell labeling dye on sorted MSCs. The cells maintained their viability after labeling and no significant difference

was found in an increase in dead cells compared to unlabeled controls (Figure 9). Tissue biopsies with the incorporated labeled and grafted cells were taken at determined time points at every dressing change on day 2, 4, 7, 9, etc. Labeled cells were present in the wound biopsy on the pig until day 7 in repeated experiments, as demonstrated via flow cytometry. The number of positive detected cells (CD90+, DiO) continually declined over time until day 7 (Figure 9). (Eylert et al. 2021)

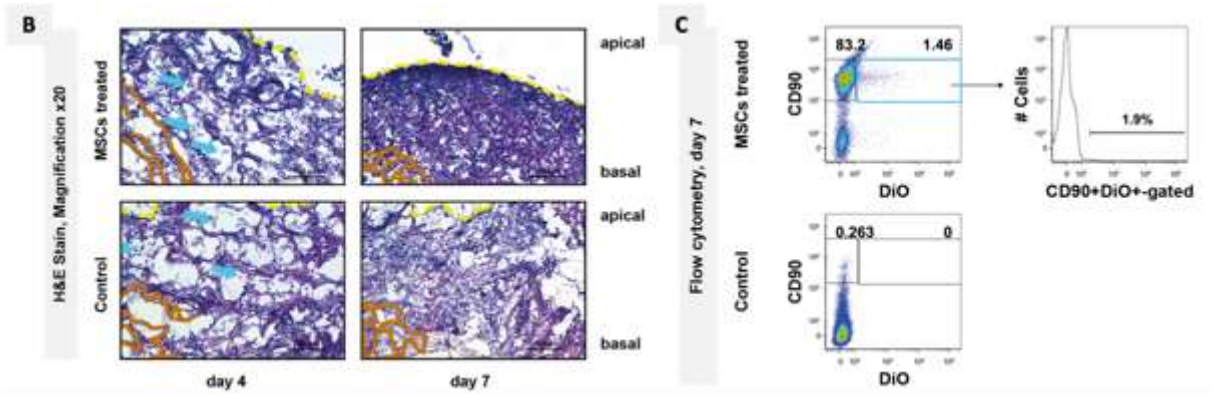

Figure 9: Cell viability after labeling cells with DiO, DRT cell infiltration and DiO detection via flow cytometry. (A) Live-dead-staining 12 hours after flow cytometry of MSCs sorting for surface markers, and DiO-labeling, confocal microscope, magnification x 20. (1, 4) Live cells (calcein) (green channel), (2, 5) dead cells (EthD) (red channel) and (3, 6) merged. (B) H&E stained DRT after tissue biopsy and tissue preparation, on day 4 and 7, magnification x 20. The dark yellow colored dotted line indicates the upper border from the Integra® scaffold. The Integra® scaffold in violet stained (as seen in both images on day 4). The brown line at the left bottom image border indicates the Integra® scaffold. The blue arrows indicate cells. (C) Flow cytometry on day 7 after tissue biopsy and tissue preparation with a double positive cell signal of a cell surface dye (DIO) on CD90+ cells. (Eylert et al. 2021)

Skin tissue regeneration after Integra® treatment

The following graph illustrates the typical appearance seen in the histology over the time course of 4 weeks. The acellular control lags behind in regeneration compared to the cellularized scaffold, as seen on the prolonged time in the acellular control to degraded the bio-degradable Integra®. In the acellular control, the DRT was not fully degraded on day 28. Cell migration subjectively occurred faster in the cellularized scaffold compared to the acellular control with a superior architecture in skin regeneration (Figure 10).

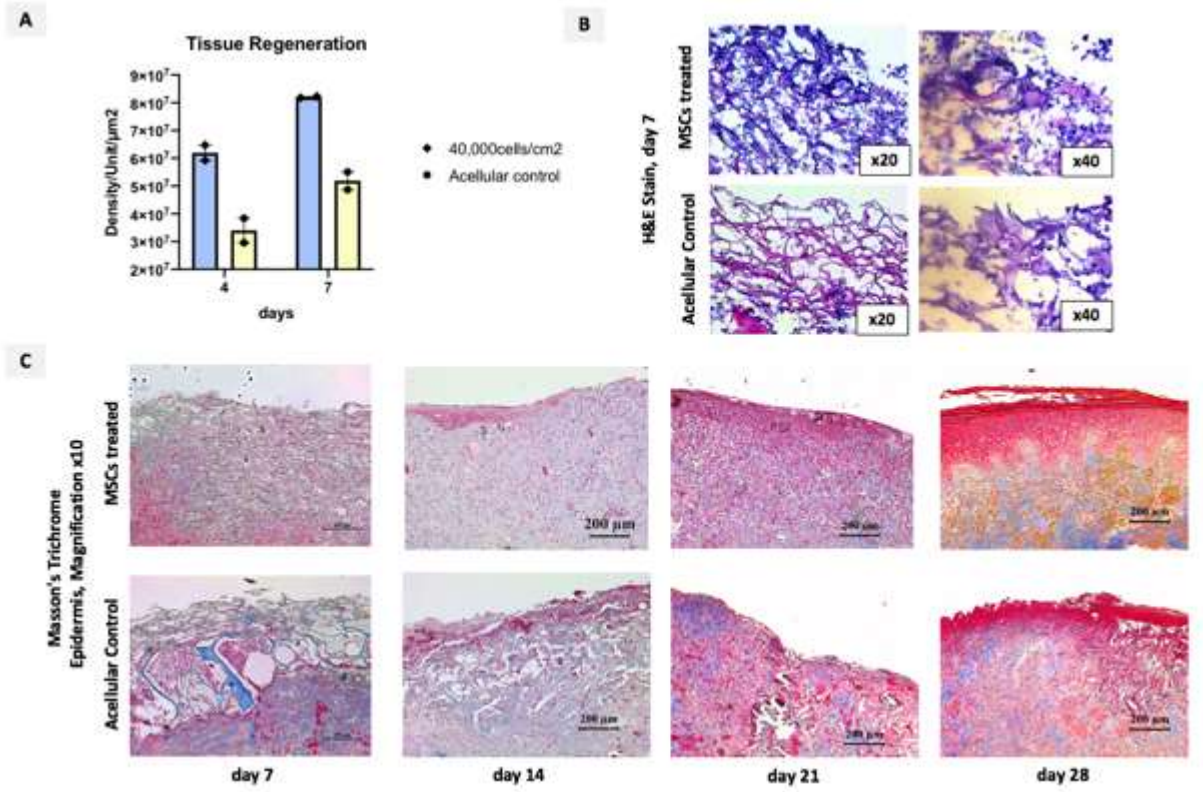

**Figure 10: Tissue regeneration, H&E stain, and Masson`s Trichrome staining histology.** (A) Graph, tissue regeneration measured in density/unit/µm2. (B) H&E Stain, day 7, magnification x 20 and x 40. (C) Masson`s Trichrome staining of histology on day 7, 14, 21 and 28. Magnification x 10.

Mesenchymal stromal/stem cells therapy enhances skin regeneration and wound healing

The newly cellularized Integra® sheets were grafted on full-thickness excised burn wounds, and tissue regeneration was assessed on day 28. To determine the efficacy of the seven applied treatments, 10 wound healing outcome measures were used. The mesenchymal stromal/stem cell treatments were compared to the acellular control, which is currently used as a gold standard in the clinic.

The following descriptive data set illustrates the different measured macroscopical and histological outcomes shown with medians and interquartile ranges (Figure 11, B). In general, the majority of the MSCs-treated groups regenerated the wounds superiorly compared to the acellular control when looking at each outcome measure separately.

A comparison assessment between acellular and cellularized treatment was made using a simple ranking system (1–7 treatments, where 7 = best, 1 = worst) based on the medians. The graph illustrates the MSCs dose concentrations in an ascending manner and the summary of the

ranked outcome parameters of the medians (Figure 11, A). All MSCs-treated groups using between 200–2,000,000 cells/cm^2 generated skin regeneration and wound healing better compared to the acellular control. We found the best outcome when using 40,000 cells/cm^2 (62 points), followed by 5,000 cells/cm^2 (52 points), and 200,000 cells/cm^2 (48 points). Furthermore, the lowest dose of 200 cells/cm^2 (43 points), the very high dose of 400,000 cells/cm^2 (32 points) and the highest dose of 2,000,000 cells/cm^2 (26 points) regenerated the skin effectively compared to the acellular control (17 points).

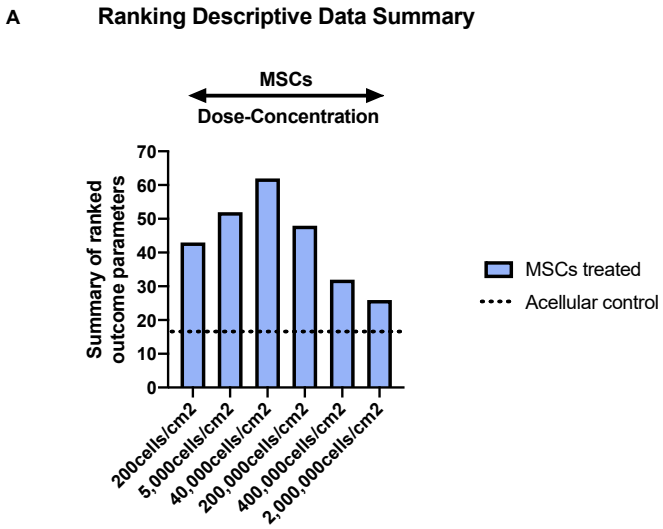

B

low-to-high dose MSCs groups | references

Cell Dose (cells/cm2)	Acellular (N=12)	200 (N=3)	5,000 (N=6)	40,000 (N=6)	200,000 (N=6)	400,000 (N=6)	2,000,000 (N=3)	Healthy Skin (N=9)	Burn alone (N=4)
Epithelialization Area (%)	92 89-95	91 88-92	96 91-97	95 89-96	88 87-89	86 84-86	81 69-87	100 100-100	51 47-52
Vancouver Scar Scale (VSS)	8 7-10	6 5-9	8 7-8	6 6-7	8 7-8	8 7-8	6 4-9	0 0	12 12-13
Epidermal Thickness (Epidermis)	177 64-383	104 77-237	284 205-286	189 132-262	157 99-198	131 116-149	201 158-262	165 159-182	63 49-75
Collagen Formation (Dermis)	490K 464-605K	639K 579-720K	554K 525-605K	539K 512-627K	567K 527-590K	513K 475-571K	551K 524-607K	924K 892-1,077K	400K 249-567K
Neovascularization (Dermis)	7 6-10	12 11-26	13 10-21	17 12-17	15 12-16	19 15-23	13 10-14	17 13-18	8 6-12
Fibrosis (Dermis)	412K 386-485K	41K 23-64K	37K 36-40K	30K 27-39K	31K 29-34K	37K 31-45K	64K 46-71K	6K 6-8K	548K 519-569K
Type 1 Macrophages (Epidermal border)	17 10-30	12 5-15	12 7-18	8 6-11	15 14-16	22 21-35	37 31-44	5 5-7	63 48-74
Type 1 Macrophages (Dermis)	32 15-49	9 6-16	9 8-10	7 6-11	14 10-22	15 13-24	36 8-50	5 5-7	63 44-77
Type 2 Macrophages (Epidermal border)	68 48-72	25 16-54	10 9-20	12 8-24	26 17-31	31 26-27	52 38-55	4 3-5	65 55-76
Type 2 Macrophages (Dermis)	68 34-72	33 22-54	8 6-13	12 4-29	31 25-34	34 29-46	46 19-51	2 2-3	78 65-87

Color bar: best (healthy) — current therapy (acellular) — worst (burn)

Figure 11: Ranking assessment, descriptive data summary of the study. (A) Ranking assessment. A comparison using a simple ranking system (1–7 treatments, where 7 = best, 1 =

worst) was made based on the medians between acellular and cellularized treatment. (B) Summary of the descriptive data. Data are expressed in median and interquartile range (IQR). K indicates 1,000. Heat-color-map: dark blue indicates healthy skin as the physiologic and best condition. Lighter blue shades are first, second and third best, respectively. The light yellow shaded color indicates the acellular control, which is the current treatment standard used in the clinic. Everything from yellow to dark orange indicates a worse outcome compared to the acellular control. Orange indicates a burn alone, the worst condition. (Eylert et al. 2021)

Efficacy of a low-to-high mesenchymal stromal/stem cells treatment

Macroscopical Wound Healing

Epithelialization

Wound healing was assessed via taken photography after four weeks of treatment, as per the definition in the remodeling phase (Gurtner et al. 2008), the last phase of wound healing. The epithelialization area per wound was calculated as [(area without epithelialization in cm^2 on day 28 x 100)/(initial wound size in cm^2 on day 0)]. The MSC-treated groups showed a median between 96%–81% epithelialization compared to the acellular control, with a median of 92% (IQR 89–95). The low dose group with 5,000 cells/cm^2 showed the fastest epithelialization with 96% epithelialization (IQR 91-97), followed by 40,000 cells/cm^2 with 95% epithelialization (IQR 89–96). The lowest dose of 200 cells/cm^2, and high doses of 200,000–2,000,000 cells/cm^2 showed inferior wound healing compared to the acellular control with epithelialization between 81%–91% (IQR 69-92) (Figure 12).

Scarring

Scarring was assessed using the Vancouver Scar Scale (VSS, assessing: vascularity, pigmentation, pliability, and height), which is the most recognized and validated (Finlay et al. 2017) scar scale (Fearmonti 2010; Zuo et al., 2019) and has been used previously for skin graft assessment (Zuo et al., 2019; Cheng & Eylert et al. 2020; Eylert et al. 2021). The MSC-treated group of 5,000 cells/cm^2 showed the lowest scarring with a median VSS of 6 with the narrowest interquartile range (IQR 6–7). The highest dose of 2,000,000 cells/cm^2 (IQR 4–9) and the lowest dose of 200 cells/cm^2 (IQR 5–9) both had the same median VSS of 6. The other MSC-treated groups of 5,000, 200,000 and 400,000 cells/cm^2 showed a median VSS of 8 (all IQR 7–8), compared to the acellular control with the same median VSS of 8 (IQR 7-10). Overall, the MSC-treated groups appeared less inflamed, with a more homogenous scar texture. The lowest

and the highest dose had a sample size of N = 3, while the other dose groups had N = 6 (Figure 12).

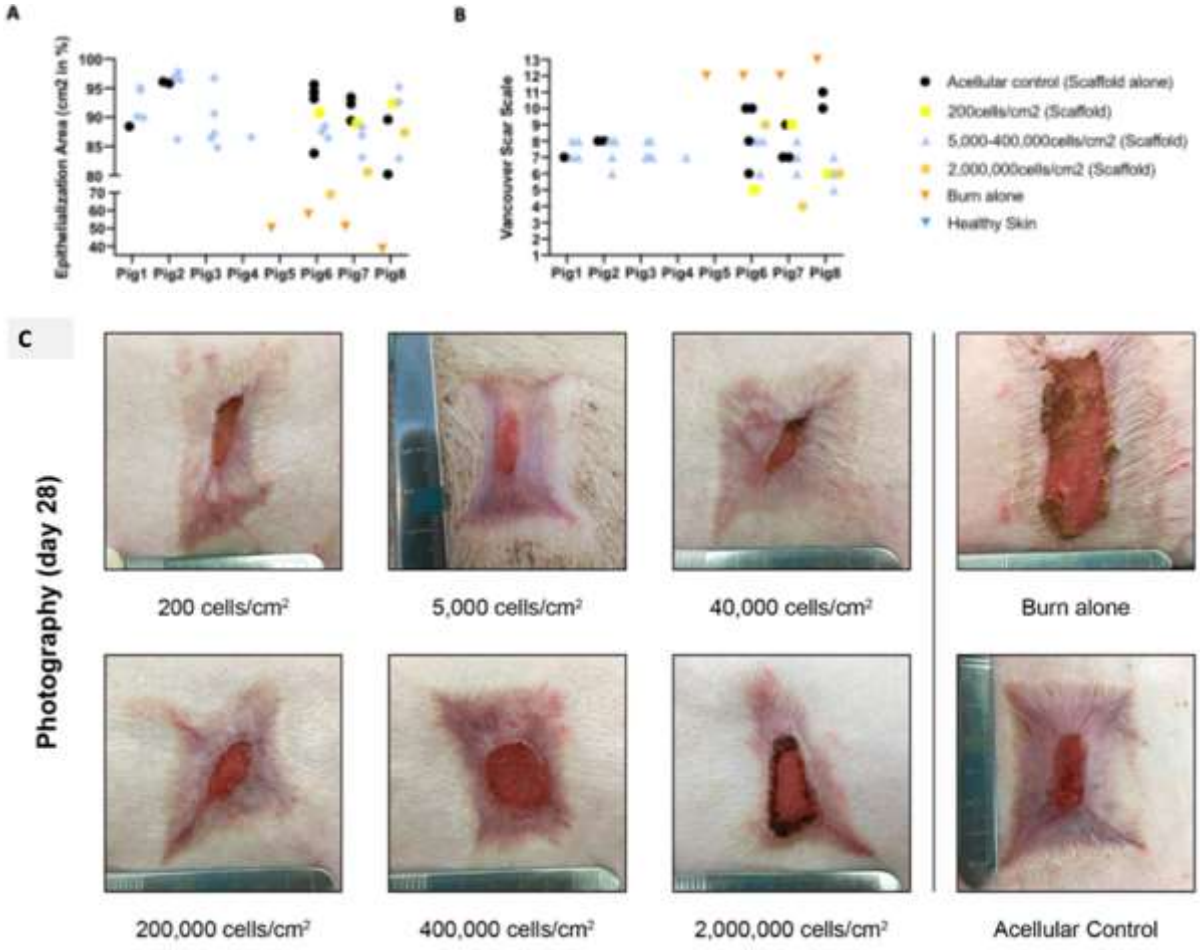

Figure 12: Data distribution, macroscopical wound healing. (A) Epithelialization area (cm^2 in %). (B) Vancouver Scar Scale. (C) Photography of macroscopical wounds on day 28 from the initial 5x5 cm full-thickness burn excised wounds. (Eylert et al. 2021)

Epidermal Regeneration

Epidermal Thickness

Histological assessment was performed accompanying the macroscopical assessment also four weeks after surgery, where tissue biopsies from the wound centers were taken and stained after Masson`s trichrome protocol. For references, healthy porcine skin representing the physiological/natural condition had a median of 165 µm (IQR 159–182 µm), and burn wounds, without any treatment, had a median of 63 µm (IQR 49–75 µm). Hypo- and hyperplasia were defined as inferior and superior epidermal thickness, respectively, from the interquartile range of the healthy skin. The most effectively regenerated epidermal thickness was achieved by the dose

of 200,000 cells/cm^2 with a median of 157 µm (IQR 99-198), followed by the dose of 40,000 cells/cm^2 with a median of 189 µm (IQR 132-262), and the dose of 400,000 cells/cm^2 with a median of 131 µm (IQR 116-149). The acellular control showed a median of 177 µm (IQR 64-383 µm), although it lagged in epidermal regeneration and demonstrated a high range of hypo- and hyperplastic epidermal thickness (64-383 µm), where the Integra® scaffold was incompletely degraded by day 28. The DRT was visible in none of the MSC-treated groups. The dose of 5,000 cells/cm^2 showed a median of 284 µm (IQR 205-286 µm) and, according to the reference, it was defined as epidermal hyperplasia, although the histology showed overall a very homogenous epidermal regenerated architecture with rete ridges comparable to the other MSC-treated groups. (Figure 13, A)

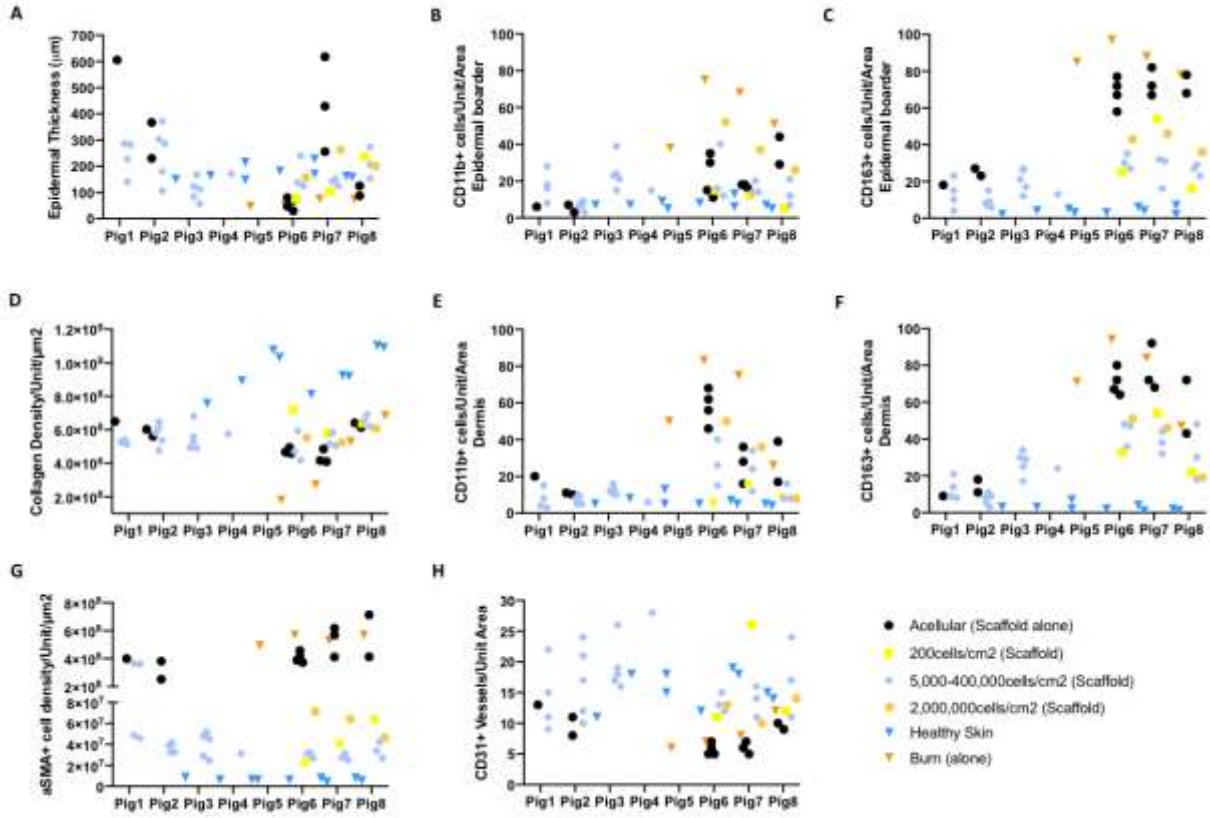

Figure 13: Data Distribution, outcome measures. (A) Epidermal thickness (µm). (B) CD11b pos. cells, type 1 macrophages per unit/image, epidermal border. (C) CD163 pos. cells, type 2 macrophages per unit/image, epidermal border. (D) Collagen formation with density per unit/image (µm^2). (E) CD11b pos. cells, type 1 macrophages per unit/image, dermis. (F) CD163 pos. cells, type 2 macrophages per unit/image, dermis. (G) Density of positive alpha-smooth muscle actin cells (a-SMA) per unit/image (µm^2). (H) Neovascularization with vessels with CD31 pos. endothelial cells per unit/image.

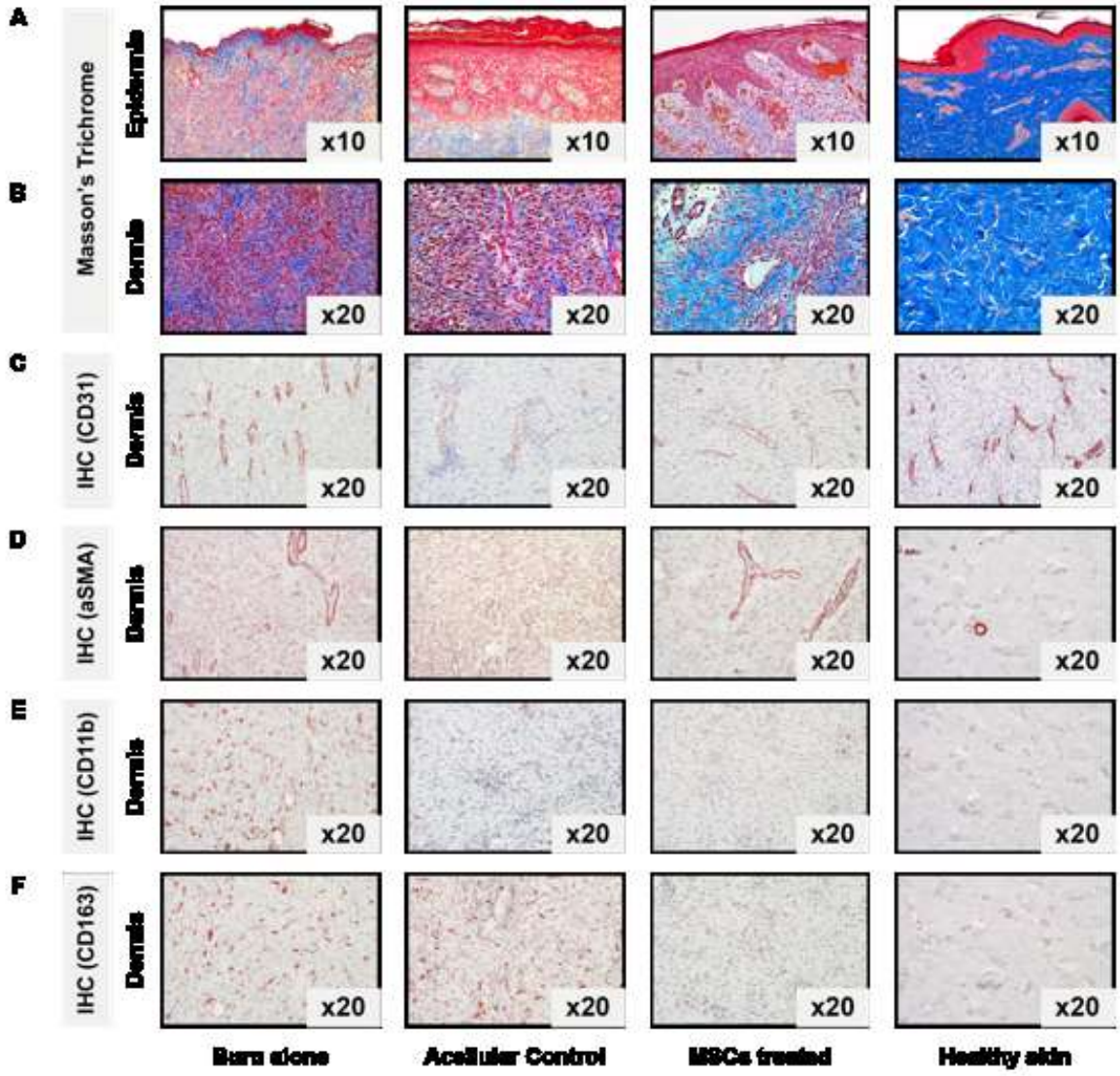

Figure 14: Epidermal and Dermal Regeneration. (A, B) Masson`s Trichrome stained epidermis with magnification x 10 and dermis with magnification x 20. (C-F) Immunohistochemically stained dermis with CD31 (C), a-SMA (D), CD11b (E), CD163 (F) with magnification x 20. (Eylert et al. 2021)

Appendages

After a severe burn injury, healed wounds leak appendages (Binghui Li et al. 2019), which is problematic for patients with, the example, the inability to transpire. The DRT with its structure allows cell ingrowth and has been shown in full-thickness burn healing to achieve regeneration of adnexal structures, such as hair follicles (Navsaria et al. 2004). This adnexal neoformation originates from the epithelial lining (Binghui Li et al. 2019; Biedermann et al. 2010; Dekoninck & Blanpain 2018) and may be attributed from the cell plasticity and neogenetic/regenerative

capability of the upper dermal fibroblastic lineage (Belokhvostova et al. 2018). In addition, (umbilical cord) mesenchymal stem cells have the ability to regenerate hair follicles sufficiently as previously shown (Sabapathy et al. 2014).

In healthy porcine skin, as reference, four different types of appendage structures were identified, such as hair follicles and the associated arrector pili muscle, sebaceous and eccrine glands. In the burn wounds, no adnexal structure was seen at any time point, presumably due to the necrotic tissue, which was scaled apart, leaving only the deep fibrotic tissue attached. In our evaluation we found in eight cellularized MSC-treated wounds (26.7%) and in one acellular control wound (8.3%) adnexal structures on day 28 in the histology. The majority in the MSC-treated group were hair follicles, but sebaceous and eccrine glands were seen as well, compared to the acellular control which showed only one single hair follicle. The adnexal neoformation was found in all treatment groups (5,000-2,000,000 cells/cm^2) except in the lowest dose with 200 cells/cm^2 (Figure 15).

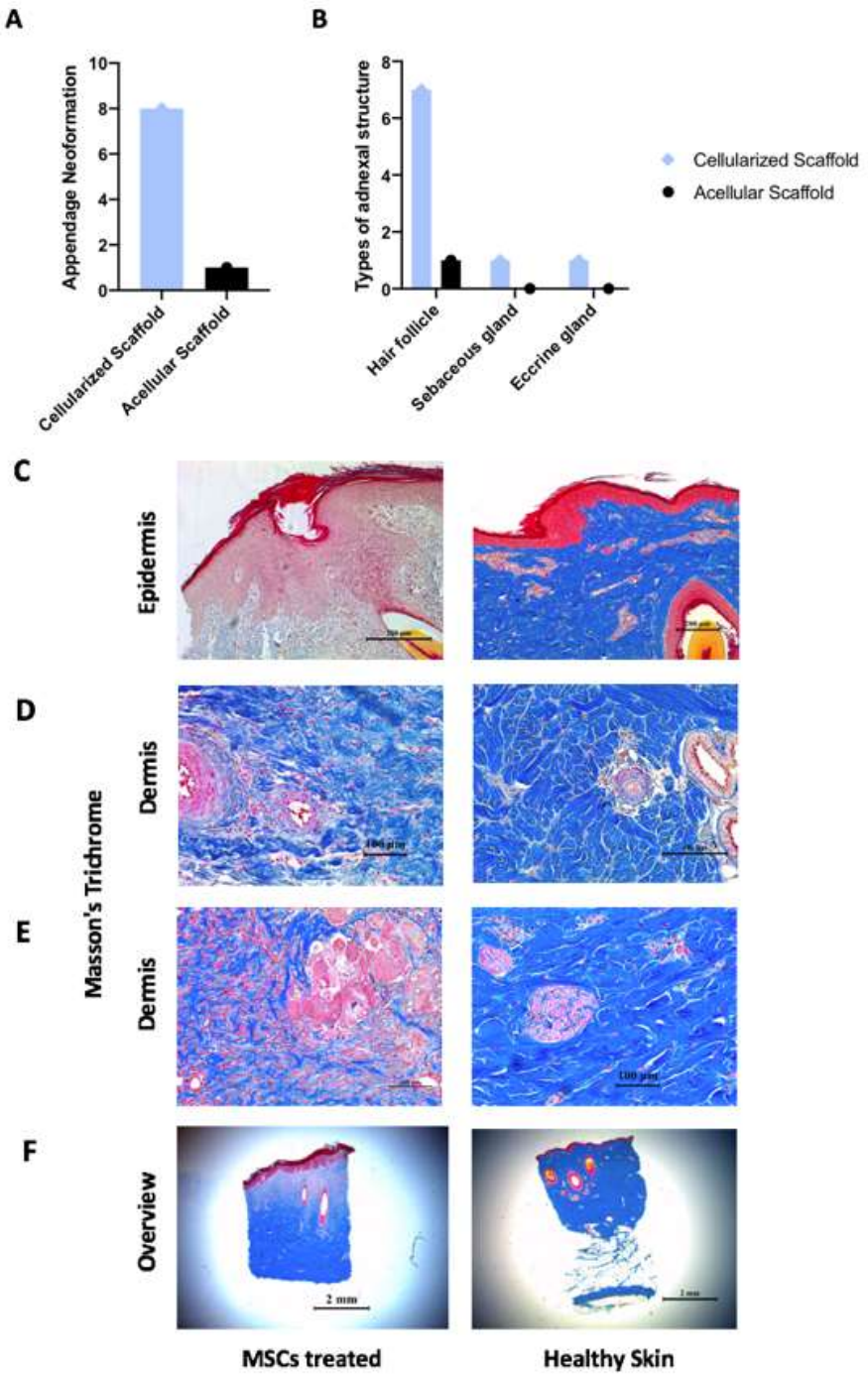

Figure 15: Appendages, Neoformation. (A) Graph, appendage neoformation. (B) Types of adnexal structures. (C–F) Histology, Masson`s Trichrome Staining, on day 28. (C) Hair follicle, magnification x 10. (D) Eccrine gland, magnification x 20. (E) Sebaceous gland, magnification x 20. (F) Overview, in the MSC-treated group, two embedded hair follicles were observed in the dermis, and in the healthy skin, hair follicles, eccrine and sebaceous glands were embedded in the dermis. Magnification x 1.25.

Dermal Regeneration

Collagen Formation

Dermal regeneration was evaluated by measuring the collagen density with an imaging software, where stained collagen fibers were extracted from digitized histology(Brianezi et al. 2015). All MSC-treated groups regenerated more collagen compared to the acellular control. Within the dose groups, the dose of 200 cells/cm^2 reached the highest collagen density (median 639K, IQR 579-720K), followed by 200,000 cells/cm^2 (median 567K, IQR 527-590K) and 5,000 cells/cm^2 (median 554K, IQR 525-605K). The acellular control reached the lowest collagen density (median 490K, IQR 464-605K) (Figure 12, 13).

Neovascularization

The tissue was also stained via immunohistochemistry for the specific endothelial marker CD31, which is indicative of neovascularization. Measurements were performed by counting each vessel with a lumen. Anatomical structure was counted once (Ertl et al. 2018; Ryan 1976). All MSC-treated groups showed higher neovascularization compared to the acellular control. Within the different dose groups, the dose of 40,000 cells/cm^2 showed the same vessel count of 17 (IQR 12–17) compared to the healthy skin (median 17, IQR 13–18). Closest to the reference, the dose of 200,000 cells/cm^2 showed 15 vessels (IQR 12–16), followed by 400,000 cells/cm^2 with 19 vessels (IQR 15–23). The acellular control regenerated 7 vessels (IQR 6–10) (Figure 12, 13).

Fibrosis

In a fibrosis assessment, positive alpha smooth muscle cells (a-SMA) were stained and measured with imaging software after extraction and an adjusted density assessment (Brianezi et al. 2015). All MSC-treated groups showed a lower positive a-SMA cell density compared to the acellular control (median 412K, IQR 386-485K). We found the lowest fibrotic appearance with lowest positive a-SMA count in the 40,000 cells/cm^2 (median 30K, IQR 27-39K) dose group, followed by 200,000 cells/cm^2 (median 31K, IQR 29-34K), and 5,000 cells/cm^2 (median 37K, IQR 36-40K) (Figure 12, 13).

Inflammation

The tissue was also stained for positive inflammatory markers. Due to the high cross-reactivity of the antibodies in the pig tissue, finding reliable markers for macrophages was challenging. However, a clear signal was found for CD11b and CD163. CD11b is a pan-macrophage marker,

which is expressed on a variety of leukocytes and is upregulated on activated cells, including type 1 macrophages (Eming et al. 2007; Schliefsteiner et al. 2017), and it is associated with a proinflammatory state, whereas the CD163 is associated with a state of repair. Due to the tissue showing different patterns of the present inflammatory cells in the remodeling phase on day 28 depending on wound location, the epidermal border region and the dermis were assessed separately to quantify differences. The tissue regeneration occurs from the deep wound bed upwards, similar to the remodeling occurrence of remodeling, and therefore the deep dermis is remodeled earlier than the superficial dermis and epidermis (Figure 12, 13, 14).

The fewest CD11b positive cells were found in the epidermal border region in the wounds with 40,000 cells/cm^2 with a median of 8 (IQR 6–11), followed by 200 cells/cm^2 with a median of 12 (IQR 5–15), and 5,000 cells/cm^2 with a median of 12 (IQR 7–18). The wounds with 400,000 cells/cm^2 showed a median of 22 (IQR 21–35), and the wounds with 2,000,000 cells/cm^2 showed a median of 37 (IQR 31–44), which was higher when compared to the acellular control with a median of 17 (IQR 10–30).

Evaluating the dermal region, the dose of 40,000 cells/cm^2 showed the lowest positive cell count of 7 (IQR 6-11), followed by the dose of 5,000 cells/cm^2 with a median of 9 (IQR 8-10), and 200 cells/cm^2 with also a median of 9 (IQR 6-16) as well. The acellular control showed a lower median of positive counted cells of 32 (IQR 15-49) compared to the highest dose group with 2,000,000 cells/cm^2 with a median of 36 (IQR 8-50). (Figure 12, 13, 14)

Along with the pro-inflammatory marker CD11b, the tissue was stained for CD163, which is a marker expressed on anti-inflammatory and pro-repair cells such as type 2 macrophages (Etzerodt & Moestrup 2013; Tang et al. 2017).

In the epidermal border region, all MSC-treated groups showed a lower positive cell count of CD163 positive cells compared to the acellular control. The wounds with 5,000 cells/cm^2 showed the lowest median of 10 (IQR 9–20), followed by 40,000 cells/cm^2 with a median of 12 (IQR 8–24), and 200 cells/cm^2 with a median of 25 (IQR 16–54), which were lower than the acellular control with a median of 68 (IQR 48–72).

In addition, in the dermal region, all MSC-treated groups showed fewer positive cells than the acellular control with a median of 68 (IQR 34–72). Within the different dose groups, we found the lowest positive cell count when treating wounds with 5,000 cells/cm^2 with a median of 8 (IQR 6–13), followed by 40,000 cells/cm^2 with a median of 12 (IQR 4–29), and 200,000 cells/cm^2 with a median of 31 (IQR 25–34) (Figure 12, 13, 14).

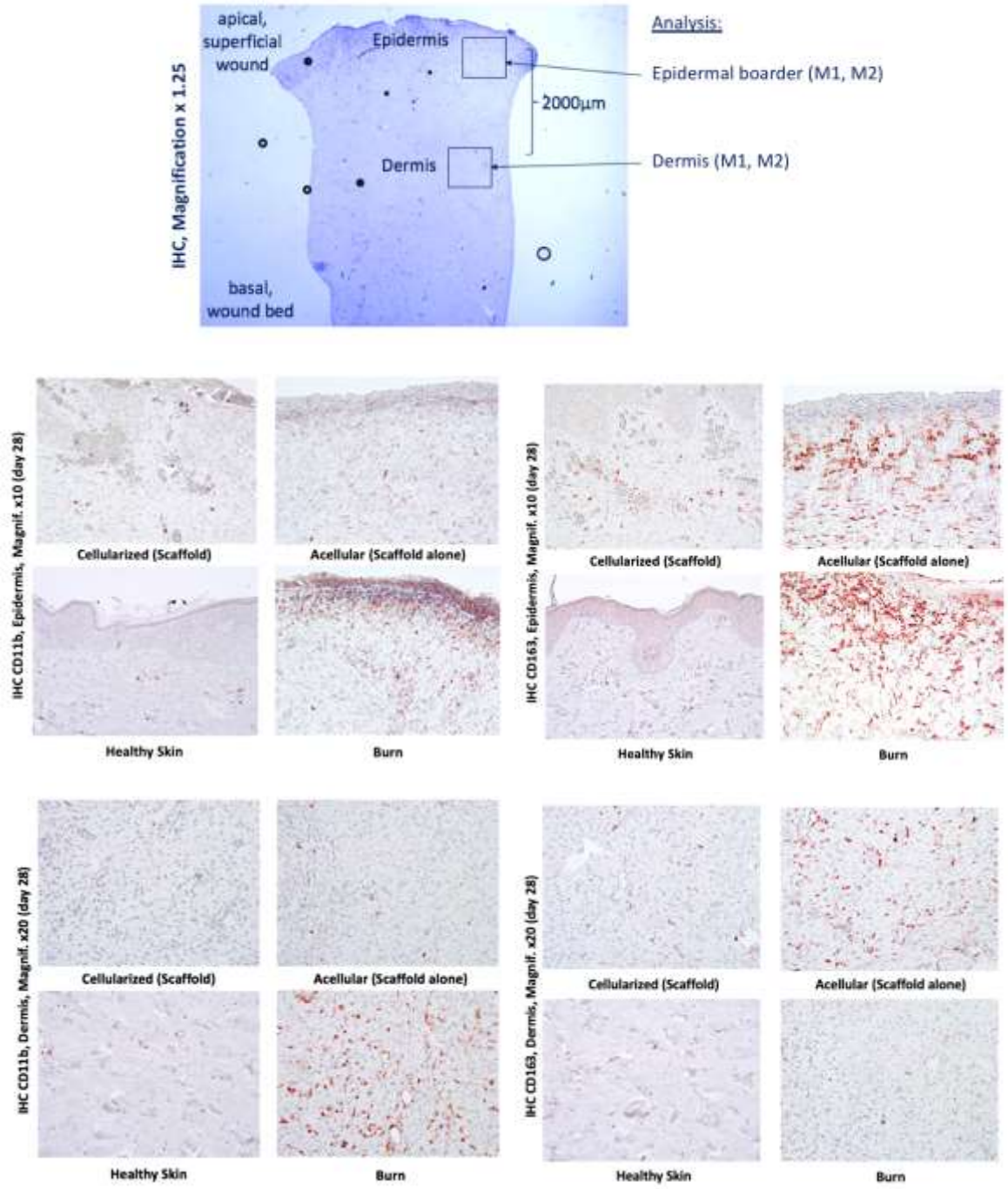

Figure 16: Inflammation. Overview of the assessment of the inflammatory cells – type 1 and type 2 macrophages in the epidermal boarder region and dermis. Immunohistochemically stained epidermis with magnification x 10 and dermis with magnification x 20.

Skin regeneration and wound healing after mesenchymal stromal/stem cell treatment is dose-dependent

The analysis of the outcome parameters suggests a dose-dependent skin regeneration and wound healing phenomenon when utilizing a low-dose. The low dose group range between 200–40,000 cells/cm^2 regenerates the full-thickness wounds most efficaciously, following by

the middle dose of 200,000 cells/cm^2 and 400,000 cells/cm^2, and lastly the extremely high dose of 2,000,000 cells/cm^2 (Figure 17).

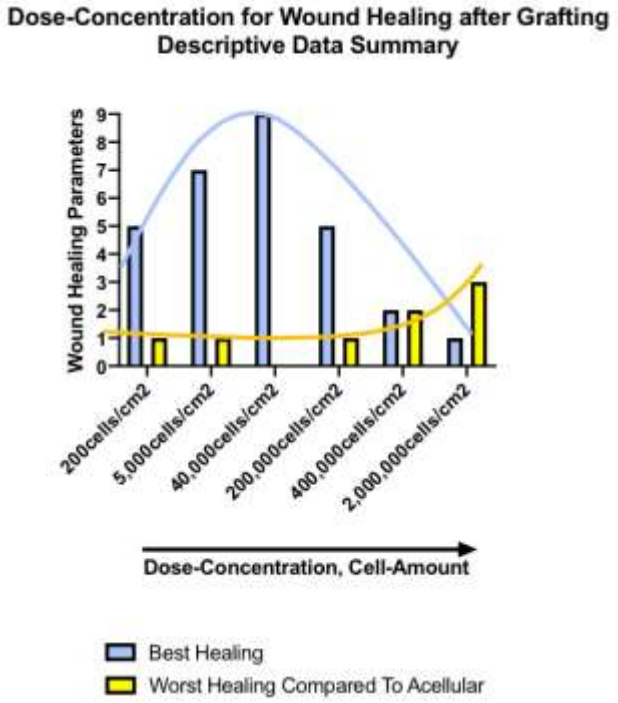

Figure 17: Data summary of the study. (A) Summary of the best outcome measures from the descriptive data set, indicative for best healing (in blue). The worst healing outcomes when compared to the acellular control is shown (in yellow). (Eylert et al. 2021)

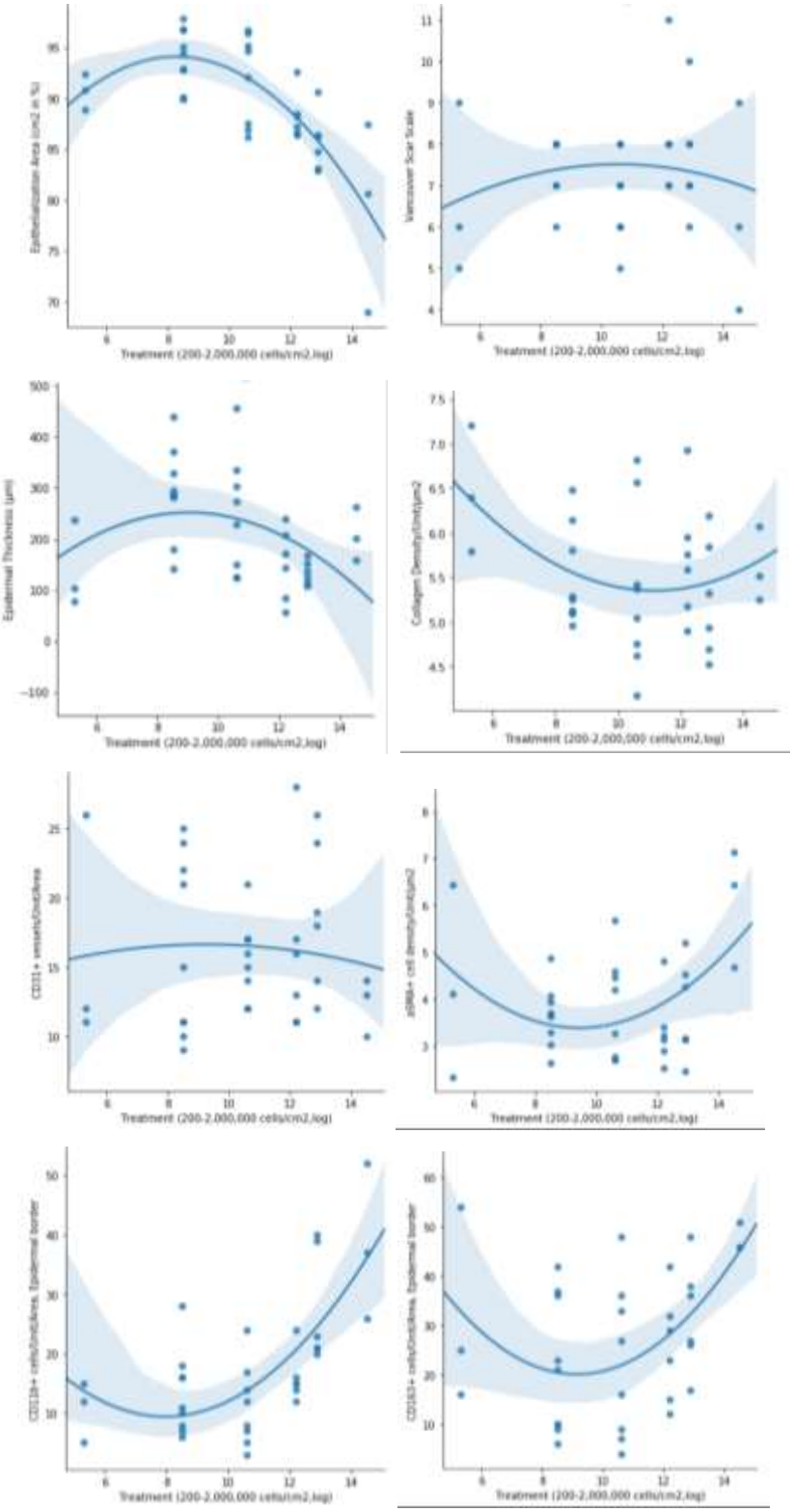
Epithelialization Area (cm2 or %)
Vancouver Scar Scale
Epidermal Thickness (µm)
Collagen Density(Units/µm2)
CD31+ vessels/Units/Area
pSMA+ cell density/Units/µm2
CD11b+ cells/Units/Area, Epidermal border
CD163+ cells/Units/Area, Epidermal border
Treatment (200-2,000,000 cells/cm2,log)

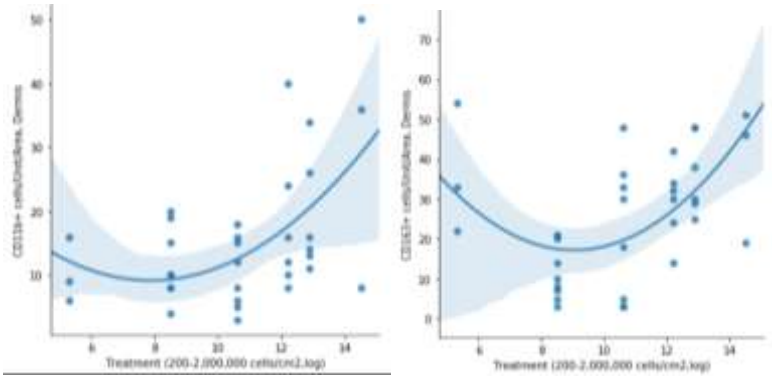

Figure 18: Cell dose curves for each outcome measures. The graphs illustrate at each parameter a plotted dose dependency, as shown on a logarithmic (x-scale, natural log) and with the cell numbers (y-scale, total cell counts) and the confidence-interval (line of best fit, blue) (area in light blue). (Eylert et al. 2021)

Chapter 5
Discussion

The contents in this chapter of this thesis have been partially published previously as follows:

- **Eylert, G**. (2019) MSc Thesis. Bio-Printing of Mesenchymal Stem Cells for Skin Reconstruction after Burns(Eylert 2019).
- Cheng & **Eylert** et al., Handheld instrument for wound-conformal delivery of skin precursor sheets improves healing in full-thickness burns. *Biofabrication*, 2020
- **Eylert** et al., Skin regeneration is accelerated by a lower dose of multipotent mesenchymal stromal/stem cells-a paradigm change. *Stem cell research & therapy*, 12(1), p.82, 2021

General Discussion

In regenerative medicine, the general goals after a burn injury is to regenerate and heal the skin. As such, the transplantation of mesenchymal stromal/stem cells is becoming increasingly feasible in (plastic, reconstructive) surgery. If ethical approval is granted, safety guidelines are followed and special GMP (Good Manufacturing Practices) facilities, as well as the knowledge in the utilization of MSCs, are available, then MSC or similar treatments could become a more widespread solution for skin regeneration. The first case studies that have transplanted (via injection) UC-MSCs in burns were successfully conducted and showed superior healing (Jeschke et al. 2019). Furthermore, the first autologous (stromal) cell therapies that spray fibroblasts and progenitor cells have been FDA approved for partial thickness therapy (Esteban-Vives et al. 2018) and are available in selected (burn) centers in Europe for study purposes in burns for skin regeneration. From a commercial standpoint, stem cells are known as the "ultimate regenerative medicine", an idea that is propagated worldwide (Connolly et al. 2014). However, many research questions are still unanswered, and failure of this treatment is possible if safety is not applied. Indeed, some stem cell trials have already been shut down as novel treatments could not be shown as the superior option (Yau et al. 2019).

Wound healing is extremely costly (Kamolz, 2014; Banfield et al. 2015), and a practical treatment that can regenerate tissue is what medical societies and professionals have been waiting for. Stem cell therapy with the property of regeneration and repair bears, therefore, a great potential to reduce current burdens and alleviate disease. This study gives new insights on the novel therapy using UC-MSCs in tissue engineering, which adds important value in the discussion of this new treatment approach in skin regeneration.

The existence of a cell-dose phenomenon

A low-to-high MSC-dose treatment model was created, full-thickness burn wounds were excised and UC-MSCs were grafted on Integra® from a low-to-high cell dose between 200 and 2,000,000 cells/cm^2 as treatment on the wounds, comparisons were made four weeks after surgery on day 28. Eight wound healing parameters indicating the progress in tissue regeneration and repair were evaluated (Gurtner et al. 2008). It was found that a low dose of 40,000 cells/cm^2 accelerates the regeneration of the epidermis and dermis most efficaciously, followed by an even lower dose of 5,000 cells/cm^2. Comparatively effective in the analysis were the dosages of 200 cells/cm^2 and 200,000 cells/cm^2 as third best, followed by higher dosages up to 400,000 cells/cm^2 and lastly 2,000,000 cells/cm^2, when compared to the acellular component and referenced to the healthy skin alone.

This finding changes the paradigm that more cells lead to a better outcome in skin healing as numerous authors have described previously investigating the MSCs grafted on Integra® (Falanga 2012b; Wood et al. 2007; Amini-Nik et al., 2018; Spater et al. 2018; Formigli et al., 2015; Fierro et al., 2015a; Meruane et al. 2012; Foubert et al. 2015). To promote MSC cell therapy, the determination of the optimized cell dosage for (pre-)clinical trials is essential for preventing this therapy from failure. The model shown here provides a wide dose range and fills a gap for the optimization of future cell-based therapy in regenerative medicine. The impact of this study includes not only the dose range for skin wound healing, but also the feasibility of cell production for (acute) burn injuries and costs for treatment production (Kamolz, et al. 2014). Knowing that a lower cell dose range promotes skin regeneration more effectively than a high dose range has immense value for cell coverage, especially in large burn wounds (with a high TBSA where potentially millions of cells are needed to cover burn wounds) and could significantly improve the potential treatment cost efficiency.

Previous studies have hypothesized that more cells lead to better outcome, such as for cell injection in the arthritic knee joint (> 50 million) (Chahal et al. 2019), or in the treatment for ischemic heart infarction (150 million) (Cha et al. 2017; Yau et al. 2019). However, these investigations showed that the abundant cells in knee joints do not result in significant improvements for patients (Chahal et al. 2019), and early clinically randomized-controlled trials have shown that such high number of mesenchymal precursor cells (MPCs) injected in ischemic heart lesions did not show curative effects (Yau et al. 2019). As such, it appears that the dose determines the success of cell therapy.

Due to the novelty of this approach, there is a lack of (MSCs) dosing studies in the literature. In numerous rodent models, for instance, MSCs and progenitor cell treatment have been shown to have valuable healing effects (Spater et al. 2018; Formigli et al., 2015; Fierro et al., 2015; Meruane et al. 2012), but currently there seem to be excessive with cell counts in the millions when researchers graft onto small wound surface areas of a few centimeters. In a study with mini-pigs, researchers demonstrated using a wound size of $10cm^2$ that 300,000 cells/cm^2 of adipose-derived regenerative cells grafted on Integra® increased granulation tissue and neovascularization in wound healing (Foubert et al. 2015). It has also been shown that 88,000-160,000 cells/cm^2 seeded on the Integra® scaffold in a comparable full-thickness burn porcine model enhances healing (Wood et al. 2007). However, this study demonstrated that even low

doses of 40,000 cells/cm^2 and 200–5,000 cells/cm^2 in large 25 cm^2 wounds result in significant wound healing and full tissue regeneration.

We hypothesize that the more beneficial outcome in the low dose range is explainable due to the simple adage "the dose makes the poison" and three underlying mechanisms (based on a publication in *Cell* showing a mathematical model of cell circuits of cell proliferation and death) might be applicable for an explanation (Hart et al., 2014). First, an excessive amount of grafted cells, such as 2,000,000 cells/cm^2, may be proliferating to a maximum consuming space and use all available growth resources. This could generate a lack of nutrients and induce hypoxia in the wound environment, all of which might lead to cell death and massive signaling (Hart et al., 2014). This massive signaling may need time to be regulated in the wound environment so that tissue regeneration can occur. Previously, it has been shown that hypoxia-induced apoptosis of MSCs showed a beneficial initial inflammatory upregulation that prevents hypertrophic scar formation (Liu et al. 2014). This would be in line with our findings, since we found reduced scarring in the extremely high dose group. Second, for extremely low cell concentrations, the cell numbers may be declining since the critical threshold of hemostasis is not reached, and the few cell-cell interconnections could to cell death (Hart et al., 2014). The paracrine signals may provide the neighboring cells in the wound bed a proliferative healing boost as demonstrated by the results for the low dosages. Given the appropriate dose, cell hemostasis may be able to be achieved faster (Hart et al., 2014), leading to most optimal accelerated healing.
The scientific underlying mechanism, however, is not being determined yet. The cell-dose model has provoked many research questions, which need to be determined in the future in separate studies due to the scope of each potential underlaying mechanism that has led to this low-dose-phenomenon (Supplementary Material Table 1). Interestingly, also other researcher descripted a dose-dependent wound healing phenomenon, for instance, when using a high dosages of Botulinum (neuro)toxin A wound closure was deteriorated in an *in vitro* model (Guger-ell et al. 2016). Following our publication (Eylert et al. 2021), we found also other review/researchers reevaluated their data and descripted a low-dose phenomenon when injecting, for instance, erythropoietin into wounds and found enhanced regeneration (Spater et al. 2021).

Regeneration findings and their meaning

This preclinical study confirmed previously described results, demonstrating that MSCs therapy improves macroscopical wound healing with faster epithelialization, reduced scarring and reduced inflammation. Furthermore, it has been shown, that the application of the cells with its

proangiogenic and fibroproliferative effects increases collagen formation, increases neovascularization and reduces fibrosis (Arno et al. 2014; Isakson et al. 2015; Rolfe et al. 2007; Liu et al. 2014). A lower dose of MSCs regenerates more efficiently than a higher dose of cells. In addition, it has been shown that regardless of the dose, the newly cellularized MSC treatment accelerates wound healing more effectively compared to the acellular control. However, it seems that in an extremely high dose range, the results trend toward the acellular component.
Specifically, the results showed that in the created 25 cm^2 large full-thickness deep wounds of the pigs, almost full epithelialization, up to 95% with residual crusts, was seen on day 28. The close results from the MSCs-treated groups compared to the acellular control could be explained due to the strong contracture in the dermis in the controls, as shown in the scar evaluation and elevated aSMA cell density, which contributed to a more mechanical wound closure. Furthermore, inflamed wounds appeared in acellular controls, but less inflammation appeared in the MSCs-treated wounds, which was in line with the increased and decreased count of type 1 and 2 macrophages.
In general, it was challenging to find reliable macrophages markers due to the high cross-reactivity of the antibodies in the pig tissue. However, the CD11b, associated with a pro-inflammatory state, was found with a higher cell count in the acellular control compared to the MSC group, where stem cells reduce inflammation (Singer & Caplan 2010). CD163 correlated with a state of repair and showed significantly higher remodeling compared to the more homogenous MSC tissue. This increased inflammation and remodeling was not just observed in the dermis, it was also observed in the epidermal-dermal border. The observed tissue remodeling reflects the wide range of epidermal thickness.
It is possible that a compensatory mechanism exists, as wounds will heal as fast as possible, but without the correct cell signaling, a paradoxical (Hart et al., 2014) regeneration might be seen, as in hypo- and hyperplasia. Recently, it has been shown that the epidermis has high plasticity when it comes to cell differentiation and migration (Dekoninck & Blanpain 2018) not just from the ectodermal region (Prodinger et al. 2017; Dekoninck & Blanpain 2018), but also from the dermal regions (Driskell et al. 2013; Philippeos et al. 2018). Another possibility could be, that the chosen umbilical cord-MSC source has a lower plasticity (Antonyshyn et al. 2018) than skin-derived stem cells, and therefore lacked in regeneration capabilities.
The increased collagen formation, increased neovascularization and reduced fibrosis are attributed due to the beneficial proangiogenic (Low et al. 2017) and fibroproliferative (Ertl et al. 2018) effects of (UC-)MSCs (Arno et al. 2014; Arno et al., 2014), as shown in numerous studies previously (Isakson et al. 2015).

Furthermore, MSCs are also known to regenerate skin appendages (Dekoninck & Blanpain 2018; Sabapathy et al. 2014), including hair follicles and skin glands. This could also be observed and measured in the cellularized groups, which is an interesting finding four weeks after the initial burn treatment. It is, however, what other authors proposed previously, demonstrating that regeneration may occurs potentially within this time frame (Biedermann et al. 2010).

Negative findings

The descriptive data table shows the negative findings of a similar outcome from the MSCs-treated groups compared to the currently most used synthetic skin substitute (Nicholas et al. 2016; Shahrokhi & Jeschke 2019) and allows comparisons through all data points. These findings were seen especially in the epithelialization speed and the type 1 macrophage assessment. First, it could also be speculated that the wound healing was not fully completed, as demonstrate with the residual crusts on top of the wound, or the low N of 3 in the extremely low dose distorted the result. Regarding the type 1 macrophages, with the inferior result from the current/acellular treatment it could be argued that the older tissue from 2015–2017 might have a lower affinity to the histological staining than the newer tissue from 2017–2019 (Supplementary Material Figure 2). Further research is needed to adjust and determine the (slight) differences.

MSCs therapy via Integra®

Mesenchymal stromal/stem cell treatments beneficially influence and promote wound healing and tissue repair (Malhotra et al. 2016). However, the ideal burn wound dressing is not determined yet (Selig et al. 2012), and cell delivery to the tissue with respect to the wound still remains a challenge. Multiple cell delivery strategies are under development and are currently being investigated, as for instance, bio-printing (Cheng & Eylert et al. 2020), cell-spraying (Wood et al. 2007), direct cell injection(Jeschke et al. 2019) and the cellularization of scaffolds (Amini-Nik et al., 2018; Ertl et al. 2018; Eylert et al. 2021; Germain 2018; Meuli et al. 2019). MSCs were incorporate into a collagen-cartilage–based synthetic acellular dermal matrix for tissue regeneration, which is available worldwide (Tompkins & Burke 1990) and used successfully in numerous stem cell research studies as a delivery structure (Amini-Nik et al., 2018; Cheng & Eylert et al. 2020; Eylert et al. 2021). In addition, as a reliable cell carrier, it has been shown that the biodegradable scaffold allows cell ingrowth (Jones et al. 2003; Wood et al. 2007; Hamrahi et al. 2012) and permits cell differentiation into the mesenchymal lineage (Morena et al. 2016). Labeled grafted cells were present until day 7, which is similar to other reports

(Hamrahi et al. 2012; Cheng & Eylert et al. 2020) that used the same cell tracing method (Clover et al. 2015). This suggests that the cells promote wound healing and tissue regeneration via their paracrine effects (Singer & Caplan 2010).

Taken together, the Integra® scaffold, which can be easily cellularized as shown previously (Amini-Nik et al., 2018; Cheng & Eylert et al. 2020; Eylert et al. 2021; Wood et al. 2007), can act as a readily applicable cell delivery system, especially when adjusted for each (burn) patient regarding cell dose, using the multiple advantages of MSCs as a new wound healing treatment.

Umbilical cord mesenchymal stromal cells in wound healing

Although the wounds were evaluated on day 28 and were not investigated longer, it has been shown that the application of UC-MSCs seems to be safe in full-thickness skin regeneration, as previous researcher have demonstrated (Davis 1910; Matthews et al. 1981). No tumorigenesis was observed in the eight pigs and thirty wounds in the macroscopical or histological tissue evaluations. The cells were applied in hemostasis, the acute inflammation phase in wound healing, and were safe in the proliferation/regeneration and beginning of the remodeling phase after 4 weeks, without any observed adverse events. This finding is in conjunction with other authors showing the safety of UC-MSCs in clinical trials (Couto et al. 2019; Can et al., 2017; Jeschke et al. 2019) were the multipotent potential for (skin) regeneration was shown (Jing Li et al. 2018; Saleh & Reza 2017). UC-MSCs have also shown immunosuppressive properties with a low risk of graft-versus-host disease (GVHD) (Jun Li et al. 2018) and their potency under ischemic-like stress-conditions (Himal et al. 2017), was valuable in the burn models previously (Cheng & Eylert et al. 2020). In addition, these fetal-derived stromal cells are associated with increased re-epithelialization, neovascularization and fibroproliferation (Arno et al. 2014; Ertl et al. 2018), which are needed in tissue regeneration. Therefore, this source of multipotent stromal cells is helpful especially in full-thickness burns, and potentially available in almost every hospital.

Animal Model

A reliable model for the investigation of the efficacy of various cell doses for tissue regeneration is crucial. The established full-thickness porcine model was used preclinical studies to research wound healing in burn research (Abdullahi et al. 2014; Amini-Nik et al., 2018; Wood et al. 2007; Cheng & Eylert et al. 2020; Eylert et al. 2021). The advantage of the Yorkshire pig as a burn model to mimic human wound healing is that they have similar anatomic and physiologic skin characteristics and a similar skin pigmentation. In the chosen model, it was possible to

study large wounds without a spontaneous healing via contracture as seen in smaller animal models (Singer & McClain 2003; Sullivan et al. 2001; Wood et al. 2007). Pig skin is slightly thicker than human skin, and therefore, the investigation of full-thickness regeneration showed reliability in the evaluation. Even though there are alternative options available for research, such as the innovative organs and lab-on-the-chip (Cheng & Eylert et al. 2020; Hakimi et al. 2018) they are not yet available to mimic the numerous functions that need to be accounted for in a full-thickness skin burn, including a complex wound healing environment (Dolp & Eylert et al. 2021) with the hypermetabolic state (Abdullahi & Jeschke 2017; Auger et al. 2021; Auger et al. 2018; Auger et al. 2020; Auger et al. 2017; Jeschke 2016; Jeschke et al., 2015; Jeschke et al. 2008).

Ethical concerns

Regenerative medicine is an exciting field with great potential. Stromal cells bear tremendous potential for curing disease; however, many research questions are still unanswered (Eylert et al. 2021). Ethical questions regarding stem cell therapy are informed by competent regulatory authorities. The Austrian Federal Office for Safety in Health Care (BASG, https://www.basg.gv.at/en/) and European Medical Agency (EMA, https://www.ema.europa.eu/en), for instance, regulate and discuss the use of stromal cells, which fall under different categories regarding their preservation, processing and purpose. Therefore, there is an essential difference regarding the ethical matters and the law if MSCs therapies remain under investigation for instance, in the laboratory (in preclinical (animal) trials), during transplantation (in (human) trials), as drug delivery systems (i.e. cytokines/vesicles), or in medical product (delivery) or devices.

The safety of any new treatment has to be proven and confirmed first. There are clear differences between the embryonic and adult (mesenchymal) stem cells (Ventura-Juncá et al. 2013). In the context of this study, it will be very interesting to assess how the dosing of MSCs will evolve in the future. If the cells are seen as a drug delivery (product); and because the dose "makes the poison", then the necessary amount for a "cytokine-cocktail" for skin (tissue) regeneration must be determined in the future, it is also possible that the cells are actually no longer needed, and furthermore, that the cells could be potentially easily be ordered. In addition, autologous burned-derived cells could be used (Amini-Nik et al., 2018; Dolp & Eylert et al. 2021) for burn treatment where stromal cells could be transplanted, which would put this cell treatment under the Tissue Safety Act and Federal Law. Another possibility is that the cells could be seen as a pharmaceutical product known as an advanced therapy medicinal product

(ATMP) (in the future) (https://www.ema.europa.eu/en/news/new-guidelines-good-manufacturing-practices-advanced-therapies), which is defined as having pharmaceutical, immunological or metabolic functions (in a human). The word "dosing" indicates that a threshold is needed for a response. This study shows the existence of a dose-phenomenon and is therefore valuable for the research community and in guiding future directions in the dosing of cell therapy in skin regeneration, especially since the vibrant (stem cell) start-up scene is pushing various wound healing products on the market as skin healing, repair and regeneration have an immense economic potential worldwide. Stem cell tourism, for instance, with promoted stem cell therapies, attract significant attention and potential patients (Ventura-Juncá et al. 2013), notably on the internet (Connolly et al. 2014). This highlights the importance of a safe cell application and the need for further (pre)clinical trials investigating the unique regenerative potential of (mesenchymal) stem cells for tissue regeneration and repair.

Limitations

Intense research is needed to determine the underlying factors and mechanism of the dose-dependent relationship in wound healing, including the various dosages and different MSC types from various sources in different (burn) skin thickness models when using different cell delivery strategies. It would be interesting if the dose phenomenon is caused by a lack of nutrients for the stromal cells and is therefore associated with a possible higher apoptosis rate leading to a worse healing outcome, or if too much cell-cell interaction and an overload of released cytokines contribute to a paradoxical cell-signaling, and therefore leads to a noncell homeostasis and cell death as researches proposed in theoretical models (Hart et al., 2014). It is believed in these mathematical models that if cell proliferation exceeds the cell death rate, the cell numbers grow, whereas in the opposite scenario the cell numbers decline (Hart et al., 2014). In addition, sophisticated hypoxia and nutrient models have to be created to account for the burn injury as well as the potential hypoxia and the wound healing environment, especially in a potential over- or under-dosed treatment in each wound in different individual. In this study, the total global viability and state of differentiation of the delivered cells were not determined, which is difficult and also not feasible in such large wounds using billions of cells. Generally, a higher N and number-needed-to-treat is necessary to calculated statistical significance. Different complex models were created together with the statistical department from the Medical University of Graz to calculate statistical significance, and they also accounted for different pigs, however, none of the models addressed the data set as well as the "simple" descriptive

data set shown in Figure 11. Using this basic method data presentation, the pure data set represented the trends for the dosing-phenomenon the best. Finally, further research with optimized conditions needs to be done in humans to determine the exact optimal dose for human (burn) wound repair and skin regeneration, which need to be pursued not only for acute but also for chronic wounds.

Chapter 6
Conclusion

The contents in this chapter of this thesis have been partially published previously as follows:

- **Eylert, G**. (2019) MSc Thesis. Bio-Printing of Mesenchymal Stem Cells for Skin Reconstruction after Burns(Eylert 2019).
- Cheng & **Eylert** et al., Handheld instrument for wound-conformal delivery of skin precursor sheets improves healing in full-thickness burns. *Biofabrication*, 2020
- **Eylert** et al., Skin regeneration is accelerated by a lower dose of multipotent mesenchymal stromal/stem cells-a paradigm change. *Stem cell research & therapy*, 12(1), p.82, 2021

Conclusion

In this work, it has been shown that different dosages of multipotent mesenchymal stromal/stem cells promote skin regeneration in full-thickness burns differently. It has also been shown and confirmed that different MSC dosages improve wound healing when compared and referenced to the initial burn and the ideal, physiologic condition of healthy skin. This study gives new insights based on a preclinical cell-dose-dependent wound healing model and demonstrates efficacy toward a low dose of MSCs, which is a helpful finding for future investigations using (mesenchymal stem) cells and allows for further considerations regarding cost efficiency and off-the-shelf cell therapies for patients.

To the best of our knowledge there are no comparisons available, including such a wide range of doses, in a large pig animal trial for skin regeneration. Importantly, this cell-dose model can be translated and implemented to various other stem cell trials in regenerative medicine, because it shows that a lower dose might be sufficient enough and high abundance might lead to misleading results tending toward a no-cell effect, which is tremendously important in future tissue repair and regeneration studies.

Recommendations

Depending on the scientific outcome measures of interest, it is recommended to create a dose-model that allows analysis on various measures and supports and complements one another to be able to accurately show created trends and interpret results. Presumably, every dose-response is based on thresholds; therefore, the underlying hypothesis should be considered first, to be able to address and determine the potentially difficult pathways for approval of any rationales. These complex considerations might be addressed accordingly in the experiments when collecting the data.

Chapter 7
Future Directions

The contents in this chapter of this thesis have been partially published previously as follows:

- **Eylert, G**. (2019) MSc Thesis. Bio-Printing of Mesenchymal Stem Cells for Skin Reconstruction after Burns(Eylert 2019).
- Cheng & **Eylert** et al., Handheld instrument for wound-conformal delivery of skin precursor sheets improves healing in full-thickness burns. *Biofabrication*, 2020
- **Eylert** et al., Skin regeneration is accelerated by a lower dose of multipotent mesenchymal stromal/stem cells-a paradigm change. *Stem cell research & therapy*, 12(1), p.82, 2021

Future Directions

The results in this pre-clinical setting highlight two directions for future research. First, the dose-model can be translated to humans for MSCs treatment studies. MSCs treatment shows efficiency for wound repair and regeneration on a wide range of dose (i.e., from low to high); however, a low dose is more effective. Knowing this, it is crucial to determine the most optimal cell therapy for patients via further fine-tuning for partial and full-thickness regeneration, as well as for acute and chronic wounds.

Second, the ultimate therapy for skin repair and generation would be a quickly available off-the-shelf therapy using the paracrine effects of MSCs. This could be feasible in the very near future if the quantitatively necessary amounts for a "cell dose cocktail" are determined successfully.

Therefore, MSC therapy can act as a frontier in regenerative medicine if safety and ethical concerns are pursued in upcoming trials. Regenerative medicine and modern, plastic, reconstructive burn surgery have the potential to pioneer the next chapter in cellular therapy in restoring the mesenchymal soft tissue.

References

Abdullahi, A. & Jeschke, M.G., 2017. Taming the Flames: Targeting White Adipose Tissue Browning in Hypermetabolic Conditions. *Endocrine Reviews*, 38(6), pp.538–549.

Abdullahi, A., Amini-Nik, S. & Jeschke, M.G., 2014. Animal models in burn research. *Cellular and Molecular Life Sciences*, 71(17), pp.3241–3255.

Adibfar, A. et al., 2019. Current State of Selected Wound Regeneration Templates and Temporary Covers. pp.1–11.

Amini-Nik, S., Dolp, R., Eylert, G., Datu, A.-K., Parousis, A., Blakeley, C. & Jeschke, M.G., 2018a. Stem cells derived from burned skin - The future of burn care. *EBIOMedicine*, 37, pp.509–520.

Antonyshyn, J.A. et al., 2018. Limited Endothelial Plasticity of Mesenchymal Stem Cells Revealed by Quantitative Phenotypic Comparisons to Representative Endothelial Cell Controls. *Stem cells translational medicine*, 8(1), pp.35–45.

Arno, A.I., Amini-Nik, S., Blit, P.H., Al-Shehab, M., Belo, C., Herer, E. & Jeschke, M.G., 2014. Effect of human Wharton's jelly mesenchymal stem cell paracrine signaling on keloid fibroblasts. *Stem cells translational medicine*, 3(3), pp.299–307.

Arno, A.I., Amini-Nik, S., Blit, P.H., Al-Shehab, M., Belo, C., Herer, E., Tien, C.H., et al., 2014. Human Wharton's jelly mesenchymal stem cells promote skin wound healing through paracrine signaling. *Stem cell research & therapy*, 5(1), p.28.

Auger, C. et al., 2021. Beyond mitochondria: alternative energy-producing pathways from all strata of life. *Metabolism*, p.154733.

Auger, C. et al., 2018. Metformin adapts its cellular effects to bioenergetic status in a model of metabolic dysfunction. *Scientific Reports*, pp.1–10.

Auger, C. et al., 2020. Regulation of glycolysis and the Warburg effect in wound healing. *JCI insight*, 5(17), pp.12–23.

Auger, C., Samadi, O. & Jeschke, M.G., 2017. The biochemical alterations underlying post-burn hypermetabolism. *BBA - Molecular Basis of Disease*, 1863(Part B), pp.2633–2644.

Bakhtyar, N. et al., 2017. Acellular Gelatinous Material of Human Umbilical Cord Enhances Wound Healing: A Candidate Remedy for Deficient Wound Healing. *Frontiers in Physiology*, 8, p.2599.

Banfield, J. et al., 2015. Healthcare Costs of Burn Patients From Homes Without Fire Sprinklers. *Journal of Burn Care & Research*, 36(1), pp.213–217.

Beier, J.P. et al., 2010. [Skin tissue engineering--from split skin to engineered skin grafts?]. *Handchirurgie, Mikrochirurgie, plastische Chirurgie :* 42(6), pp.342–353.

Belokhvostova, D. et al., 2018. Homeostasis, regeneration and tumour formation in the mammalian epidermis. *The International Journal of Developmental Biology*, 62(6-7-8), pp.571–582.

Biedermann, T. et al., 2010. Human Eccrine Sweat Gland Cells Can Reconstitute a Stratified Epidermis. *The Journal of investigative dermatology*, 130(8), pp.1996–2009.

Bielefeld, K.A., Amini-Nik, S. & Alman, B.A., 2012. Cutaneous wound healing: recruiting developmental pathways for regeneration. *Cellular and Molecular Life Sciences*, 70(12), pp.2059–2081.

Brianezi, G. et al., 2015. Dermal type I collagen assessment by digital image analysis. *Anais Brasileiros de Dermatologia*, 90(5), pp.723–727.

Yau T.M., Noiseux N., & Sarkissian, 2017. Cell therapies: The next-generation clinical trials. *The Journal of thoracic and cardiovascular surgery*, 154(2), pp.556–557.

Can, A., Celikkan, F.T. & Cinar, O., 2017a. Umbilical cord mesenchymal stromal cell transplantations: A systemic analysis of clinical trials. *Cytotherapy*, 19(12), pp.1351–1382.

Caplan, A.I., 2019. Medicinal signalling cells: they work, so use them. *Nature*, 566(7742), p.39.

Cha, J. & Falanga, V., 2007. Stem cells in cutaneous wound healing. *Clinics in dermatology*, 25(1), pp.73–78.

Chahal, J. et al., 2019. Bone Marrow Mesenchymal Stromal Cell Treatment in Patients with Osteoarthritis Results in Overall Improvement in Pain and Symptoms and Reduces Synovial Inflammation. *Stem cells translational medicine*, 8(8), pp.746–757.

Cheng, R.Y. & Eylert, G. et al., 2020. Handheld instrument for wound-conformal delivery of skin precursor sheets improves healing in full-thickness burns. *Biofabrication*, 12(2), p.025002.

Germain L. et al., 2018. Autologous bilayered self-assembled skin substitutes (SASSs) as permanent grafts: a case series of 14 severely burned patients indicating clinical effectiveness. *European Cells and Materials*, 36, pp.128–141.

Clark, R.A.F., Ghosh, K. & Tonnesen, M.G., 2007. Tissue engineering for cutaneous wounds. *The Journal of investigative dermatology*, 127(5), pp.1018–1029.

Clover, A.J.P. et al., 2015. Allogeneic mesenchymal stem cells, but not culture modified monocytes, improve burn wound healing. *Burns*, 41(3), pp.548–557.

Connolly, R., O'Brien, T. & Flaherty, G., 2014. Stem cell tourism--a web-based analysis of clinical services available to international travellers. *Travel medicine and infectious disease*, 12(6 Pt B), pp.695–701.

Couto, P.S. et al., 2019. First decade of clinical trials and published studies with mesenchymal stromal cells from umbilical cord tissue. *Regenerative Medicine*, 14(4), pp.309–319.

Davis, J.S., 1910. *Skin transplantation with a review of 550 cases at the Johns Hopkins Hospital*, Available at: https://scholar.google.at/scholar?hl=de&as_sdt=0%2C5&q=davis+js+skin+transplantation&btnG=.

Dekoninck, S. & Blanpain, C., 2018. Stem cell dynamics, migration and plasticity during wound healing. *Nature cell biology*, pp.1–7.

Dindo, D., Demartines, N. & Clavien, P.-A., 2004. Classification of Surgical Complications. *Annals of surgery*, 240(2), pp.205–213.

Dolp, R., 2017. Burn-Derived Stem Cells - A Promising New Cell Source For Skin Regeneration. *TSpace, University of Toronto*, 1(1), pp.1–160.

Dolp, R. & Eylert, G. et al., 2021. Biological characteristics of stem cells derived from burned skin-a comparative study with umbilical cord stem cells. *Stem cell research & therapy*, 12(1), p.137.

Dominici, M. et al., 2006. Minimal criteria for defining multipotent mesenchymal stromal cells. The International Society for Cellular Therapy position statement. *Cytotherapy*, 8(4), pp.315–317.

Driskell, R.R. & Watt, F.M., 2015. Understanding fibroblast heterogeneity in the skin. *Trends in Cell Biology*, 25(2), pp.92–99.

Driskell, R.R. et al., 2013. Distinct fibroblast lineages determine dermal architecture in skin development and repair. *Nature*, 504(7479), pp.277–281.

Eming, S.A., Krieg, T. & Davidson, J.M., 2007. Inflammation in Wound Repair: Molecular and Cellular Mechanisms. *The Journal of investigative dermatology*, 127(3), pp.514–525.

Ertl, J. et al., 2018. Comparative study of regenerative effects of mesenchymal stem cells derived from placental amnion, chorion and umbilical cord on dermal wounds. *Placenta*, 65, pp.37–46.

Esteban-Vives, R. et al., 2018. Cell-spray auto-grafting technology for deep partial-thickness burns: Problems and solutions during clinical implementation. *Burns*, 44(3), pp.549–559.

Etzerodt, A. & Moestrup, S.K., 2013. CD163 and inflammation: biological, diagnostic, and therapeutic aspects. *Antioxidants & redox signaling*, 18(17), pp.2352–2363.

Eylert, G., 2019. *Bio-Printing of Mesenchymal Stem Cells for Skin Reconstruction after Burns. Thesis for the degree of Master of Science, University of Toronto, 2019*,

Eylert, G. et al., 2021. Skin regeneration is accelerated by a lower dose of multipotent mesenchymal stromal/stem cells-a paradigm change. *Stem cell research & therapy*, 12(1), p.82.

Falanga, V., 2012a. Stem Cells in Tissue Repair and Regeneration. *Journal of Investigative Dermatology*, 132(6), pp.1538–1541.

Fearmonti, R., 2010. A Review of Scar Scales and Scar Measuring Devices. pp.1–10.

Fierro, F.A., O'Neal, A.J., Beegle, J.R., Chavez, M.N., Peavy, T.R., Isseroff, R.R. & Egana, J.T., 2015a. Hypoxic pre-conditioning increases the infiltration of endothelial cells into scaffolds for dermal regeneration pre-seeded with mesenchymal stem cells. *Frontiers in cell and developmental biology*, 3, p.68, pp964-9.

Finlay, V. et al., 2017. Increased burn healing time is associated with higher Vancouver Scar Scale score. *Scars, Burns & Healing*, 3(121), pp.DOI: 10.1177–2059513117695324.

Finnerty, C. et al., 2016. Hypertrophic scarring: the greatest unmet challenge after burn injury. *Lancet (London, England)*, 388(10052), pp.1427–1436.

Fitzsimmons, R.E.B. et al., 2018. Mesenchymal Stromal/Stem Cells in Regenerative Medicine and Tissue Engineering. *Stem Cells International*, 2018, p.8031718.

Fletcher, J., 2010. Development of a new wound assessment form. *Wounds : a compendium of clinical research and practice*, 6, pp.1–7.

Formigli, L., et al., 2015. MSCs seeded on bioengineered scaffolds improve skin wound healing in rats. *Wound repair and regeneration : official publication of the Wound Healing Society [and] the European Tissue Repair Society*, 23(1), pp.115–123.

Foubert, P. et al., 2015. Uncultured adipose-derived regenerative cells (ADRCs) seeded in collagen scaffold improves dermal regeneration, enhancing early vascularization and structural organization following thermal burns. *Burns*, 41(7), pp.1504–1516.

Friedenstein, A.J., Piatetzky-Shapiro, I.I. & Petrakova, K.V., 1966. Osteogenesis in transplants of bone marrow cells. *Journal of embryology and experimental morphology*, 16(3), pp.381–390.

Frueh, F.S. et al., 2017. Adipose Tissue-Derived Microvascular Fragments Improve Vascularization, Lymphangiogenesis, and Integration of Dermal Skin Substitutes. *The Journal of investigative dermatology*, 137(1), pp.217–227.

Grada, A., Mervis, J. & Falanga, V., 2018. Research Techniques Made Simple: Animal Models of Wound Healing. *The Journal of investigative dermatology*, 138(10), pp.2095–2105.e1.

Greenhalgh, D.G., 2019. Management of Burns D. L. Longo, ed. *New England Journal of Medicine*, 380(24), pp.2349–2359.

Grinnell, F., 2003. Fibroblast biology in three-dimensional collagen matrices. *Trends in Cell Biology*, 13(5), pp.264–269.

Gugerell, A. et al., 2016. Botulinum Toxin A: Dose-dependent Effect on Reepithelialization and Angiogenesis. *Plastic and Reconstructive Surgery Global Open*, 4(8), p.e837.

Gurtner, G.C. et al., 2008. Wound repair and regeneration. *Nature*, 453(7193), pp.314–321.

Hakimi, N. et al., 2018. Handheld skin printer: in situ formation of planar biomaterials and tissues. *Lab on a Chip*, pp.1–12.

Hamrahi, V.F. et al., 2012. In vivo molecular imaging of murine embryonic stem cells delivered to a burn wound surface via Integra(R) scaffolding. *Journal of Burn Care & Research*, 33(2), pp.e49–54.

Hart, Y., et al., 2014. Paradoxical Signaling by a Secreted Molecule Leads to Homeostasis of Cell Levels. *Cell*, 158(5), pp.1022–1032.

Himal, I., Goyal, U. & Ta, M., 2017. Evaluating Wharton's Jelly-Derived Mesenchymal Stem Cell's Survival, Migration, and Expression of Wound Repair Markers under Conditions of Ischemia-Like Stress. *Stem Cells International*, pp.1–13.

Hinz, B., 2016. Experimental Eye Research. *Experimental Eye Research*, 142(C), pp.56–70.

Hinz, B. et al., 2001. Alpha-smooth muscle actin expression upregulates fibroblast contractile activity. *Molecular biology of the cell*, 12(9), pp.2730–2741.

Idriss, N. & Maibach, H.I., 2009. Scar assessment scales: a dermatologic overview. *Skin Research and Technology*, 15(1), pp.1–5.

Isakson, M. et al., 2015. Review Article Mesenchymal Stem Cells and Cutaneous Wound Healing: Current Evidence and Future Potential. *Stem Cells International*, pp.1–12.

Jeschke, M.G., 2016. Postburn Hypermetabolism. *Journal of Burn Care & Research*, 37(2), pp.86–96.

Jeschke, M.G. et al., 2019. Allogeneic mesenchymal stem cells for treatment of severe burn injury. *Stem cell research & therapy*, 10(337), pp.1–6.

Jeschke, M.G. et al., 2008. Pathophysiologic response to severe burn injury. *Annals of surgery*, 248(3), pp.387–401.

Jeschke, M.G. et al., 2013. Wound Coverage Technologies in Burn Care. *Journal of Burn Care & Research*, 34(6), pp.612–620.

Jeschke, M.G., Kamolz, L.P., et al., 2017. Handbook of Burns, Volume1, Acute Burn Care SpringerWienNewYork, ed., pp.1–20.

Jeschke, M.G., Patsouris, D., Stanojcic, M., Abdullahi, A., Rehou, S., Pinto, R., Chen, P., Burnett, M. & Amini-Nik, S., 2015a. Pathophysiologic Response to Burns in the Elderly. *EBIOMedicine*, 2(10), pp.1536–1548.

Jeschke, M.G., Sadri, A.-R., et al., 2017. A Surgical Device to Study the Efficacy of Bioengineered Skin Substitutes in Mice Wound Healing Models. *Tissue engineering. Part C, Methods*, 23(4), pp.237–242.

Jones, I. et al., 2003. Upward migration of cultured autologous keratinocytes in Integra artificial skin: a preliminary report. *Wound repair and regeneration : official publication of the Wound Healing Society [and] the European Tissue Repair Society*, 11(2), pp.132–138.

Kamolz, L.-P. et al., 2015. Skin Regeneration, Repair, and Reconstruction. *BioMed Research International*, 2015, p.892031.

Kamolz, L.-P., Keck, M. & Kasper, C., 2014. Wharton's jelly mesenchymal stem cells promote wound healing and tissue regeneration. *Stem cell research & therapy*, 5(3), p.62.

Kamolz, L.-P., Koller, H., et al., 2014. Skin substitutes: which one do we know, which one do we use? *Burns*, 40(5), pp.1053–1054.

Kamolz, L.-P., Sendlhofer, G. & Lumenta, D., 2014. Future burn care: balancing the relationship between cost and quality. *Wound repair and regeneration : official publication of the Wound Healing Society [and] the European Tissue Repair Society*, 22(4), pp.433–434.

Kretzschmar, K. & Watt, F.M., 2014. Markers of Epidermal Stem Cell Subpopulations in Adult Mammalian Skin. *Cold Spring Harbor Perspectives in Medicine*, 4(10), pp.a013631–a013631.

Le Blanc, K. & Davies, L.C., 2018. MSCs—cells with many sides. *Cytotherapy*, pp.1–6.

Lee, D.E., Ayoub, N. & Agrawal, D.K., 2016. Mesenchymal stem cells and cutaneous wound healing: novel methods to increase cell delivery and therapeutic efficacy. *Stem cell research & therapy*, pp.1–8.

Li, Binghui et al., 2019. Skin Epidermis and Adnexa Regrowth Induced by Treatment With Artificial Dermal Template After Full-Thickness Skin Wound. *The International Journal of Lower Extremity Wounds*, 33, pp.153473461881890–14.

Li, Jing et al., 2018. Comparison of the biological characteristics of human mesenchymal stem cells derived from exfoliated deciduous teeth, bone marrow, gingival tissue, and umbilical cord. *Molecular Medicine Reports*, pp.1–9.

Li, Jun, Huang, H. & Xu, X., 2018. Biological and genetic characteristics of mesenchymal stem cells in vitro derived from human adipose, umbilical cord and placenta. *Int J Clin Exp Med*, pp.1–9.

Lindberg, R.B. et al., 1965. The successful control of burn wound sepsis. *The Journal of trauma*, 5(5), pp.601–616.

Liu, S. et al., 2014. Mesenchymal Stem Cells Prevent Hypertrophic Scar Formation via Inflammatory Regulation when Undergoing Apoptosis. *Journal of Investigative Dermatology*, 134(10), pp.2648–2657.

Low, M., Eisner, C. & Rossi, F., 2017. Fibro/Adipogenic Progenitors (FAPs): Isolation by FACS and Culture. *Methods in molecular biology (Clifton, N.J.)*, 1556, pp.179–189.

Lynch, M.D. & Watt, F.M., 2018a. Fibroblast heterogeneity: implications for human disease. *The Journal of clinical investigation*, 128(1), pp.26–35.

Mahmood, R. et al., 2015. Research Article In Vitro Differentiation Potential of Human Placenta Derived Cells into Skin Cells. *Stem Cells International*, pp.1–11.

Malhotra, S. et al., 2016. Review Article: Mesenchymal Stromal Cells as Cell-Based Therapeutics for Wound Healing. *Stem Cells International*, pp.1–6.

Matthews, R.N., Bennett, J.P. & W, P.F., 1981. Wound Healing Using Amniotic Membranes. *British Journal of Plastic Surgery*, 34(1981), pp.76–78.

Meruane, M.A., Rojas, M. & Marcelain, K., 2012. The use of adipose tissue-derived stem cells within a dermal substitute improves skin regeneration by increasing neoangiogenesis and collagen synthesis. *Plastic and reconstructive surgery*, 130(1), pp.53–63.

Meuli, M. et al., 2019. A Cultured Autologous Dermo-epidermal Skin Substitute for Full-Thickness Skin Defects: A Phase I, Open, Prospective Clinical Trial in Children. *Plastic and reconstructive surgery*, 144(1), pp.188–198.

Morena, F. et al., 2016. Ex-Vivo Tissues Engineering Modeling for Reconstructive Surgery Using Human Adult Adipose Stem Cells and Polymeric Nanostructured Matrix. *Nanomaterials (Basel, Switzerland)*, 6(4), pp.57–13.

Mathew N Nicholas, 2016. Cellularized Bilayer Pullulan-gelatin Hydrogel for Skin Regeneration. pp.1–42.

Navsaria, H.A. et al., 2004. Reepithelialization of a full-thickness burn from stem cells of hair follicles micrografted into a tissue-engineered dermal template (Integra). *Plastic and reconstructive surgery*, 113(3), pp.978–981.

Nicholas, M.N., Jeschke, M.G. & Amini-Nik, S., 2016. Methodologies in creating skin substitutes. *Cellular and molecular life sciences : CMLS*, 73(18), pp.3453–3472.

Niels, T. & Stephen, B., 2006. Global burden of injury in the year 2000: an overview of methods. *WHO Global Burden of Injury - World Health Organization*, pp.1–22.

Nolte, S.V. et al., 2008. Diversity of fibroblasts--a review on implications for skin tissue engineering. *Cells Tissues Organs*, 187(3), pp.165–176.

Oltulu, P. et al., 2018. Measurement of Epidermis, Dermis, and Total Skin Thicknesses from Six Different Body Regions with a new Ethical Histometric Technique. *Turkish Journal of Plastic Surgery*, pp.1–6.

Philippeos, C. et al., 2018. Spatial and Single-Cell Transcriptional Profiling Identifies Functionally Distinct Human Dermal Fibroblast Subpopulations. *The Journal of investigative dermatology*, 138(4), pp.811–825.

Prodinger, C.M. et al., 2017. Current and Future Perspectives of Stem Cell Therapy in Dermatology. *Annals of Dermatology*, 29(6), pp.667–21.

Qomi, R.T. & Sheykhhasan, M., 2017. Adipose-derived stromal cell in regenerative medicine: A review. *World Journal of Stem Cells*, 9(8), p.107.

Reinisch. *Dissertation PhD-Thesis Medical University of Graz*, Toward a better understanding of non-hematopoietic stem and progenitor cell biology and function, 2010.

Rolfe, K.J. et al., 2007. A role for TGF-beta1-induced cellular responses during wound healing of the non-scarring early human fetus? *The Journal of investigative dermatology*, 127(11), pp.2656–2667.

Ruddy, R.M. & Morshead, C.M., 2018. Home sweet home: the neural stem cell niche throughout development and after injury. *Cell and tissue research*, 371(1), pp.1–17.

Ryan, T.J., 1976. The Blood Vessels of the Skin. *The Journal of investigative dermatology*, 67(1), pp.110–118.

Sabapathy, V. et al., 2014. Human Wharton's Jelly Mesenchymal Stem Cells Plasticity Augments Scar-Free Skin Wound Healing with Hair Growth A. B. Pant, ed. *PloS one*, 9(4), pp.e93726–10.

Saleh, R. & Reza, H.M., 2017. Short review on human umbilical cord lining epithelial cells and their potential clinical applications. pp.1–9.

Schliefsteiner, C. et al., 2017. Human Placental Hofbauer Cells Maintain an Anti-inflammatory M2 Phenotype despite the Presence of Gestational Diabetes Mellitus. *Frontiers in Immunology*, 8, pp.6166–17.

Selig, H.F. et al., 2012. The properties of an "ideal" burn wound dressing--what do we need in daily clinical practice? Results of a worldwide online survey among burn care specialists. *Burns*, 38(7), pp.960–966.

Shahrokhi, S. & Jeschke, M., 2019. Skin substitutes - UpToDate. pp.1–20.

Shahrokhi, S., Arno, A. & Jeschke, M.G., 2014. The use of dermal substitutes in burn surgery: Acute phase. *Wound repair and regeneration : official publication of the Wound Healing Society [and] the European Tissue Repair Society*, 22(1), pp.14–22.

Sheikholeslam, M. et al., 2018. Biomaterials for Skin Substitutes. *Advanced healthcare materials*, 7(5).

Singer, A.J. & Clark, R.A., 1999. Cutaneous wound healing. *New England Journal of Medicine*, 341(10), pp.738–746.

Singer, A.J. & McClain, S.A., 2003. A porcine burn model. *Methods in molecular medicine*, 78, pp.107–119.

Singer, A.J. et al., 2016. Effects of burn location and investigator on burn depth in a porcine model. *Burns*, 42(1), pp.184–189.

Singer, N.G. & Caplan, A.I., 2010. Mesenchymal Stem Cells: Mechanisms of Inflammation. pp.1–22.

Spater, T. et al., 2018. Prevascularization of collagen-glycosaminoglycan scaffolds: stromal vascular fraction versus adipose tissue-derived microvascular fragments. *Journal of biological engineering*, 12, p.24.

Spater, T. et al., 2021. Systemic low-dose erythropoietin administration improves the vascularization of collagen-glycosaminoglycan matrices seeded with adipose tissue-derived microvascular fragments. *Journal of tissue engineering*, 12, p.20417314211000304.

Sullivan, T. et al., 1990. Rating the burn scar. *The Journal of burn care & rehabilitation*, 11(3), pp.256–260.

Sullivan, T.P. et al., 2001. The pig as a model for human wound healing. *Wound repair and regeneration : official publication of the Wound Healing Society [and] the European Tissue Repair Society*, 9(2), pp.66–76.

Takeo, M., Lee, W. & Ito, M., 2015. Wound healing and skin regeneration. *Cold Spring Harbor Perspectives in Medicine*, 5(1), p.a023267.

Tang, L. et al., 2017. M2A and M2C Macrophage Subsets Ameliorate Inflammation and Fibroproliferation in Acute Lung Injury Through Interleukin 10 Pathway. *Shock*, 48(1), pp.119–129.

Thulabandu, V., Chen, D. & Atit, R.P., 2017. Dermal fibroblast in cutaneous development and healing. *Wiley interdisciplinary reviews. Developmental biology*, 3, pp.e307–13.

Tompkins, R.G. & Burke, J.F., 1990. Progress in burn treatment and the use of artificial skin. *World journal of surgery*, 14(6), pp.819–824.

Ventura-Juncá, P., Erices, A. & Santos, M.J., 2013. [Bioethical challenges of stem cell tourism]. *Revista medica de Chile*, 141(8), pp.1034–1040.

Wagner, J.M. et al., 2019. Bone allografts combined with adipose-derived stem cells in an optimized cell/volume ratio showed enhanced osteogenesis and angiogenesis in a murine femur defect model. pp.1–12.

Walraven, M. & Hinz, B., 2018. Therapeutic approaches to control tissue repair and fibrosis: Extracellular matrix as a game changer. *Matrix biology : journal of the International Society for Matrix Biology*, pp.1–20.

Watt, F.M., 2014. Mammalian skin cell biology: at the interface between laboratory and clinic. *Science (New York, N.Y.)*, 346(6212), pp.937–940.

Weiss, M.L. & Troyer, D.L., 2006. Stem cells in the umbilical cord. *Stem Cell Reviews*, 2(2), pp.155–162.

WHO, World Health Organization, 2002. World Health Organization Dept. of Injuries and Violence Prevention. The injury chart book: a graphical overview of the global burden of injuries. 29, (World Health Organization, 2002). pp.1–83.

Wood, F.M. et al., 2007. The use of a non-cultured autologous cell suspension and Integra® dermal regeneration template to repair full-thickness skin wounds in a porcine model: A one-step process. *Burns*, 33(6), pp.693–700.

Wurzer, P. et al., 2016. The use of skin substitutes and burn care-a survey. *Journal of Surgical Research*, 201(2), pp.293–298.

Yannas, I.V. & Burke, J.F., 1980. Design of an artificial skin. I. Basic design principles. *Journal of biomedical materials research*, 14(1), pp.65–81.

Yannas, I.V., Orgill, D.P. & Burke, J.F., 2010. Template for Skin Regeneration. *Plastic and Reconstructive Surgery Global Open*, pp.1–11.

Yau, T.M. et al., 2019. Intramyocardial Injection of Mesenchymal Precursor Cells and Successful Temporary Weaning From Left Ventricular Assist Device Support in Patients With Advanced Heart Failure. *JAMA*, 321(12), pp.1176–11.

Yousef, H. & Badri, T., 2019. Histology, Skin Appendages.

Yousef, H. & Varacallo, M., 2019. Physiology, Thermal Regulation.

Zuo, K.J., Umraw, N. & Cartotto, R., 2019a. Scar Quality of Skin Graft Borders: A Prospective, Randomized, Double-Blinded Evaluation. *Journal of Burn Care & Research*, 40(5), pp.529–534.

Appendix I: Timeframe, Milestones of the Thesis project

1 AUSTRIA, Graz: Preliminary Work (Prof. Lang-Olip Lab) 02/2017-08/2017

MSCs Isolation from Umbilical Cord/Wharton`s Jelly

MSCs Differentiation Assays

Cell Work, Cell Culturing, Freezing and Banking

2 CANADA, Toronto: Study, Collecting Data (Dr. Jeschke Lab) 09/2017-06/2019

Animal Training (Animal Course, Anesthesia, Regulations, Safety, and After Care)

Mesenchymal Stromal/Stem Cell Isolation, Culturing, Expansion from various sources

Mesenchymal Stromal/Stem Cell Grafting Experiments on the Pigs

Flowcytometry

Histology, Immunohistochemistry, Analysis

3 AUSTRIA, Graz: Data Analysis, Publications 07/2019-06/2021

Histology, Immunohistochemistry Analysis

Statistical Analysis

Publication, Writing Thesis

Course Work at the Medical University of Graz and at the Medical University of Vienna

Defense of the Doctoral Degree

Appendix II: Publication list for this Thesis project

(2018)

Amini-Nik, Dolp, **Eylert**, et. al, Stem cells derived from burned skin - The future of burn care. *EBIOMedicine*, 37, pp.509–520, 2018, **IF 5.6**

(2020)

Cheng & **Eylert** et al., Handheld instrument for wound-conformal delivery of skin precursor sheets improves healing in full-thickness burns. *Biofabrication*, 2020, **IF 7.2**

(2021)

Eylert et al., Skin regeneration is accelerated by a lower dose of multipotent mesenchymal stromal/stem cells-a paradigm change. *Stem cell research & therapy*, 12(1), p.82, 2021, **IF 5.4**

Supplementary Material

Supplementary Material Figure 1

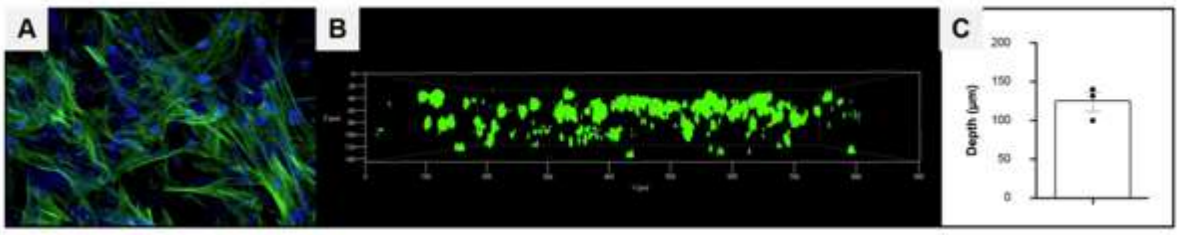

Supplementary Material Figure 1. **Evaluation of the seeding depth of the cells in the DRT Integra®** (Contribution: Reinhard Dolp, available: MSc Thesis, T-Space, University of Toronto; Figure modified by Gertraud Eylert and published as followed: Eylert, Dolp, Parousis et al., in Stem Cell Research Therapy, 2021(Eylert et al. 2021)).

Supplementary Material Figure 2

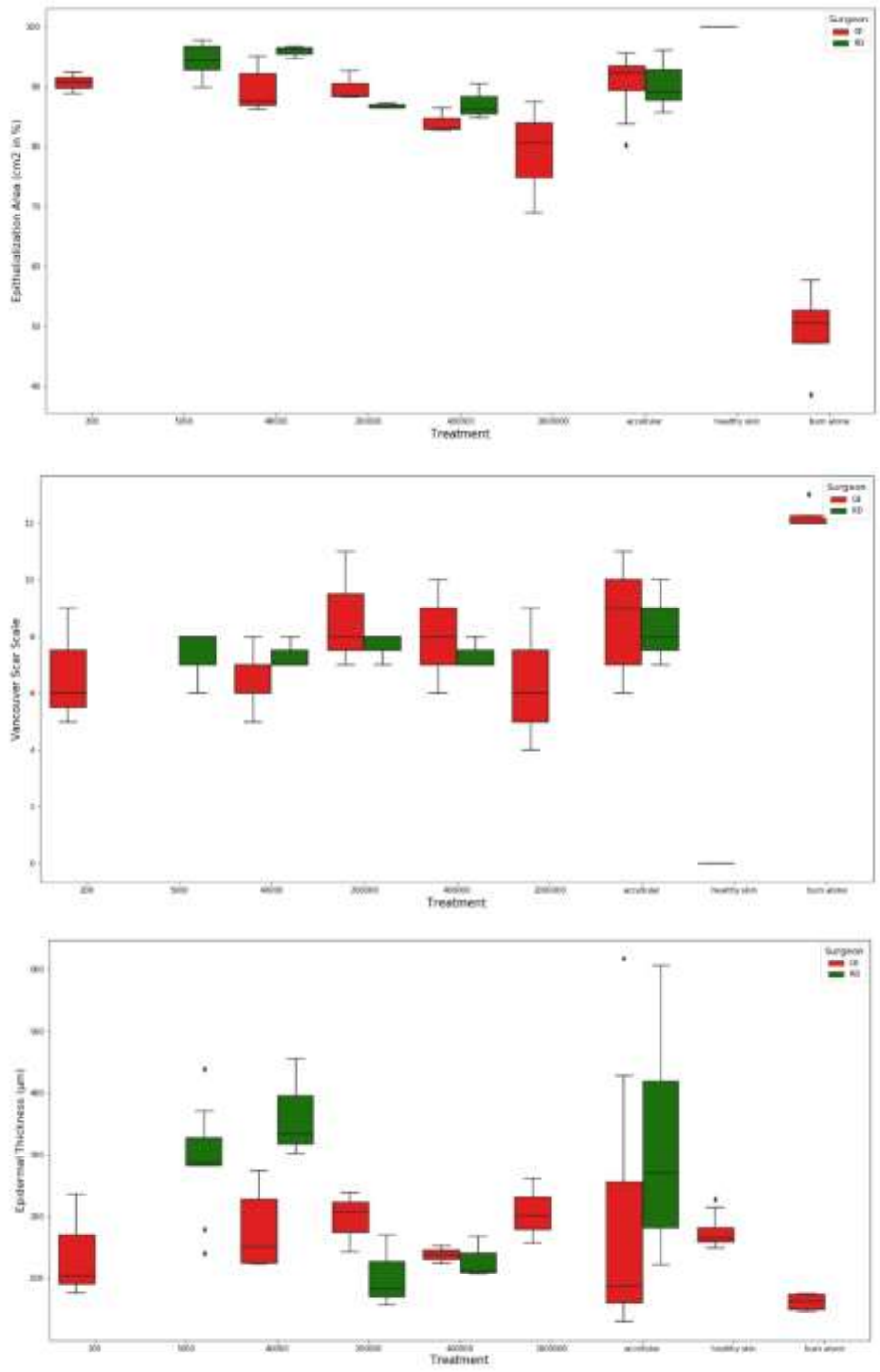

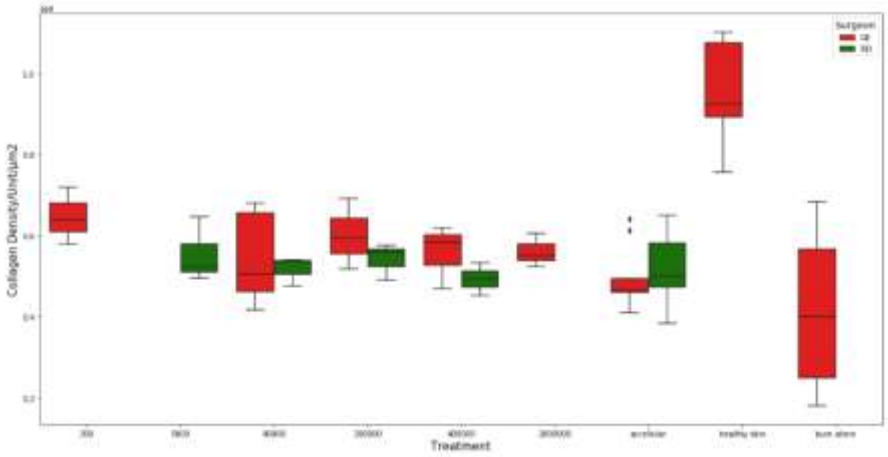
Collagen Density/Unit/µm2
Treatment

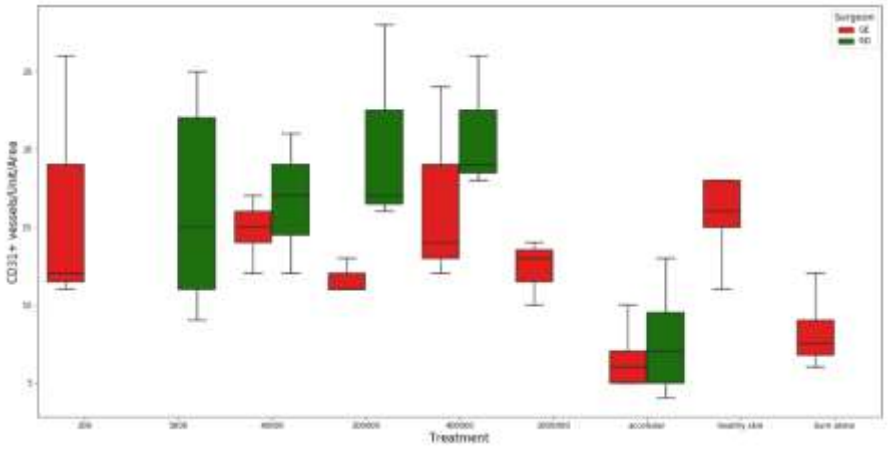
CD31+ vessels/Unit/Area
Treatment

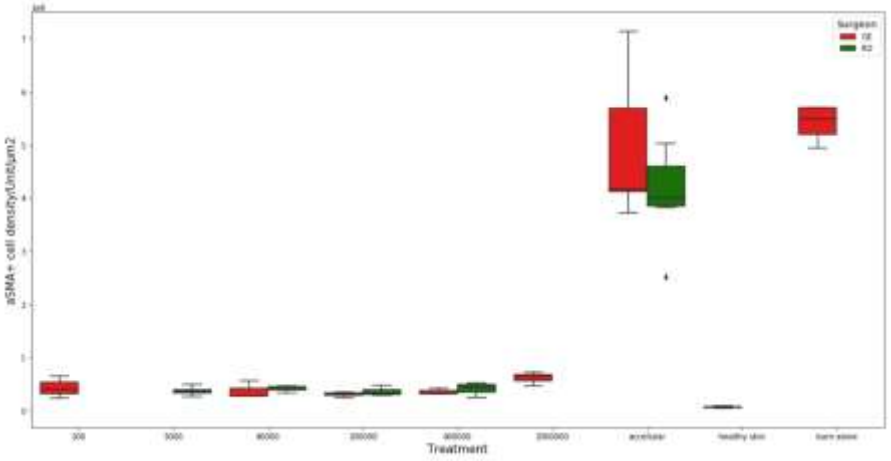
αSMA+ cell density/Unit/µm2
Treatment

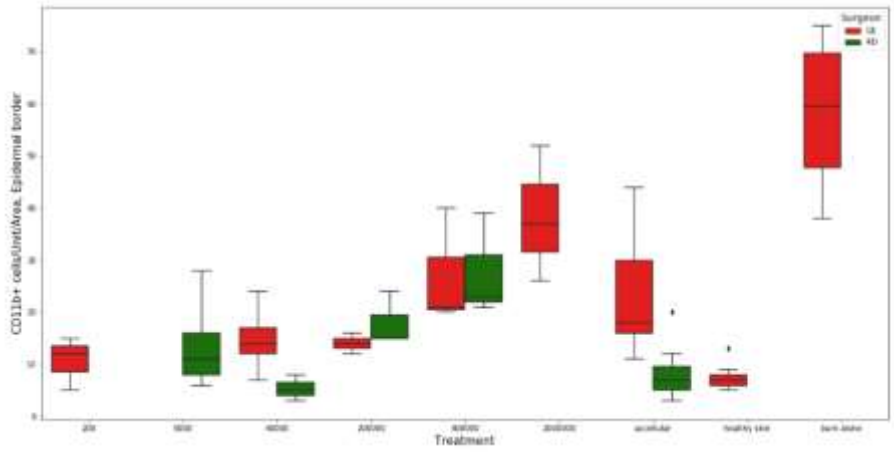
CD11b+ cells/Unit/Area, Epidermal border
Treatment

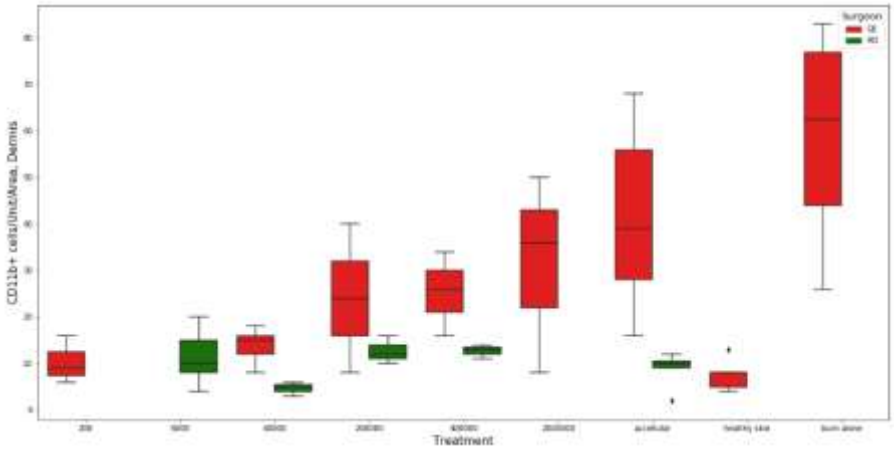
CD11b+ cells/Unit/Area, Dermis
Treatment

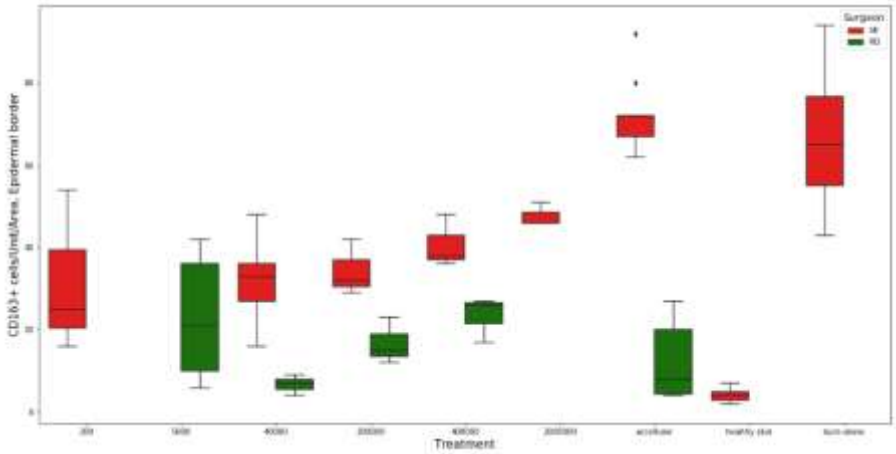
CD163+ cells/Unit/Area, Epidermal border
Treatment

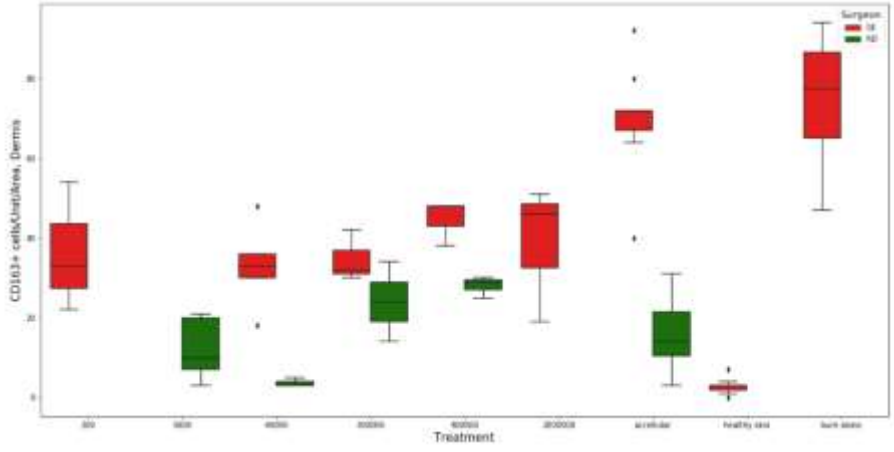
CD163+ cells/Unit/Area, Dermis
Treatment

Supplementary Material Figure 2. Outcome from the two collected data sets. Evaluation of the range of outcome measures between the two surgeon RD (green) and GE (red) from the collected tissue 2015-2017 vs. 2017-2019.

Supplementary Material Table 1

Supplementary Material Table 1.		
Intra-cellular	Cell source	Juvenile UC-MSCs vs. adult skin derived, precursor vs. progenitor cells, quiescence of (adult) cells, level of differentiation of the transplanted cells
	Cell type	Not long cultured vs. long cultured cells (with already initiated downstream differentiation)
	Cell state	Level of internal cell energy and available intracellular nutrients/resources, internal hypermetabolic cell stress levels and mechanism to cope with cell stress, e.g., mitochondrial status (ATP, ADP, glycolytic function, mitochondrial function), strategies to cope with hypoxia, mechanism to cope with (nutrient, energy) starvation, intracellular mechanism to cope with (outside/downstream) cell competition, cell cycle phase of (transplanted) cells, regenerative potential of the transplanted cells
Extra-cellular	(Host) Environment	Burn (inflicted) wounds, wound bed, host tissue/viability, preconditioned host tissue, (already) "homed" repair cells at the wounded side (e.g., migrated bone-marrow stem cells, bandage/dressing, warmth/temperature of the wound, manipulation of wounds, healing potential such as immobilization of the wound (sheer/mechanical stress, range-of-motion of wounds))
	Cell Delivery, Carrier	Quality of cell delivery/grafting/transplantation/setting, cell carrier, (traumatic) cell transplantation
	Biomaterial	Environment for cells, e.g., soft, stiff material, nutrients available, (space for) cell adherence, cell competition, triggers for cell-cell interaction, potential of biodegradability of the biomaterial, external mechanical stress for cells, migration from cells from the host toward the wound dressing, duration of wound dressing onto wounds (dressing changes, disinfection of wounds, toxicity of dressing changes)
	Cell Integration and Migration	Host Tissue and cells distance (cell-adherence, cell integration, migration), orchestrate cutaneous wound healing cascade including e.g., a potential healing environment, nutrients for cells, accurate temperature for cells to migrate/proliferate, outside/wound triggers of the host (chemokines, cytokines), cell environment in the biomaterial, cell-competition, toxicities of/from the host tissue (burn, preconditioned wound, repair potential)
	Cell Therapy (Quantity, Dose)	Quality of cell therapy, contamination, cell-cell-interactions, nutrients, (overload) on cytokines/chemokines from other cells - toxicity, paradoxical cell signaling (from to many, to few cells)

Supplementary Material Table 1. Future directions, outlook and other research questions. (Eylert et al. 2021)